Flexibility in Multi Energy Systems

Models and Metrics to Assess Future Energy Systems

Gusain, D.

DOI
10.4233/uuid:3e857b6c-b028-4f40-9625-54ca79477be8

Publication date
2022

Document Version
Final published version

Citation (APA)
Gusain, D. (2022). *Flexibility in Multi Energy Systems: Models and Metrics to Assess Future Energy Systems*. [Dissertation (TU Delft), Delft University of Technology]. https://doi.org/10.4233/uuid:3e857b6c-b028-4f40-9625-54ca79477be8

FLEXIBILITY IN MULTI ENERGY SYSTEMS

MODELS AND METRICS TO ASSESS FUTURE ENERGY SYSTEMS

FLEXIBILITY IN MULTI ENERGY SYSTEMS

MODELS AND METRICS TO ASSESS FUTURE ENERGY SYSTEMS

Dissertation

for the purpose of obtaining the degree of doctor
at Delft University of Technology,
by the authority of the Rector Magnificus Prof. dr. ir. T.H.J.J. van der Hagen,
chair of the Board for Doctorates,
to be defended publicly on Monday 17, October 2022 at 17:30 o'clock

by

Digvijay GUSAIN

MSc in Electrical Engineering,
Delft University of Technology, Delft, The Netherlands,
born in Kotdwara, India.

This thesis has been approved by

promotor: prof. dr. P. Palensky
copromotor: dr. M. Cvetković

Composition of the promotion committee:

Rector Magnificus,	Chairperson
Prof. dr. P. Palensky,	Technische Universiteit Delft
Dr. M. Cvetković,	Technische Universiteit Delft
Independent members:	
Prof. dr. A. Monti	RWTH Aachen, Germany
Prof. dr. M. Gibescu	Utrecht University, The Netherlands
Prof. dr. ir. P. Bauer	Technische Universiteit Delft
Dr. ir. R. M. Stikkelman	Technische Universiteit Delft
Dr. E. Widl	Austrian Institute of Technology, Austria
Prof. dr. ir. M. Zeman	Technische Universiteit Delft, reserve member

Keywords: power-to-x, flexibility, multi-energy systems, co-simulation

Printed by:

ISBN 000-00-0000-000-0

An electronic version of this dissertation is available at
http://repository.tudelft.nl/.

Dedicated to Maa, Papa, Shalen, and Ruti.
Your support was invaluable.

दुनिया बहुत मतलबी है,
साथ कोइ क्यूँ देगा ।
मुफ़्त का तो यहा कफन भी नही मिल्ता,
बिना गम के प्यार कौन देगा ॥

सरिता गुसाईं

Contents

SUMMARY

The transition to sustainable energy is well underway and is introducing changes on both sides of the electricity balance scale – generation and demand. On the generation side, emissions-free renewable generation resources such as wind and solar are replacing the pollution-emitting thermal power plants. On the demand side, energy sectors traditionally dependent on fossil fuels such as heat, mobility, gas, chemicals, and others are being coupled to electricity using Power to X (or P2X) technologies. These developments are introducing changes to the planning and operation of the electricity grid. Large-scale power generation from renewables and an increased demand for power resulting from the electrification of energy sectors in a grid with limited capacity is causing congestion challenges. Increased penetration of renewables is also driving demand for power system services that can complement the uncertainty and intermittency associated with renewable power generation. Until sufficient capacity is installed, mitigating these challenges requires the grid, especially its participants, to be flexible.

To provide for an increasing amount of flexibility in a rapidly evolving power system, new entities that specifically provide such services are emerging. These Flexibility Service Providers (FSPs) include entities such as aggregators or virtual power plants. The flexibility provided by the FSPs often comes from demand-side resources, especially the sector coupling P2X resources. However, in the current energy landscape, there are only FSPs with resource-specific portfolios, such as FSPs with EV (Electric Vehicles) portfolios, FSP with residential heat pump portfolios, etc. Being resource-specific helps the FSP to quantify its available flexibility since the operational characteristics of a single type of resource in the portfolio can be characterized and aggregated. Quantification of flexibility becomes complicated in portfolios consisting of resources with different operational characteristics. Therefore, the research in this thesis focuses on an FSP with a portfolio of more than one type of P2X resource. The main objective of this research is to develop metrics that can help FSPs quantify its flexibility from such a portfolio.

Assessment of this objective starts with understanding the importance of modeling P2X resources. Here, with the help of several case studies involving models of different types of P2X resources, differences in simplistic and detailed modeling approaches are highlighted. The case studies also show the benefits of using detailed models in understanding phenomena that impact flexibility avail-

able from P2X resources. The observations from these case studies form the basis for recommendations regarding modeling approaches for assessing flexibility from P2X resources. Once the need for appropriate modeling is established, the focus in this research shifts toward model-based simulation methods for the assessment of sector-coupled energy systems (also known as multi-energy systems). Here, co-simulation is proposed as a tool for the FSP to simulate systems consisting of models of different technologies and networks, developed in different programming languages and with different levels of detail. Finally, the thesis brings attention to developing metrics for measuring the flexibility available in the FSP's portfolio. An assessment of existing metrics is presented, and the inaccuracy in existing metrics to quantify flexibility is shown. Consideration is given to operational time frames – minutes to hours to a day – where extracting flexibility from P2X resources is of most value to the FSP. Taking inspiration from long-term power system adequacy studies three metrics are designed to help the FSP quantify flexibility from a portfolio of flexible energy resources. The applicability of these metrics to power system challenges listed previously is shown. Recommendations are made on the use and applicability of the proposed method and metrics for other power system challenges, such as frequency regulation.

The final chapter of this thesis provides conclusions to the research conducted and answers the research questions posed at the onset. In summary, the following conclusions are drawn. First, the observations from studies and simulations advocate that model detail is essential when characterizing flexibility from P2X resources. An analogy is made between current P2X modeling techniques in power systems studies and early-stage modeling of renewables as negative loads in power system studies. With the increasing adoption of these technologies and their growing impact on power system operation, the use of models that appropriately describe their behavior is essential. Second, co-simulation as a method to assess a portfolio offers significant benefits over monolithic simulation. Co-simulation facilitates model exchange between different stakeholders and allows the FSP to understand the operation of P2X resources in a setting where the resources dynamically interact with both the power system and the coupled energy sector. The third and final conclusion pertains to the usability of the proposed metrics for the FSP. The designed metrics can encapsulate the behavior of different types of P2X resources in a portfolio, each with unique operational characteristics and constraints that impact their and, consequently, portfolio flexibility. The ability to quantify flexibility in a diverse portfolio paves the way for FSPs to extract flexibility from more than one type of flexible energy resource, quantify it, and offer it in the market. Ultimately, this also benefits the consumer, which does not need to contract multiple P2X technology-specific FSPs to participate in the market to provide its flexibility.

SAMENVATTING

De overgang naar duurzame energie is in volle gang en brengt veranderingen met zich mee aan beide zijden van de elektriciteitsbalans - opwekking en vraag. Aan de opwekkingszijde worden de vervuilende thermische centrales vervangen door emissievrije hernieuwbare energiebronnen zoals wind- en zonne-energie. Aan de vraagzijde worden energiesectoren die traditioneel afhankelijk zijn van fossiele brandstoffen, zoals warmte, mobiliteit, gas en chemicaliën, gekoppeld aan elektriciteit met behulp van Power to X-technologieën (of P2X). Deze ontwikkelingen brengen veranderingen teweeg in de planning en de werking van het elektriciteitsnet. Grootschalige stroomopwekking uit hernieuwbare energiebronnen en een toegenomen vraag naar stroom als gevolg van de elektrificatie van energiesectoren in een net met beperkte capaciteit veroorzaken congestieproblemen. De toegenomen penetratie van hernieuwbare energiebronnen leidt ook tot een grotere vraag naar energiesysteemdiensten die de onzekerheid en intermitterendheid van de hernieuwbare energieproductie kunnen aanvullen. Zolang er niet voldoende capaciteit is geïnstalleerd, moeten het net en vooral de deelnemers aan het net flexibel zijn om deze problemen op te lossen.

Om te zorgen voor een toenemende mate van flexibiliteit in een snel evoluerend elektriciteitssysteem, ontstaan er nieuwe entiteiten die specifiek dergelijke diensten verlenen. Deze aanbieders van flexibiliteitsdiensten (FSP's) omvatten entiteiten zoals aggregatoren of virtuele elektriciteitscentrales. De door de FSP's geleverde flexibiliteit is vaak afkomstig van middelen aan de vraagzijde, met name de sectorale koppeling van P2X-middelen. In het huidige energielandschap zijn er echter alleen FSP's met hulpbronspecifieke portefeuilles, zoals FSP's met EV-portefeuilles (elektrische voertuigen), FSP's met warmtepomp-portefeuilles voor woningen, enz. Middelengebondenheid helpt de FSP om zijn beschikbare flexibiliteit te kwantificeren, aangezien de operationele kenmerken van één type middel in de portefeuille kunnen worden gekarakteriseerd en samengevoegd. De kwantificering van flexibiliteit wordt ingewikkeld in portefeuilles die bestaan uit hulpbronnen met verschillende operationele kenmerken. Daarom richt het onderzoek in dit proefschrift zich op een FSP met een portefeuille van meer dan één type P2X-middelen. Het hoofddoel van dit onderzoek is metrieken te ontwikkelen die FSP's kunnen helpen hun flexibiliteit van een dergelijke portefeuille te kwantificeren.

Beoordeling van deze doelstelling begint met inzicht in het belang van het

modelleren van P2X-middelen. Aan de hand van een aantal case studies met modellen van verschillende soorten P2X-middelen worden de verschillen tussen simplistische en gedetailleerde modelbenaderingen belicht. De case studies laten ook de voordelen zien van het gebruik van gedetailleerde modellen bij het begrijpen van verschijnselen die de beschikbare flexibiliteit van P2X-middelen beïnvloeden. De bevindingen van deze case studies vormen de basis voor aanbevelingen betreffende modelbenaderingen voor de beoordeling van de flexibiliteit van P2X-middelen. Zodra de noodzaak van passende modellering is vastgesteld, verschuift de aandacht in dit onderzoek naar modelgebaseerde simulatiemethoden voor de beoordeling van sectoraal gekoppelde energiesystemen (ook bekend als multi-energiesystemen). Hier wordt co-simulatie voorgesteld als instrument voor het FSP om systemen te simuleren die bestaan uit modellen van verschillende technologieën en netwerken, ontwikkeld in verschillende programmeertalen en met verschillende detailniveaus. Tenslotte wordt in het proefschrift aandacht besteed aan de ontwikkeling van metrieken voor het meten van de beschikbare flexibiliteit in de portefeuille van het FSP. Een beoordeling van bestaande metrieken wordt gepresenteerd, en de onnauwkeurigheid in bestaande metrieken om flexibiliteit te kwantificeren wordt aangetoond. Er wordt gekeken naar de operationele tijdsbestekken - van minuten tot uren tot een dag - waarin het onttrekken van flexibiliteit aan P2X-middelen het meest waardevol is voor het FSP. Geïnspireerd door studies naar de toereikendheid van het elektriciteitssysteem op lange termijn, worden drie maatstaven ontworpen om het FSP te helpen de flexibiliteit van een portefeuille van flexibele energiebronnen te kwantificeren. De toepasbaarheid van deze maatstaven op de eerder genoemde uitdagingen voor het energiesysteem wordt aangetoond. Er worden aanbevelingen gedaan voor het gebruik en de toepasbaarheid van de voorgestelde methode en metrieken voor andere uitdagingen in het energiesysteem, zoals frequentieregeling.

Het laatste hoofdstuk van dit proefschrift geeft conclusies over het uitgevoerde onderzoek en beantwoordt de onderzoeksvragen die aan het begin zijn gesteld. Samengevat worden de volgende conclusies getrokken. Ten eerste pleiten de waarnemingen uit studies en simulaties ervoor dat modeldetails essentieel zijn bij het karakteriseren van flexibiliteit van P2X-middelen. Er wordt een analogie gemaakt tussen de huidige P2X-modelleringstechnieken in studies van energiesystemen en de vroege modellering van hernieuwbare energiebronnen als negatieve belastingen in studies van energiesystemen. Met de toenemende invoering van deze technologieën en hun groeiende invloed op het functioneren van het energiesysteem, is het gebruik van modellen die hun gedrag adequaat beschrijven essentieel. Ten tweede biedt co-simulatie als methode om een portfolio te beoordelen aanzienlijke voordelen ten opzichte van monolithische simu-

latie. Co-simulatie vergemakkelijkt de uitwisseling van modellen tussen verschillende belanghebbenden en stelt het FSP in staat de werking van P2X-middelen te begrijpen in een omgeving waarin de middelen dynamisch interageren met zowel het elektriciteitssysteem als de gekoppelde energiesector. De derde en laatste conclusie betreft de bruikbaarheid van de voorgestelde meetgegevens voor het FSP. De ontworpen metrieken kunnen het gedrag van verschillende soorten P2X-middelen in een portefeuille inkapselen, elk met unieke operationele kenmerken en beperkingen die hun flexibiliteit en bijgevolg de flexibiliteit van de portefeuille beïnvloeden. Het vermogen om de flexibiliteit in een gevarieerde portefeuille te kwantificeren maakt de weg vrij voor FSP's om flexibiliteit uit meer dan één type flexibele energiebron te halen, deze te kwantificeren en op de markt aan te bieden. Uiteindelijk komt dit ook ten goede aan de consument, die niet meerdere P2X-technologie-specifieke FSP's hoeft te contracteren om deel te nemen aan de markt voor zijn flexibiliteit.

ACKNOWLEDGEMENTS

Many people have played a vital role in this long journey. First and foremost, my promoter, Prof. Peter Palensky. He has given me time to explore new ideas, investigate them, and implement them, no matter how absurd they sound. Without his support and belief in me, I would not have been able to complete this project. I have thoroughly enjoyed our engaging discussions and your mentorship. Next, I would like to thank Dr. Milos Cvetkovic, my daily supervisor, for his valuable guidance and mentorship throughout the project. His enthusiastic support, his willingness to discuss anything and everything whenever I wanted to, and most importantly, his ability to be appreciative and, at the same time, rational when I have proposed all sorts of ideas was critical in my journey of achieving this doctorate. I have been fortunate to have shared this experience with you.

Next, I would like to acknowledge the love and support of the people closest to me. My mother, with her lovely and thought-provoking poems, her lovely laughter, and her infectious ability to discuss and debate with me on topics ranging from god to life, managed to keep me in high spirits, even when I felt helpless. My father, who was always eager to listen to any problem I had and offer his help, wisdom, experience, and advice on the matter. Whether it concerned my research or not, I could always rely on him to give me his best, unbiased advice, which has helped me immensely. My sister, who is the source of my strength and bravery. She is my constant cheerleader, someone who never fails to cheer me up with her silly jokes and impersonations. She believes in me more than I do in myself, and for that, I am indebted to you. My partner, who has been instrumental in the progress I have made in my personal and professional life. Her love, patience, and kindness has helped me immensely navigate mentally and emotionally challenging periods. She has been encouraging when I have been at my lowest and has been a crucial part of my support system whenever I have needed her. She is a kind-hearted but intensely fearless woman whom I am lucky to have by my side. To be able to share everything with these four people, to have them celebrate my achievements and share my lows, has kept me moving forward. I am immensely grateful to you all.

Another band of four people, whom I also consider my family and whose contributions I would like to acknowledge, is Krishna, Sunny, Rahul, and Sharath. It is said that friends are the family you choose. It could not have been more truer in this case. We started out as confused 20-somethings when we first came to

Delft in 2014. Over the years, we have helped each other, rejoiced in each other's successes, and shared our lows. I have been truly blessed to have you; I hope this bond we share remains as strong as ever.

My colleagues at TU Delft Hazem, Haiyan, Shantanu, Roland, Chenguang, Aihui, Rishabh, Swasti, Matija, Vinay, Arun, Nakisa, Arcadio, Shubhangi, Simon, Jose, Marjan, Pedro, Arjen, Elyas, Wouter, Vetri, Ajay, Ties and many others in the research group, with whom I shared countless beers and many interesting conversations. Thank you for your support. You all made the work environment so much less stressful and enjoyable. I have enjoyed working with all of you. I would also like to thank my closest friends, Sidharth and Bhavesh, with whom I have shared the closest bond for the longest time. Even though the opportunities for us to meet and enjoy have been far and few over the years, spending time with you guys every year is the highlight of my trip back home to India. My *dehaatis*: Agrata, Aparna, Shikhar, Chayan, Mouli, Arti, and Prachi, thank you for your continuous support, regular calls, and your cheeky jokes about the duration of this thesis. Unfortunately for you, this is done now, and so you will have to find new jokes!

ABBREVIATIONS

VRES	Variable Renewable Energy Sources
TSO	Transmission System Operator
DSO	Distribution System Operator
BRP	Balance Responsible Party
VPP	Virtual Power Plant
FSP	Flexibility Service Provider
P2X	Power to X
P2H	Power to Heat
P2G	Power to Gas
MES	Multi Energy System
DRP	Demand Response Program
CoP	Coefficient of Performance
PEM	Proton Exchange Membrane
HVAC	Heat Ventilation and Air Conditioning
EBST	Electric Boiler and Storage System
AGC	Automatic Generation Control
WTO	Wind Turbine Operator
PTU	Program Time Unit
API	Application Programming Interface
FMI	Functional Mockup Interface
FMU	Functional Mockup Unit
CTDS	Continuous Time Dynamic Simulator
CHP	Combined Heat and Power
EN	Electrical Network
DG	Distributed Generators
TCL	Thermostatically Controlled Loads
EV	Electric Vehicles
DRX	Demand Response Market
FRP	Flexibility Requesting Party
FR	Flexibility Request
IPP	Individual Power Profile
IRRE	Insufficient Ramp Resource Expectation
PFD	Periods of Flexibility Deficit

UF	Unserved Flexibility
UFE	Unserved Flexibility Energy
EUFE	Expected Unserved Flexible Energy
EFI	Expected Flexibility Index
EDIF	Expected Durations of Insufficient Flexibility
EG	External Grid
EB	Electrical Boiler
FC	Fuel Cell
GH	Greenhouse
GB	Gas Boiler
TS	Thermal Storage
HP	Heat Pump
MILP	Mixed Integer Linear Program

NOMENCLATURE

Variables

ΔP	Change in Power
Δ_t	Time interval
$\dot{m}$	Mass Flow Rate
η	Efficiency
Λ	Cell Current
λ	Cell Current Density
ν	Flexibility Set
Π	FR Signal Set
π	FR Signal
τ	Time to Ramp
θ	Temperature
f	Electrical Frequency
i	Electrical Current
N_x	Total Number of x
P	Electrical Power
p	Pressure
p_a	Probability of acceptance
P_{th}	Thermal Power
r	Ramp Rate
S	Thermal Storage Capacity

T	Total Simulation Time
t	Time variable
V	Electrical Voltage

Subscripts

agg	Aggregated
amb	Ambient
ava	Available
a	Actual
c	Specific Heat Capacity
d	Index of electric load
el	Electrolyzer
e	Electric
fc	Forecast
ID	Intraday
i	Index of flexible resource in the portfolio
k	Index of PTU
l	Loss
max	Maximum
min	Minimum
ms	Minkowski Summation
nom	Nominal
n	n^{th} value
op	Operational
p	Pump
ref	Reference

req	Required
sp	Setpoint
s	Index of scenario
t	Index of time
UF	Unserved Flexibility
w	Wind

Superscripts

π	FR signal
$\uparrow$ $\downarrow$	Upward and downward directions
avg	Average
$real$	Real
ss	Substation

Others

$\overline{x}$, $\underline{x}$	Lower and upper bounds on x

1

INTRODUCTION

1.1. FLEXIBILITY NEEDS IN POWER SYSTEMS

The adoption of variable renewable energy sources (VRES) such as wind and solar PV has been phenomenal in recent years, as shown in Fig. 1.1. According to data published by the *Centraal Bureau voor de Statistiek* (CBS), [1], the share of wind energy increased from 3391 MW in 2015 to 6619 MW in 2020 within the Netherlands (shown in green). The adoption of solar PV technology has been even more explosive than wind energy, increasing from just 1526 MW in 2015 to 10717 MW in 2020 in the same time frame (shown in pink). This trend is expected to continue in the near future as the Netherlands looks to achieve its 2030 and 2050 renewable energy and CO_2 emissions targets.

A more significant share of VRES in our energy system also comes with its share of challenges. Consider the following example. In regions of high solar PV penetration, sunrise and sunset times correspond to events of a significant amount of solar PV generation turning on and turning off, respectively. A planned and coordinated transition from solar PV to other generation forms is needed when the sun goes down. This means that other power-generating resources must come up online and ramp up their power production quickly. Consider the net load (demand minus renewable generation) curve in Fig. 1.2 from a typical day in Germany. There is a need for almost 15500 MW of power (almost 30% of peak load) to come up online within two hours.

To address scenarios such as one listed above, the future power system must be flexible. It is for this reason that flexibility in electric power systems has become an area of keen interest in recent years [2–9]. A study was conducted by the *Nederlandse Organisatie voor Toegepast Natuurwetenschappelijk Onderzoek* (TNO) [4] to evaluate the demand and supply of flexibility in the Dutch power

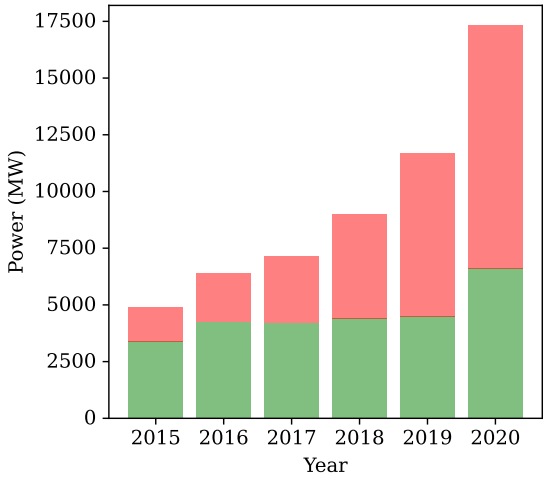

Figure 1.1: Recent growth in adoption of renewable energy in The Netherlands. Green represents wind energy capacity, while pink represents the capacity of solar energy in the Netherlands. Data taken from CBS.

system between 2015 and 2050. The authors noted in this report that demand for flexibility in 2050 will increase almost six-fold compared to 2015, thanks to the aforementioned increase in the adoption of VRES across various voltage levels in the Dutch power grid.

The topic of flexibility is vast and deep. Therefore, before commencing any further into the commentary and discussion on this topic, a clear and concise definition of flexibility must be first established in the context of electric power and energy systems.

> *Flexibility is defined as the ability of the power system to respond to any event, planned or unplanned, such that the balance between supply and demand of electricity is always maintained and therefore operational reliability of the system is preserved.*

There are two critical points in the definition mentioned above: 1) flexibility is tied to the idea of ensuring the dynamic balance of demand and supply, and 2) this balance has to be maintained in case of any event, planned or unplanned. The first point can be seen as composed of two sub-points 1a) the ability to respond quickly to ensure the balance, that is, ramping flexibility, and 1b) the ability to provide a certain amount of power and energy, that is, power and energy flexibility [10]. The second point refers to the timing of the request for flexibility. In essence, both have to be satisfied simultaneously.

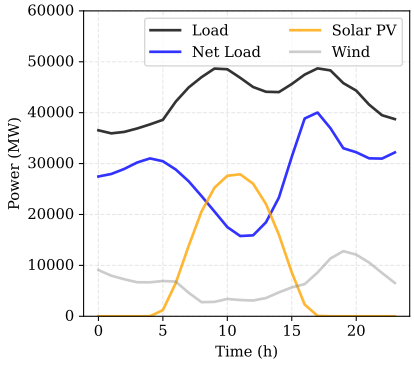

Figure 1.2: VRE generation, load, and net-load on September 20, 2020, in Germany. Data taken from www.open-power-system-data.org.

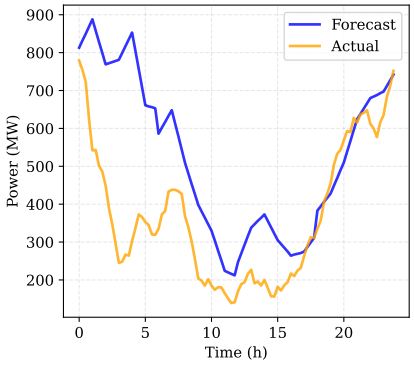

Figure 1.3: Wind power generation in Ireland over 24 hours on November 15, 2021. Data taken from smartgriddashboard.eirgrid.com.

1.2. POWER SYSTEMS CHALLENGES REQUIRING FLEXIBILITY

There are several events in the power system every day which require it to be flexible. In this section, I list some of these challenges.

Renewable Forecasting Errors Unlike conventional power generation plants, which depend on a steady supply of fossil fuels, wind and solar PV power output depends on weather conditions, which are volatile and unpredictable. Power systems might experience missing generation when the wind does not blow, or there is a cloud cover. Alternatively, systems might experience a generation surplus due to excessive, unpredictable winds. For an economical operation of a power system, the amount of power produced by each generator (including VRES) is fixed a day before the actual time of delivery. Due to volatile and unpredictable weather, there is almost always a difference between the projected and actual values of power generated, causing scenarios of generation deficits and surpluses, as illustrated in Fig. 1.3. The power grid, therefore, needs to be flexible in accommodating such scenarios.

Net Load Ramping The phenomena illustrated in the example in Section 1.1 reflects the need for flexibility to fulfill the net load ramp requirements. The curve in Fig. 1.2 is called the Duck Curve since the net load curve (blue-solid) looks like a duck silhouette. The California Independent System Operator (CAISO) first observed this while analyzing the impact of increased solar PV adoption in their grid. However, the large ramps in net load occur from predictable events such as sunrises and sunsets and other unpredictable events such as forecasting

errors in VRES power generation. When a large deficit or surplus of generation is produced, apart from requiring flexibility in the form of power and energy to fill the gap, it is also required that this flexibility is obtained quickly, i.e., ramping flexibility.

Congestion Management A typical challenge faced by distribution and transmission system operators is congestion. Congestion in power networks occurs when the line capacity constrains the power transfer from one point to the other. In the transmission grid, transporting cheap renewable energy generated from a rapidly growing portfolio of utility-scale VRES such as offshore wind farms to load centers several hundred (and even thousands) kilometers away on existing infrastructure causes congestion issues. For the system operator, who is required to maintain system reliability and stability, this congestion becomes a re-dispatching problem, which can be expensive. In Germany, the frequency of re-dispatching operations done by the system operator to tackle local VRES-induced congestion issues is increasing the costs in the electricity market [11]. Within the distribution grid as well, congestion problems can cause issues for the distribution system operator. In the Netherlands, it is expected that by 2050, almost 45% of distribution substation transformers will be congested due to over-generation from distributed VRES [12]. To tackle these issues, the system requires flexibility to adapt generation or consumption when congestion occurs.

Frequency regulation The power system is a highly dynamic entity that requires a constant, second-by-second balance between load and generation to maintain frequency near a constant value. The system operator keeps an excess capacity known as an operating reserve to ensure this balance. Calculating capacity in operating reserve is determined using expected load and generation values, as well as anticipated reserve triggering events. With an increasing amount of VRES, the expected generation is known with much less confidence compared to conventional power plants owing to uncertainties in weather predictions. If the system operator has to rely solely on operating reserve, the cost of electricity for the final consumer will be impacted [13, 14]. This is because the cost of this reserve power is much higher than the cost of power available from energy markets [15]. The grid operator, therefore, needs flexibility in procuring the operating reserves in the face of uncertain VRES power generation.

1.3. POWER SYSTEM ENTITIES AND FLEXIBILITY

The challenges highlighted in the previous section represent the requirement for flexibility in power systems in the face of both planned and unplanned events.

The responsibility to address the listed challenges lies with various entities within the power system. These entities are the transmission system operator (frequency regulation, congestion, net load ramping), the distribution system operator (congestion, net load ramping), and the balance responsible party (forecast error correction). A balance responsible party (BRP) is a power system entity consisting of one or more power producers and/or consumers. A BRP interacts with the system operator to exchange energy. It submits a schedule of its expected energy exchange with the grid, which is fixed a day in advance. The system operator expects the BRPs to adhere to the agreed schedule, ensuring the balance of the power system is maintained (hence the name, balance responsible party). If the BRP deviates from the agreed schedule of energy exchange and causes a deviation, the system operator covers up for it using the operating reserve. However, it levies a penalty upon the BRP, which can be a significant expense. Therefore, the BRP has an obligation and a financial incentive to maintain it's internal balance.

For a BRP with significant VRES, such as a prominent wind power park owner, or a solar PV farm owner, the uncertainty in VRES's power production affects its ability to accurately determine its energy exchange schedule with the system operator in advance. Hence, such a BRP will require flexibility to counter the uncertainty from VRES and avoid imbalance. Such a BRPs' need for flexibility has enabled entities such as aggregators and virtual power plants (VPP) to emerge as Flexibility Service Providers (FSPs). FSPs rely heavily on controlling and coordinating flexibly operated distributed flexible energy resources. By controlling a portfolio of flexible energy resources, the FSP can modulate aggregated power profile of its portfolio as needed, providing required flexibility [2, 16–18] to a Flexibility Requesting Party such as the BRPs. The FSPs are a new power system entity that can provide flexibility as a resource in electricity markets. Alternatively, FSPs can also make bilateral contracts with the BRP to provide flexibility [19]. This makes FSPs an essential component of current and future power systems where flexibility is and will increasingly be an indispensable commodity to ensure a safe, reliable, and economic operation of the power system.

In this thesis, I assess flexibility from the perspective of an FSP and look at some of the aforementioned technical challenges which require flexibility.

1.4. MULTI ENERGY SYSTEMS AS FLEXIBLE RESOURCES

One type of the aforementioned flexible resources which an FSP can control is the power and energy conversion devices that couple the electricity sector to other energy sectors such as heat (electric boilers and heat pumps), gas (electrolyzers), transportation (electric vehicles), etc. These energy converters are called Power to X or P2X devices. P2X devices act as energy transformers and couple energy sectors to electricity. Such coupled systems are known as multi-energy

systems or MES. Coincidentally, while VRES introduces the need for greater flexibility in power systems, MES offers a potential source of the needed flexibility [3] in the form of P2X devices. The P2X devices have characteristics that can be exploited to provide flexibility to the power system. These include:

- P2X devices can be extremely flexible in operation with high operational ramp rates, allowing them to quickly shift their operating power set point as needed by the power system.
- In the case where P2X resources are spatially distributed and have diverse technical characteristics, the aggregated and coordinated control of these resources can provide a significant and granular control on aggregated power demand at any time.
- Integrated communication capabilities allow P2X devices to be seamlessly incorporated into a smart energy management systems (Smart EMS) framework and control their operation as required. In industrial areas where robust communication infrastructure is already well established, large-scale P2X devices can be easily set up to offer flexibility to the power system.

For some FSPs, P2X devices form an integral component of their portfolio of controllable resources. Controlling and modulating their power demand to support the power system operation is known as Demand Side Management or Demand Response [20]. It has been shown in studies around the world that Demand Response is a key, affordable, and viable solution to the power system's flexibility needs. Demand Response is defined and enacted using programs called Demand Response Programs, or DRPs. A DRP defines the conditions under which participating resources will be controlled to provide demand response. This includes setting parameters between which device will be asked to operate (such as defining the temperature range for heating system in buildings), setting times, and durations during which device will be asked to modulate its consumption pattern. In a report published by US Energy Information Administration [21], the authors reported that DRP was responsible for saving energy and reducing the peak demand in a pilot program in the USA. In another pilot study in the USA [22], authors showed that DRP was a cost-effective option for providing frequency response. The authors in [23] use DRP in a VPP portfolio to assist the distribution system operator in maintaining the voltage in its network within an acceptable range. The problem of congestion management using DRP was tackled in [24, 25]. In Norway, a pilot study involving residential P2H electrical water heaters showed that DRP was an effective tool in reducing peak demand [26]. Therefore, the FSP with a diverse set of flexible resources requires a DRP to coordinate and control the power consumption to provide flexibility.

1.5. UNDERSTANDING THE RESEARCH PROBLEMS

To sell flexibility as a product, the FSP (with multiple controllable resources in its portfolio), must:

1. study the constraints and operational behavior of the controllable resource in its portfolio,
2. evaluate the impact these constraints have on the flexibility provided by the portfolio as an entity itself, and finally,
3. use this information to design a DRP that can maximize the flexibility available from the portfolio.

The first step is to model and evaluate the various types of resources in the portfolio. Each P2X device's behavior, and consequently the flexibility extractable from it, is dependent upon two key factors:

1. the operational constraints of the device itself, such as maximum available ramping capability from the current operating condition, and
2. the operational constraints of the sector it couples, for example, unavailability of flexibility from a P2H resource due to high heat demand.

The FSP needs to ensure that the models used to compute the flexibility available are an acceptable representation of the system or device's behavior. The used model should be of sufficient resolution (i.e., it should be modeled with sufficient detail) to evaluate operational constraints and dynamics. Therefore, for my first research problem, I focus on the value of including various constraints that define the operational behavior of P2X devices, that is, the importance of detail in the modeling of P2X devices.

To assess flexibility from various P2X resources, it is crucial to evaluate the operation of these P2X devices in an MES setting. Since the P2X devices used by the FSPs couple various energy domains to electricity, an approach to evaluate the flexibility of P2X devices must consider its operation and implication in the electricity domain and the coupled domain. Traditionally, modeling and simulation of different domains in energy system analysis have been done in domain-specialized monolithic modeling and simulation environments. This has allowed using state-of-the-art modeling languages and solvers to obtain accurate system responses. However, as systems get increasingly integrated and their behavior and operation more dynamically interluded, it becomes essential to evaluate this system on an integrated, holistic level rather than an individual

subsystem. Therefore, in the second part of the research, I focus on the usefulness of an integrated simulation-based approach to an FSP.

The final research problem I tackle in this thesis is the design of metrics that can help the FSP assess its portfolio's flexibility by considering the relevant P2X resource characteristics and their operation in an integrated MES setting. Given the research problems, the objective of this thesis is therefore stated as follows:

> *The objective of this thesis aims to develop adequacy metrics that quantify the operational flexibility available to the electric power systems from various flexible energy resources in an integrated energy system setting.*

1.6. RESEARCH QUESTIONS

The following research questions are posed in line with the problems and objective stated in Section 1.5.

1. The amount of flexibility must be expressed with respect to the nature of flexibility requests. What are the flexibility requests of interest for an FSP?

2. The level of detail in a model directly influences outputs obtained from that model. What impact does model detail have on the accurate assessment of operational behavior and, consequently, accurate assessment of flexibility available from P2X devices?

3. Evaluation of flexibility from P2X devices must be done by considering its operation in an integrated setting. How can this be achieved?

4. The metric must convey information on the ability of a portfolio with flexible resources to fulfill flexibility requests. How can such metric(s) be formulated?

5. Activation of flexibility from a device at any time can lead to changes in the subsequent ability of devices to provide flexibility. How can the time-dependent behavior of P2X resources be accounted for in the formulation of the metric(s) describing flexibility?

6. Flexibility requests and availability of P2X devices for providing flexibility are uncertain quantities to determine. How can the metric(s) capture this uncertainty?

7. How will such metric(s) be helpful for an FSP?

1.7. PROPOSED APPROACH

Technical modeling and simulation-based assessment form a key first step in any power and energy system analysis [27]. In the ever-changing energy landscape, the modeling and simulation approach is pervasive in determining the efficacy of a technology: studying its impact on the power grid, assessing its long-term impacts, and the usefulness of the resource itself in the short and long term on the grid, and the energy landscape. However, different users can employ different models with different level of model details for the same study, since there is no rule guiding the selection of models for a particular study. Therefore, insights generated from using different models for the same study can vary. To properly understand and quantify this, I will develop models of different P2X devices in different resolutions using Modelica modeling language. This is done for the reason that Modelica allows acausal, equation-based modeling of the physical systems. In addition, it is open source and a widely used modeling language for modeling physical systems in various industries such as energy and automobile. The development of these models and accompanying studies will provide important insights on why model detail is needed, addressing the first two research questions.

For the research objective, which is centered around developing metrics for flexibility assessment, I take inspiration from the power systems planning and operations domain. The system operator performs studies such as transmission expansion planning, and generation adequacy [28, 29] to determine the expansion plan of the grid and adequacy of generation capacity to service an expected load demand in the future. These studies employ specific metrics designed to "quantify performance of the power system" operation under different conditions and guide the system operator's decision-making process. Examples of these metrics are Loss of Load Expectation (LOLE) and Expected Unserved Energy (EUE). LOLE describes the expected number of hours when a given generation capacity will not serve the load. This information helps the TSO determine if the generation amount is adequate for the forecasted demand.

Similarly, EUE uses the forecasted data for a given time horizon (typically, a year) and calculates the expected amount of energy that would not be served with the given generation portfolio. The TSO uses these metrics extensively in generation planning and network expansion planning. The usage of these metrics is shown in Fig. 1.4.

A similar approach with appropriate metrics can also benefit the FSP. These metrics would serve as a measure for the FSP to quantify available flexibility, enabling it to maximize available flexibility from the portfolio. This requires investigation of the abilities and limits of the existing metrics, identification of requirements for a useful flexibility metric, and derivation of such a metric.

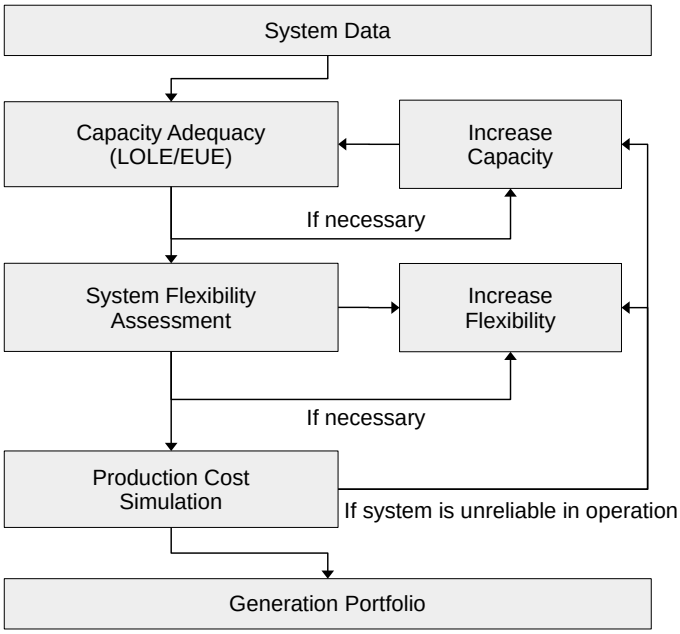

Figure 1.4: Traditional generation expansion planning process adopted by the system operator. Metrics quantifying power system performance play an important role in guiding the decision-making process of the system operator to plan the grid expansion. Taken from [7]

1.8. RESEARCH CONTRIBUTIONS

The main contribution of this thesis is to provide a thorough discussion on flexibility in the context of integrated energy systems and to enrich the current knowledge on flexibility available to power systems from the integration of energy sectors. More specifically, for the first time ever, this thesis introduces metrics that help to assess the flexibility of a portfolio of flexible energy resources. The distinguishing feature of the proposed metrics is that they explicitly consider the operational limitations of the coupling P2X device as well as the constraints in the coupled energy sector. This consideration is absent from current metrics.

During this thesis, along with several M.Sc. student contributions, models of various P2X devices (of various modeling resolutions) were developed and analyzed in a synthetic test case setting. The developed models, grid networks, and other research output is made publicly available for reuse and extension with an open source license. During this research project, I also developed software packages to assist in developing, simulating, and optimizing integrated energy systems. These include:

- ENERGYSIM: A modular co-simulation tool to simplify the setup and analysis of multi-energy system cosimulation
- DELMOD: A Modelica library designed to assist in the modeling of Smart Grids.

1.9. SOFTWARE TOOLS

This thesis used only open-source modeling languages and tools to describe various physical systems. Specifically, I have employed OpenModelica to describe physical processes and understand the dynamics of physical systems. OpenModelica is an open-source modeling tool based on the Modelica language. The Modelica language provides an acausal way to describe equations governing the behavior of a process. It is used extensively in various fields of study, including thermal systems, fluid dynamics, automotive design, control systems, and electrical power systems. For assessing electric power systems, I use Python programming language. Specifically, I employ the use of the pandapower package. Unless specified otherwise, the models, algorithms, and simulation frameworks used or developed in this thesis use open-source software.

1.10. OUTLINE OF THESIS

Chapter 2 is dedicated to modeling P2X devices to investigate the role model resolution plays in flexibility assessment studies. In this chapter, I develop detailed and simplified models of various P2X technologies, which are then embedded in

different power system flexibility assessment studies to evaluate the additional value that detailed models offer over simplified models. I also evaluate the impact these insights have on not only the device but also on the system itself.

In Chapter 3, I introduce a co-simulation toolchain for simulation-based assessment of integrated energy systems. After highlighting the usefulness of using detailed models of P2X devices, this toolchain combines these models, which could be developed in mature, domain-specific software and solved using state-of-art solvers. I motivate the reasons for the development of ENERGYSIM and its feature set, which differentiates it from current co-simulation tools. An example is provided where I showcase the usefulness of ENERGYSIM to conduct a multi-stakeholder, flexibility assessment study using a detailed model of power-to-gas hydrogen electrolyzer.

Once the role of modeling and simulation is established, and their relevance is placed in the context of flexibility assessment, I shift focus to quantification of flexibility. In Chapter 4, I take the perspective of an FSP controlling a portfolio of flexible energy resources. I evaluate currently used metrics for flexibility assessment in literature, arguing against their accuracy, especially for quantifying short-term operational flexibility. The limitation of the most prominent method, which uses Minkowski Summation for assessing flexibility, is analytically shown to be inaccurate. Here, I propose a simulation-based approach for more accurate quantification of short-term operational flexibility. Taking inspiration from the metrics used in determining the power system's resource adequacy, I specify the requirements for appropriate metric(s) for assessing flexibility and the method to derive and interpret them.

Chapter 5 demonstrates the applicability of the simulation-based approach and the proposed flexibility metrics using two case studies. Examples in the two case studies are designed so that the usefulness of the proposed metrics to an FSP is clearly and easily visible. The examples consider the most common power system issues which require flexibility, namely, renewable forecasting errors and congestion in the distribution grid. Further, results from the proposed method are compared with the Minkowski Summation method to illustrate the differences in quantified flexibility. For each of the two examples, I provide qualitative and quantitative discussion on the value of the proposed method and metrics for the FSP.

Finally, in Chapter 6, I present a discussion on the research, results obtained in this thesis, and conclusions. I highlight the gaps that remain to be researched and provide ideas for future research on the topic of flexibility in integrated energy systems.

BIBLIOGRAPHY

[1] *StatLine*. https://opendata.cbs.nl/statline/#/CBS/en/.

[2] Antti Alahäivälä et al. "A Virtual Power Plant for the Aggregation of Domestic Heating Load Flexibility". In: *IEEE PES Innovative Smart Grid Technologies, Europe*. Oct. 2014, pp. 1–6. DOI: 10.1109/ISGTEurope.2014.7028861.

[3] Sannamari Pilpola and Peter D. Lund. "Different Flexibility Options for Better System Integration of Wind Power". In: *Energy Strategy Reviews* 26 (Nov. 2019), p. 100368. ISSN: 2211-467X. DOI: 10.1016/j.esr.2019.100368.

[4] Jos Sijm et al. "Energy Transition Implications for Demand and Supply of Power System Flexibility: A Case Study of the Netherlands Within an EU Electricity Market and Trading Context". In: *The European Dimension of Germany's Energy Transition: Opportunities and Conflicts*. Ed. by Erik Gawel et al. Cham: Springer International Publishing, 2019, pp. 363–394. ISBN: 978-3-030-03374-3. DOI: 10.1007/978-3-030-03374-3_21.

[5] Ming Jin et al. "MOD-DR: Microgrid Optimal Dispatch with Demand Response". In: *Applied Energy* 187 (Feb. 2017), pp. 758–776. ISSN: 0306-2619. DOI: 10.1016/j.apenergy.2016.11.093.

[6] Eamonn Lannoye et al. "Assessing Power System Flexibility for Variable Renewable Integration: A Flexibility Metric for Long-Term System Planning". In: *CIGRE Science and Engineering Journal* 3 (Oct. 2015), pp. 26–39. ISSN: 2426-1335.

[7] Eamonn Lannoye, Damian Flynn, and Mark O'Malley. "Evaluation of Power System Flexibility". In: *IEEE Transactions on Power Systems* 27.2 (May 2012), pp. 922–931. ISSN: 1558-0679. DOI: 10.1109/TPWRS.2011.2177280.

[8] Lin Zhao et al. "A Geometric Approach to Aggregate Flexibility Modeling of Thermostatically Controlled Loads". In: *IEEE Transactions on Power Systems* 32.6 (Nov. 2017), pp. 4721–4731. ISSN: 0885-8950, 1558-0679. DOI: 10.1109/TPWRS.2017.2674699.

[9] Jinye Zhao, Tongxin Zheng, and Eugene Litvinov. "A Unified Framework for Defining and Measuring Flexibility in Power System". In: *IEEE Transactions on Power Systems* 31.1 (Jan. 2016), pp. 339–347. ISSN: 1558-0679. DOI: 10.1109/TPWRS.2015.2390038.

[10] Andreas Ulbig and Göran Andersson. "Analyzing Operational Flexibility of Electric Power Systems". In: *International Journal of Electrical Power & Energy Systems*. The Special Issue for 18th Power Systems Computation Conference. 72 (Nov. 2015), pp. 155–164. ISSN: 0142-0615. DOI: 10.1016/j.ijepes.2015.02.028.

[11] P. Staudt et al. "Analysis of Redispatch and Transmission Capacity Pricing on a Local Electricity Market Setup". In: *2017 14th International Conference on the European Energy Market (EEM)*. June 2017, pp. 1–6. DOI: 10.1109/EEM.2017.7981959.

[12] Jos Sijm et al. "The Demand for Flexibility of the Power System in the Netherlands, 2015-2050". In: (), p. 140.

[13] Marissa Hummon et al. *Fundamental Drivers of the Cost and Price of Operating Reserves*. Tech. rep. NREL/TP-6A20-58491. National Renewable Energy Lab. (NREL), Golden, CO (United States), July 2013. DOI: 10.2172/1220216.

[14] Shadi Goodarzi, H. Niles Perera, and Derek Bunn. "The Impact of Renewable Energy Forecast Errors on Imbalance Volumes and Electricity Spot Prices". In: *Energy Policy* 134 (Nov. 2019), p. 110827. ISSN: 0301-4215. DOI: 10.1016/j.enpol.2019.06.035.

[15] *Annual Market Update 2020 - Electricity Market Insights*. Apr. 2021.

[16] Zhongkai Yi et al. "A Multi-Time-Scale Economic Scheduling Strategy for Virtual Power Plant Based on Deferrable Loads Aggregation and Disaggregation". In: *IEEE Transactions on Sustainable Energy* 11.3 (2019), pp. 1332–1346. DOI: 10.1109/TSTE.2019.2924936.

[17] Zheng Ma, Joy Dalmacio Billanes, and Bo Nørregaard Jørgensen. "Aggregation Potentials for Buildings—Business Models of Demand Response and Virtual Power Plants". In: *energies* 10.10 (2017), p. 1646. DOI: 10.3390/en10101646.

[18] Marialaura Di Somma, Giorgio Graditi, and Pierluigi Siano. "Optimal Bidding Strategy for a DER Aggregator in the Day-Ahead Market in the Presence of Demand Flexibility". In: *IEEE Transactions on Industrial Electronics* 66.2 (Feb. 2019), pp. 1509–1519. ISSN: 1557-9948. DOI: 10.1109/TIE.2018.2829677.

[19] *Peeeks - Eneco*. https://www.eneco.nl/over-ons/wat-we-doen/duurzame-bronnen/peeeks.

[20] Peter Palensky and Dietmar Dietrich. "Demand Side Management: Demand Response, Intelligent Energy Systems, and Smart Loads". In: *IEEE Transactions on Industrial Informatics* 7.3 (Aug. 2011), pp. 381–388. ISSN: 1941-0050. DOI: 10.1109/TII.2011.2158841.

[21] Lori Aniti. *Demand-Side Management Programs Save Energy and Reduce Peak Demand - Today in Energy - U.S. Energy Information Administration (EIA)*. https://www.eia.gov/todayinenergy/detail.php?id=38872.

[22] Doug Hurley. *Demand Response as a Power System Resource*. Tech. rep. Synapse Energy, May 2013, p. 99.

[23] Sung-Won Park and Sung-Yong Son. "Interaction-Based Virtual Power Plant Operation Methodology for Distribution System Operator's Voltage Management". In: *Applied Energy* 271 (Aug. 2020), p. 115222. ISSN: 0306-2619. DOI: 10.1016/j.apenergy.2020.115222.

[24] Mohammad Ali Fotouhi Ghazvini et al. "Congestion Management in Active Distribution Networks through Demand Response Implementation". In: *Sustainable Energy, Grids and Networks* 17 (Mar. 2019), p. 100185. ISSN: 2352-4677. DOI: 10.1016/j.segan.2018.100185.

[25] A. N. M. M. Haque et al. "Demand Response for Real-Time Congestion Management Incorporating Dynamic Thermal Overloading Cost". In: *Sustainable Energy, Grids and Networks* 10 (June 2017), pp. 65–74. ISSN: 2352-4677. DOI: 10.1016/j.segan.2017.03.002.

[26] Hanne Saele and Ove S. Grande. "Demand Response From Household Customers: Experiences From a Pilot Study in Norway". In: *IEEE Transactions on Smart Grid* 2.1 (Mar. 2011), pp. 102–109. ISSN: 1949-3061. DOI: 10.1109/TSG.2010.2104165.

[27] M. Kezunovic et al. "The Role of Digital Modeling and Simulation in Power Engineering Education". In: *IEEE Transactions on Power Systems* 19.1 (Feb. 2004), pp. 64–72. ISSN: 1558-0679. DOI: 10.1109/TPWRS.2003.821002.

[28] Saeed Zolfaghari Moghaddam. "Generation and Transmission Expansion Planning with High Penetration of Wind Farms Considering Spatial Distribution of Wind Speed". In: *International Journal of Electrical Power & Energy Systems* 106 (Mar. 2019), pp. 232–241. ISSN: 0142-0615. DOI: 10.1016/j.ijepes.2018.10.007.

[29] Simon Tindemans and Goran Strbac. “Accelerating System Adequacy Assessment Using the Multilevel Monte Carlo Approach”. In: *arXiv:1910.13013 [cs, eess, stat]* (Apr. 2020). arXiv: 1910.13013 [cs, eess, stat].

2

Modeling Flexible Energy Resources

2.1. Introduction

As stated previously, P2X technology is a viable source to supply the increasing demand for power system flexibility [3, 4]. By integrating P2X into the electrical power systems, P2X devices can absorb over- and under-generation VRES by modulating their power consumption. Using storage systems as buffers, such a flexible operation of P2X can provide ample opportunities for effective demand side management [5, 6]. A detailed technical assessment is usually needed to properly assess the value of these technologies as sources of flexibility for electric power systems. Modeling and simulation form the first step in such a technical assessment. The availability of representative models of components and systems is vital in this process, and so, the importance of modeling cannot be understated.

Models for assessing flexibility from P2X devices can generally be divided into three broad categories. In the first category, the most common one, studies look at the problem of P2X device integration into the grid from the perspective of the electrical grid operator. Typically, in electrical power system modeling and simulations, loads are modeled with Eq. (2.1). This equation describes the dependence of electrical power demand of a load in Watts as a function of the voltage and change in frequency at the connected bus bar [7]. Load models described by Eq. (2.1) are one-dimensional, i.e., modeled from the electrical grid operator perspective.

Parts of this chapter have been published in IEEE PowerTech 2019 [1], ISIE 2020 [2], and ISGT NA 2022.

$$P = P_0 \cdot \left[P_1 \left(\frac{V}{V_0} \right)^2 + P_2 \left(\frac{V}{V_0} \right)^1 + P_3 \left(\frac{V}{V_0} \right)^0 \right] (1 + L_{DP} \Delta f) \tag{2.1}$$

P2X resources are therefore modeled as a simplified power system static load model described by Eq. (2.1). In [8], the electrolyzer is used as a fast ramping resource to provide frequency regulation. Here, the authors focus on assessing the electrolyzer's ability to help the grid frequency. Hence, the electrical grid is modeled in detail, while the electrolyzer system is a static load model with a high ramp rate characteristic. Similarly, in [9], the authors focus solely on the applicability of an intelligently controlled hydrogen electrolyzer and fuel cell to provide voltage stability and transient stability for the DC power grid. Therefore, voltage control and grid transient control models are prioritized, whereas the electrolyzer model is simplified.

The second category includes studies that focus strongly on device physics, ignoring the grid entirely. For example, in [10], the author assesses the utilization of the PEM electrolyzer and fuel cell and quantify the PEM cell's energy efficiency sensitivity to operating temperature, current density, electrolyte thickness, and electrode catalytic activity. The detailed electrolyzer cell model can also provide insights into how the device will behave when provided with renewable solar and wind power for hydrogen generation. The model of the grid or the renewable technologies are not presented.

The third category includes studies where the focus is put on energy carrier coupling via P2X devices. Here, the discussions on the multi-energy system tend to ignore the P2X device completely, treating them as ideal energy converters. This is reflected in concepts such as the energy hub proposed in [11] to assess multiple energy carriers. Here, the P2X devices linking the energy carriers are represented as a transformation matrix consisting of energy efficiency factors. The insufficient detail in modeling P2X resources is an issue with the energy hub approach to assessing multi-energy systems.

It has been shown in [12] that simplifications in the modeling of components and systems can limit the accuracy of the results obtained from such analysis. In each category described above, there is either a lack or an excess of detail in the modeling effort. This can lead to a system representation where dynamic system interactions between system components are absent, and linearization of important non-linear characteristics of physical systems is incorrectly done.

OUTLINE OF CHAPTER

In the following sections, I provide examples and case studies to motivate, illustrate, and quantify the need and use of detailed models. The first section quantifies the difference between simplified and detailed models. Using a P2H electric

heat pump and a P2G electrolyzer system, I compare the two levels of model detail — low and high — to establish the motivation for using detailed models. In the second section, I delve deeper into using such detailed models to assess these devices. Using examples of an integrated electric boiler and storage tank system, and an electrolyzer system, I investigate the factors influencing the flexibility available to these P2X devices. I also derive conclusions for the level of detail to be included for modeling P2X devices in energy system analyses.

2.2. THE NEED FOR DETAILED MODELS

An issue with existing studies assessing the viability of P2X devices in current and future energy systems is that available models and methods in the literature [5, 13, 14] make significant simplifications on physical characteristics of these P2X devices. This is particularly true considering the impacts of operational temperature and pressure conditions on device performance in P2H electric heat pumps and P2G electrolyzer systems. Authors in [15–17] employ simplified and generic representations such as equations with constant relation between the power input and energy output of P2X, often using an averaged value of efficiency or coefficient of performance available from manufacturer's data as models to represent these technologies. Using the characteristics published in the manufacturer's data sheet for these devices can be helpful in obtaining a high-level indication of the applicability of these devices. Manufacturers calculate these metrics by considering operation under ideal conditions and averaging results over test periods, such as seasonally or yearly (commonly seen with the heat pump's coefficient of performance (COP)). From the manufacturer's point of view, it is more important to show that the device's overall characteristics and performance comply with the regulation in place for the device. Therefore, these systems are characterized in their datasheet by overarching statistics such as average efficiency and average COP. In reality, however, the performance of a P2X device is complex. It depends on operational conditions such as ambient temperature and pressure values within the device, among many other variables. Using the aforementioned simplified representations and averaged values for modeling purposes in a simulation-based technical analysis, especially from a user perspective (as opposed to a manufacturer perspective), will impact the results of such studies. This could result in incorrect estimates of operational costs and miscalculation of required capacity [18]. When P2X devices are even more pervasive in the energy landscape, the impact of these erroneous assessments could be higher for the user.

Therefore, in this section, I investigate the P2X technologies — P2G electrolyzer and P2H electric heat pump to evaluate the differences in simplified and detailed models. Mainly, I investigate the impact of simplifying temperature dy-

namics on the characteristics of both the P2H and P2G devices. The simplified models are referred to as *Model A* while the detailed models are referred to as *Model B* in the following sections.

2.2.1. THE HYDROGEN ELECTROLYZER SYSTEM

P2G electrolyzers use electrical current to split water molecules to produce hydrogen and oxygen. In this example, I model an electrolyzer cell that forms the core component of a large electrolyzer system. The considered system has a capacity of 50 MW and is a proton-exchange membrane (PEM) electrolyzer. It is assumed that electrolyzer cells are assembled into stacks and connected in series and parallel configurations. It is also assumed that the scaled electrolyzer system consisting of stacks of electrolyzer cells behaves precisely similarly to a single electrolyzer stack. Four physical domains are modeled: electrochemical, pressure, mass flow, and thermal. Each sub-model has input and output variables connected as illustrated in Fig. 2.1.

ELECTROCHEMICAL MODEL

The electrolyzer cell voltage is given by Eq. (2.2). It is composed of open circuit voltage and associated overpotentials. The open-circuit voltage is necessary to start the water electrolysis reaction under ideal conditions, while the overpotentials are needed to model the energy losses within the PEM cell stack.

$$V_{\text{cell}}(\theta) = V_{\text{ocv}}(\theta, p) + V_{\text{act}}(\theta) + V_{\text{ohm}}(\theta) + V_{\text{conc}}(\theta) \tag{2.2}$$

Here, V_{ocv} is the open-circuit voltage and is dependent on the temperature (θ) and pressure (p) in the cell. V_{act} is the activation overpotential, depending only on the temperature. It is the dominant overpotential at low current densities and is modeled using Eq. (2.3).

$$V_{\text{act}} = \frac{R \cdot \theta_{\text{op}}}{2 \cdot \alpha_{\text{an}} \cdot F} \cdot asinh\left(\frac{\lambda_{\text{dens}}}{2 \cdot \lambda_{0,\text{an}}}\right) \tag{2.3}$$

Here, λ_{dens} is the electric current density of stack electrodes expressed in A/m^2, $\lambda_{0,\text{an}}$ is the exchange current density (for the considered platinum electrodes, $\lambda_{0,\text{an}} = 1.0205E-3$), α_{an} is the charge transfer coefficient of the anode and is calculated experimentally [19], θ_{op} is the stack operating temperature, R is the ideal gas constant, and F is Faraday's constant.

V_{ohm} in Eq. (2.2) is ohmic overpotential which is necessary to model the energy loss due to resistance of the cell membrane. It dominates at nominal current densities and is calculated using Eq. (2.4).

$$V_{\text{ohm}} = R_{\text{mem}} \cdot \lambda_{\text{d}} \tag{2.4}$$

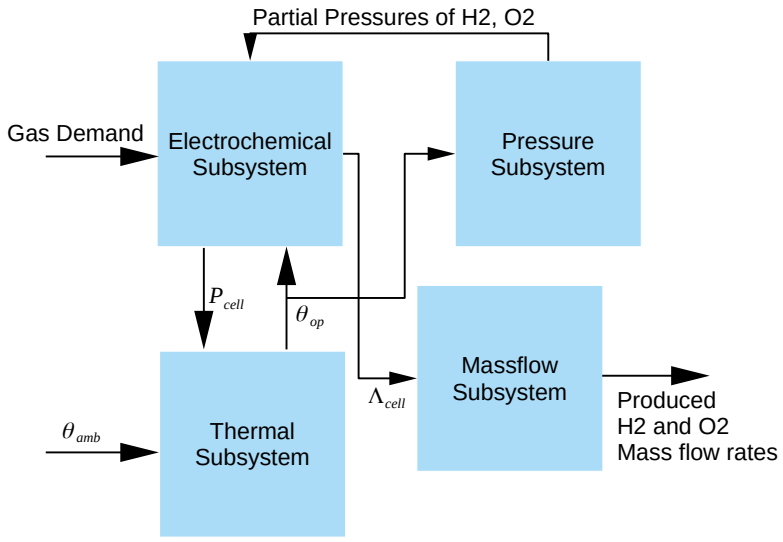

Figure 2.1: Block diagram of the electrolyzer model developed in OpenModelica with thermal dependencies between various subsystem models. The electrochemical subsystem model takes as input the gas demand, partial pressure of gases produced in the cell (calculated in pressure subsystem model), and the operating temperature of the cell (calculated in thermal subsystem model) and outputs quantities Eqs. (2.2) to (2.7). The thermal subsystem model takes as input the ambient temperature (θ_{amb}) and cell power (P_{cell}) and outputs the operational temperature of the cell. The pressure subsystem model takes as input operating temperature of the cell and outputs the partial pressure of the produced gases. The massflow subsystem model takes as input the cell current (Λ_{cell}) (calculated in the electrochemical subsystem model) and outputs the gas flow rates for hydrogen and oxygen produced in the cell. Each subsystem model depends directly or indirectly on the operational temperature, which further depends on the ambient temperature. To compare simple and detailed models, for Model A, θ_{amb} is set constant, while for Model B, θ_{amb} is variable.

Here, R_{mem} is membrane resistance. The temperature dependence of membrane conductivity can be modeled using the Arrhenius expression as shown in [20]. Finally, V_{conc} is concentration (saturation) overpotential which occurs when the electrolysis reaction is fast, and the mass transport is relatively slow. Its effect is dominant at very high current densities. Concentration overpotential is ignored in this study, assuming nominal cell current never reaches high current densities that concentration overpotential is dominant.

Over time, especially with dynamic use, the wear and tear of the electrolytic cell membrane is inevitable. This results in an increase in the ohmic overpotential in PEM cells over time as electrolysis goes on. According to [21], the ohmic overpotential increases approximately at the rate of 2-3 μV/hr for the duration of its lifetime.

The electrolyzer cell current Λ_{cell} and active power consumption P_{cell} is calculated using Eqs. (2.5) and (2.6).

$$\Lambda_{\text{cell}} = A_{\text{mem}} \cdot \lambda_{\text{dens}} \tag{2.5}$$

Here, A_{mem} in Eq. (2.5) is the membrane area. The power consumption of the cell is given by Eq. (2.6), which is a product of cell current and voltage. The cell efficiency η is calculated using Eq. (2.7).

$$P_{\text{cell}} = \Lambda_{\text{cell}} \cdot V_{\text{cell}} \tag{2.6}$$

$$\eta = \frac{V_{\text{ocv}}}{V_{\text{cell}}} \tag{2.7}$$

PRESSURE MODEL

The input of the pressure sub-model is stack operation temperature θ_{op}, and the output is the partial pressures of water, hydrogen, and oxygen as described in Eq. (2.8).

$$pp_{\text{H2O}} = 6.1078.10^{-3} \cdot exp\left(17.2694 \cdot \frac{\theta_{\text{op}} - 273.15}{\theta_{\text{op}} - 34.85}\right) \tag{2.8}$$

Here, pp_{H2O} is the partial pressure of water and is calculated using the empirical expression in [19],

MASSFLOW MODEL

The massflow sub-model describes the mass flow rates in electrolysis cell with Eqs. (2.9) and (2.10). The input of this sub-model is cell current calculated in the electrochemical sub-model, η_f is the Faraday efficiency and is assumed to be 1, n_{cells} is the number of electrolyzer cells.

$$\dot{n}_{H_2} = \frac{n_{\text{cells}} \cdot \Lambda_{\text{cell}}}{2 \cdot F} \cdot \eta_f \tag{2.9}$$

$$\dot{n}_{O_2} = \frac{n_{\text{cells}} \cdot \Lambda_{\text{cell}}}{4 \cdot F} \cdot \eta_f \tag{2.10}$$

THERMAL MODEL

The electrochemical, pressure, and massflow sub-models are the same for both Model A, and Model B. In Model B, the thermal domain is taken into account using a lumped thermal capacitance model. The temperature of the electrolyzer system is modeled with Eq. (2.11).

$$C_{\text{th}} \frac{d\theta}{dt} = P_{\text{th,el,h}} + W_{\text{pum,l}} - P_{\text{th,c}} - P_{\text{th,l}}(\theta) - \sum_{\text{j}} \dot{n}_{\text{j}} \cdot \Delta h_{\text{j}} \tag{2.11}$$

Here, C_{th} is the lumped thermal capacity of the cell. The first term on the right side, $P_{\text{th,el,h}}$, describes the heat lost during the electrolysis reaction, and it depends on cell voltage and current. The second term, $W_{\text{pum,l}}$ represents the heat losses by the circulation pump. The third term, $P_{\text{th,c}}$, represents the heat removed by the heat exchanger, and it has a linear relation with the consumed active power. The fourth term, $P_{\text{th,l}}$, is for the heat lost to ambient, and it depends on operational temperature θ_{op} and ambient temperature θ_{amb}. The last term comes from enthalpy lost with the products leaving the system (which can be seen as sensible heat leaving the system), and it has an empirical equation that depends on the operating temperature. For more details, reader is referred to [22]. Eqs. (2.2) to (2.6) and (2.8) to (2.10) describe Model A. Adding thermal dynamic sub-model described in Eq. (2.11) to Model A creates a non-linear, dynamic Model B of the electrolyzer system where each sub-model depends on the temperature parameter directly or indirectly.

2.2.2. THE ELECTRIC HEAT PUMP SYSTEM

Electric Heat Pumps are devices that use electric energy to transport heat from a colder to a hotter region. These systems are characterized by a parameter called the coefficient of performance or COP. The COP of a heat pump reflects its ability to transfer heat. As opposed to efficiency, the COP is a value that is always greater than 1. The reader is directed to [23] for more information on this. The coefficient of performance (COP) of an electric heat pump depends on the choice of refrigerant and the Rankine cycle efficiency (Carnot efficiency) of the refrigerant inside the heat pump, as described in Eq. (2.12).

$$COP = \frac{P_{\text{th}}}{P} \tag{2.12}$$

Here, P_{th} is the thermal power (heat flow) output, and P is the electrical power consumed by the heat pump. In this section, the refrigerant used for modeling is R134a, a common refrigerant in heat pumps. Again, two models are developed — Model A representing a simplified model and Model B representing a more dynamic and complex model which depends on the ambient temperature. Model A uses a constant COP and has no dependency on ambient temperature. It is described with Eq. (2.13).

$$P = \frac{P_{\text{th}}}{COP^{\text{avg}}} \tag{2.13}$$

The COP strongly depends on the source or inlet temperature. In this example, I assume that the inlet temperature of the fluid is equal to ambient temperature. Using the pressure-enthalpy table of R134a, COP values are calculated for various θ_{amb} conditions. This data set of COP and θ_{amb} is then used to create a fifth order polynomial function of COP that depends on ambient temperature, as shown in Eq. (2.14). Eq. (2.14) is then used to calculate the power consumption of the heat pump as shown in Eq. (2.15). Eq. (2.14) and Eq. (2.15) represent Model B of the heat pump.

$$\begin{aligned} COP^{\text{real}}(\theta_{\text{amb}}) = a_1\theta_{\text{amb}}^5 + a_2\theta_{\text{amb}}^4 + \\ a_3\theta_{\text{amb}}^3 + a_4\theta_{\text{amb}}^2 + a_5\theta_{\text{amb}} + a_6 \end{aligned} \tag{2.14}$$

$$P_{\text{el}} = \frac{P_{\text{th}}}{COP^{\text{real}}(\theta_{\text{amb}})} \tag{2.15}$$

Using curve fitting functionality in Python [24], the coefficients a_1, a_2, a_3, a_4, a_5, a_6 of Eq. (2.14) are calculated to 3.46E-8, 1.29E-6, 4.35E-5, 2.387E-3, 1.186E-1, and 5.063 respectively. Eq. (2.14) with aforementioned coefficients therefore represents COP-θ_{amb} curve for any heat pump using R134a refrigerant.

2.2.3. STUDY CASE

Model A and Model B of each technology are given the same demand profiles to compare the two models. Corresponding to this demand specification, both models' active power consumption is noted and compared.

GENERATING DEMAND PROFILES

The gas demand for the electrolyzer is assumed to come from an industrial process, whereas the heat demand for the P2H heat pump comes from district heating. This assumption is valid since most applications of electrolyzers are found in an industrial setting, whereas heat pumps, especially large heat pumps, find applications in district heating.

Without real-world data, artificial demand profiles need to be generated. To generate these artificial demand profiles for each P2X models, the approach adopted in reference [25] is used. The benefit of this approach is that it only requires historical ambient temperature data to generate the time-series scheduled energy demand profiles. Equation (2.16) describes the model in reference [25]. Here, $P_{th,dem}$ is the heat demand but can also be replaced by $H2_{dem}$ to obtain gas demand.

$$P_{\text{th,dem}}(t) = P_{\text{th,base}} + \frac{P_{\text{th,max}} - P_{\text{th,base}}}{\theta_{\text{ref}} - \theta_{\text{min}}} \cdot max(0,\ \theta_{\text{ref}} - \theta(t)) \tag{2.16}$$

Piecewise linear temperature dependency of heat demand ($P_{\text{th,dem}}$) (hydrogen demand $H2_{\text{dem}}$) in equation 2.16 is illustrated in Fig. 2.2. Here, $P_{\text{th,base}}$ ($H2_{\text{base}}$) is the base demand, which occurs at temperatures above the reference temperature θ_{ref}. Variable $P_{\text{th,max}}$ ($H2_{\text{max}}$) represents maximum heat (hydrogen) demand, corresponding to the minimum ambient temperature θ_{min}. The demand in district heating networks is certainly sensitive to ambient temperature changes. On the other hand, industrial hydrogen demand is expected to be less dependent on ambient temperature. Therefore, the slope of the linear line in figure Fig. 2.2 is larger for power-to-heat than power-to-gas. This means industrial hydrogen demand has fewer variations with respect to varying ambient temperature than district heating demand. Values of the parameter are shown in table 2.1 and are taken directly from [26].

	Industrial P2G	**District Heating P2H**
$\theta_{\text{ref}}[°C]$	25	25
$\theta_{\text{min}}[°C]$	5	5
Base Demand $[m^3/s]$	3.13E-3	3
Max Demand $[m^3/s]$	3.85E-3	4

Table 2.1: Ambient temperature - demand relation parameters

To conduct the experiment, set points from demand profile and temperature values to both the models are provided for 7 representative days. For the electrolyzer system, Model A is given a constant temperature input, while Model B

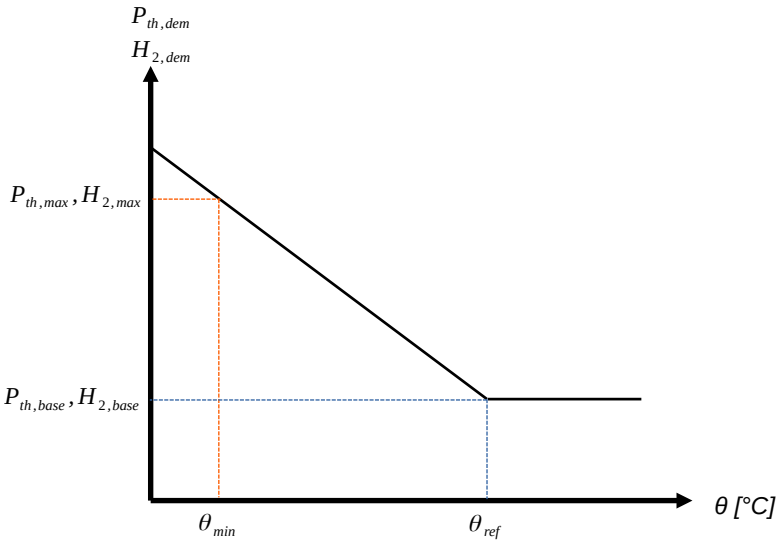

Figure 2.2: The relationship between ambient temperature and hydrogen and heat demand (taken from [25]) was used to model the demand for this experiment.

is given a variable temperature input Fig. 2.3. For the heat pump system, Model A is given a daily average temperature input, while Model B is given an hourly temperature time series.

2.2.4. RESULTS AND DISCUSSION

The effect of operational temperature evolution on the efficiency curve of the electrolyzer and ambient temperature evolution on COP of the heat pump can be observed in figures 2.4 and 2.6 respectively.

The efficiency plots of the two models are shown in Fig. 2.4. It is observed that due to the temperature deviation, the maximum efficiency difference between the two models is 0.6%.

Figure 2.5 shows the power consumption of the electrolyzer Model A and Model B corresponding to the gas demand provided as input. The maximum power consumption difference between them is 0.4 MW for a 50 MW electrolyzer system. This corresponds to 0.8% of the total capacity. This can represent a significant deviation for power system applications requiring precise power consumption knowledge, such as for frequency response. This is compounded when the number of units providing this service increases. On the other side, such deviations also impact the design and sizing of the auxiliary units for temperature regulation within the electrolyzer system. For example, consider the cooling system. If the cooling capacity of the designed system is calculated to be less than

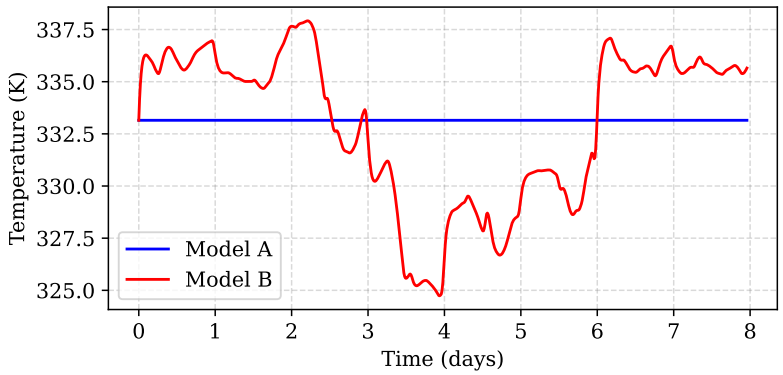

Figure 2.3: The calculated operating temperature of the electrolyzer cell in Model A and Model B. For Model A, the equation determining relationship between θ_{amb} and θ_{op} is removed, resulting in a constant θ_{op} throughout the simulation time, while for Model B, an hourly variable θ_{amb} is provided, which consequently generates a variable θ_{op} used by other subsystem models.

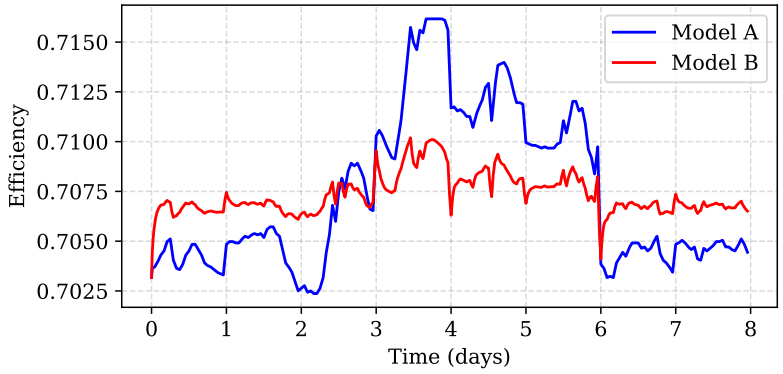

Figure 2.4: Efficiency characteristics of the electrolyzer Model A and Model B corresponding to the θ_{op}.

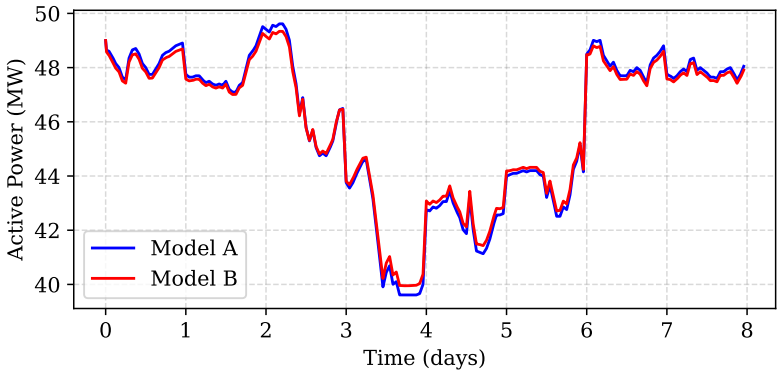

Figure 2.5: Power consumption characteristics of electrolyzer system based on efficiency characteristics. The differences between the outputs of the two models substantiate the importance of using detailed models considering thermal dynamics.

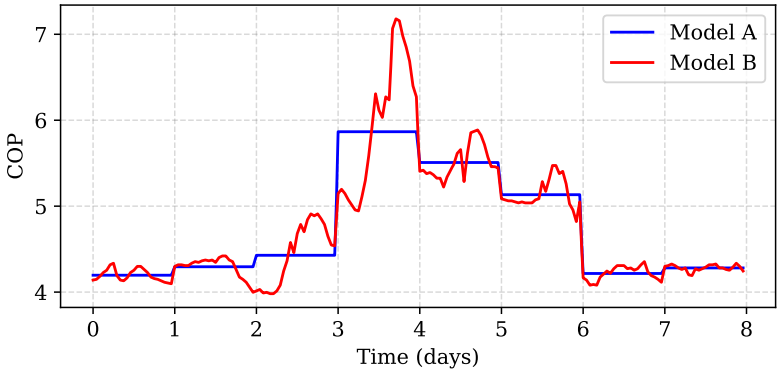

Figure 2.6: Coefficient of Performance (COP) values for heat pump Model A and Model B. Significant deviations between the COP characteristics of the two models can be seen.

required, it would lead to more considerable temperature differences between Model A and Model B. This would result in an even more significant deviation in the calculated and actual efficiency of the system.

Figure 2.6 compares the COP of Model A and Model B. In Model A, the COP is calculated from the daily average temperature; therefore, it is constant during the day. Model B uses the hourly measured temperature to calculate the COP. The maximum difference in COP values between Model A and Model B is seen to be 1.4. These results also show that temperature considerations significantly affect the COP characterization of the examined heat pump.

Figure 2.7 compares the active power consumption of Model A and Model B of the heat pump corresponding to the heat demand profile. The maximum power consumption difference between Model A and Model B is 9 MW. This rep-

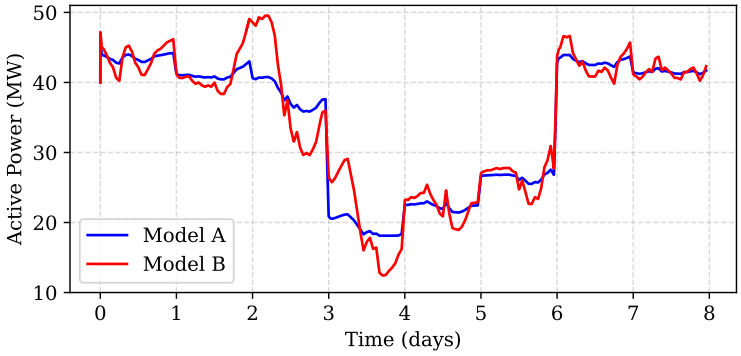

Figure 2.7: Comparison of active power consumption of heat pump Model A and Model B. A significant difference (almost 9 MW) in power consumption between Model A and Model B can be seen. These deviations can influence the contribution of this heat pump to providing power system services such as intraday load shifting and frequency response. More generally, neglecting the influence of temperature on heat pump behavior can also impact long-term economic assessment and resource sizing studies.

resents a maximum error of 18% for a 50 MW electric heat pump system. For power system services where participation from devices is required for a short interval of time, such as reducing peak load for an hour or correcting a 15-minute renewable forecast error, incorrect estimation of power consumption of the device can represent a lost economic opportunity to provide valuable flexibility.

It is clear from this experiment that detailed models offer significant advantages over simple model representations, especially when assessing their operation in the sub-hourly time scales. Now that the need for detailed models has been established, I seek to investigate the use of detailed models and explore the impact they can have on the flexible operation of the device and its consequences on the power system.

2.3. USING THE DETAILED MODELS

The previous section established the need for using detailed models over simplified ones. In this section, I delve deeper into the use of detailed models. This is shown using two examples of P2X devices — a P2H electric boiler and storage tank (EBST) system and the P2G electrolyzer system developed in Section 2.2.

2.3.1. TEMPERATURE DYNAMICS INSIDE THERMAL STORAGE TANKS

Coupling electricity and heat domains have shown to offer considerable flexibility opportunities due to the heat sector's unique characteristics [27]. Specifically, coupling thermal storage tanks with an electric boiler for temperature regulation

can provide flexibility to the power system. This is because thermal storage systems have inherent thermal inertia associated with them. Modulating the electric boiler's electrical energy input does not immediately impact the thermal dynamics of the storage system it regulates, taking minutes to hours to reflect any temperature change. This makes such systems ideal for shifting loads in time without significantly impacting operation in the coupled system.

The underlying physics of such a system is often ignored in technical assessments. Typically, such an analysis, in [28], relies on modeling the temperature dynamics using a first-order model. The temperature evolution at each time step t is obtained using Eq. (2.17).

$$\theta(t+1) = \theta(t) + \frac{P_{\text{th,in}}(t) - P_{\text{th,out}}}{\dot{m} \cdot c} \tag{2.17}$$

Here, $P_{\text{th,in}}$ is the thermal power added to the system (thermal power input) and $P_{\text{th,out}}$ is the thermal power taken out of the system (thermal power demand) at time step t, $\dot{m}$ is the mass flow rate of the fluid flowing through the system, while c is the specific heat capacitance of the flowing fluid. This model, a simplified representation of the actual system, works exceptionally well when considering small systems such as residential refrigerators. However, when large systems, such as industrial thermal storage tanks (for example, oil storage tanks in industrial areas) or building heat, air conditioning, and ventillation (HVAC) system is to be analyzed, such a representation is unsuitable [29]. Large systems require more detail in their modeling to capture complex dynamics and adequately assess the system. Modeling these dynamics can be important for an entity such as an FSP looking to flexibly operate, for example, a group of oil storage tanks in an industrial area.

In this section, I consider the example of an integrated electric boiler and storage tank (EBST) system. It represents a large thermal storage system with a height of 10 meters and a volume of 50.000 liters. It is also assumed that fluid in the tank is to be maintained at 50°C. The integrated electric boiler system has a rated power of 8 kW, and the system uses a simple on-off controller to maintain the temperature of the fluid between 49.75°C and 50.25°C. The storage tank also loses energy to the ambient environment.

As mentioned, an EBST is ideal for shifting loads in time. For the system described above, operating with an on-off control strategy, I consider the case where the EBST is required to increase its power consumption when requested. This is a practical request; for example, an increase in power consumption may be requested to correct an unexpected surplus of renewable generation. The ability of the EBST to accept this request to increase its power consumption depends on the temperature of the fluid. To evaluate this ability, I developed a first-

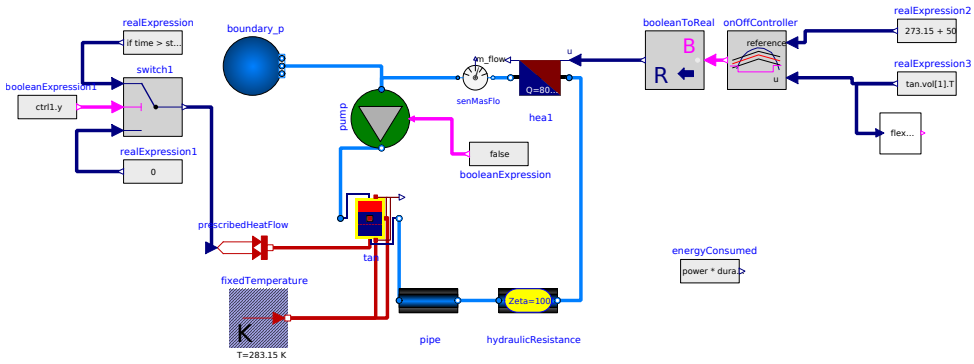

Figure 2.8: Integrated storage and boiler system model developed in OpenModelica using the AixLib. The detailed model allows us to investigate complex dynamics which cannot be captured in simple models, such as thermal stratification.

order model based on Eq. (2.17) and a more detailed model using OpenModelica and components from the thermal systems modeling library AixLib [30]. The OpenModelica model is shown in Fig. 2.8.

Figure 2.9 compares the temperature dynamics of the fluid in the EBST obtained from the two models. As can be seen, the temperature profiles obtained from the two models are very different. This means that any decision to shift the power consumption of the EBST based on the temperature of the fluid obtained from the two models will be different, too, resulting in a different estimate of the ability of such a system to provide the load shifting service.

It is of interest to investigate this extreme difference in temperature dynamics between the two models. The tank model used in the detailed representation of the EBST system includes several characteristics of the physical storage that are not present in the model described by Eq. (2.17). There is thermal stratification in a thermal storage tank such as that described in this example. At a given time, there are three zones: hotter fluid near the top, colder fluid at the bottom, and an intermediate zone known as the thermocline. This thermocline can be considered a boundary between the hotter and colder zones. When the storage is "charged," the "hotter" fluid fills from the top while simultaneously, the "colder" fluid is withdrawn from the lower side of the tank. This leads to the thermocline shifting lower. The reverse is true for "discharging". To model this phenomenon, the tank volume is discretized into smaller *segments*, or *layers* as shown in Fig. 2.10. Within each layer, the temperature of the fluid is modeled to remain constant, its dynamics evolving as it interacts with other layers. Ideally, as more layers are considered, storage behavior is closer to reality. However, computational costs are attached to considering an increasing number of layers.

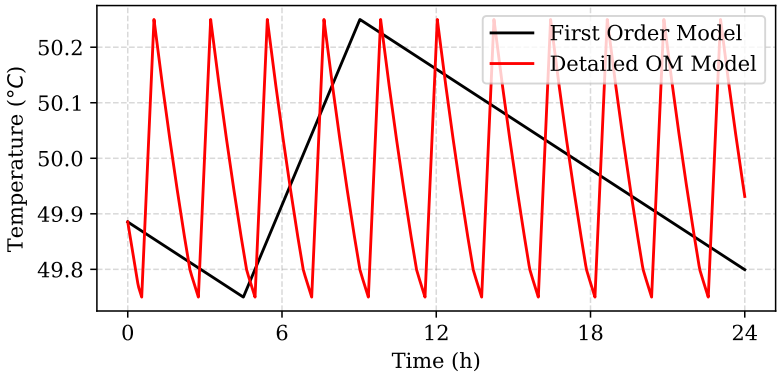

Figure 2.9: Comparing temperature dynamics of integrated storage and boiler system obtained from the first order simple model and those from a detailed model. Despite both the models being initialized with the same starting temperature, the temperature evolution dynamics from the first-order model are extremely different from the detailed model.

As is shown in Fig. 2.11, increasing the number of layers leads to an exponential increase in simulation time. In this case, I consider ten layers. The temperature is typically measured at the top of the tank.

In contrast, the first-order model considers temperature as a single parameter of the entire volume of the fluid. Hence, heating a 50.000-liter volume by 0.5°C with an 8kW heating system takes much longer than heating the top layer of the stratified thermal storage system. Therefore, to investigate the flexibility available from the integrated storage and boiler system, I use the detailed OpenModelica model.

When flexibility needs to be activated, it can be done only when the temperature of the fluid is lower than 50°C. A simple boolean controller is therefore implemented, which provides a boolean indicator depending on the fluid's temperature inside the tank when the boiler can be activated to provide flexibility (such that the fluid temperature inside the tank can be increased). In this example, the electrical boiler is activated to absorb additional energy when the boiler is turned OFF, and the fluid temperature crosses 50°C for the first time (around t = 2.8h). A sensitivity analysis is conducted by changing the duration of boiler ON operation from 0 to 60 mins in intervals of 5 mins. Figure 2.12(a) highlights the temperature profile of the boiler's top layer under nominal operation, while the temperature of fluid for three selected times: 20 mins, 40 mins, and 60 mins, can be seen in Fig. 2.12 (b,c,d) respectively.

An interesting point to note is that once the electric boiler provides flexibility, the temperature of the fluid takes some time to get back below 50°C mark. Therefore, in this period, the EBST cannot provide any flexibility. This is known as the

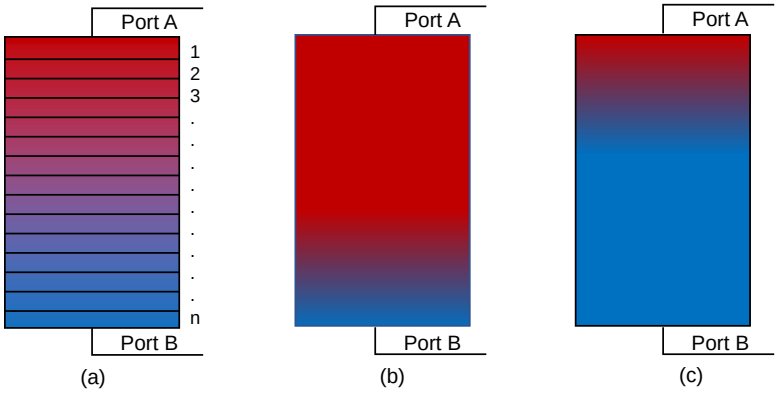

Figure 2.10: (a) A stratified thermal storage system with the presence of temperature gradient. (b) Charging the thermal storage tank moves the thermocline lower. (c) Discharging the tank moves the thermocline higher.

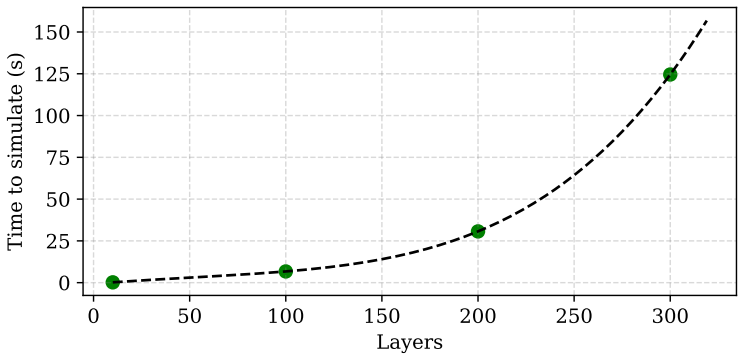

Figure 2.11: As the number of layers in the storage model is increased, the time to simulate the same experiment increases exponentially.

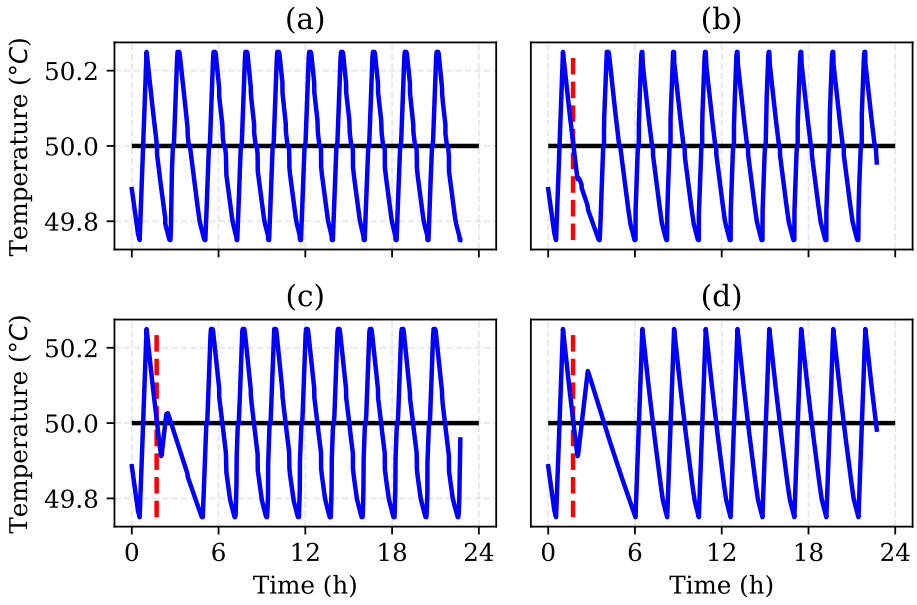

Figure 2.12: Temperature dynamics in the integrated storage and boiler system on activation of flexibility. (a) represents normal evolution temperature in the top layer of the EBST system. (b), (c) and (d) represent the scenarios when the boiler is instructed to turn ON for 20 minutes, 40 minutes, and 60 minutes respectively. The red dotted line indicates the instant when the boiler is instructed to turn ON.

rebound effect (also known as *kickback effect*), and the time for which the boiler and storage system are unavailable to provide flexibility is known as *down time*. In Fig. 2.13, the results from sensitivity analysis are plotted, illustrating the energy absorbed by the boiler and storage combination system and the downtime for this configuration.

Generally speaking, using insights from the presented example, downtime for a P2H system utilizing thermal inertia depends a lot on the time duration of the flexibility request. Other factors which impact the downtime for such systems include:

- instance of flexibility activation,
- duration of flexibility activation,
- energy and power content of the flexibility provided, for example, if instead of activating the boiler completely, it is only turned on partially,

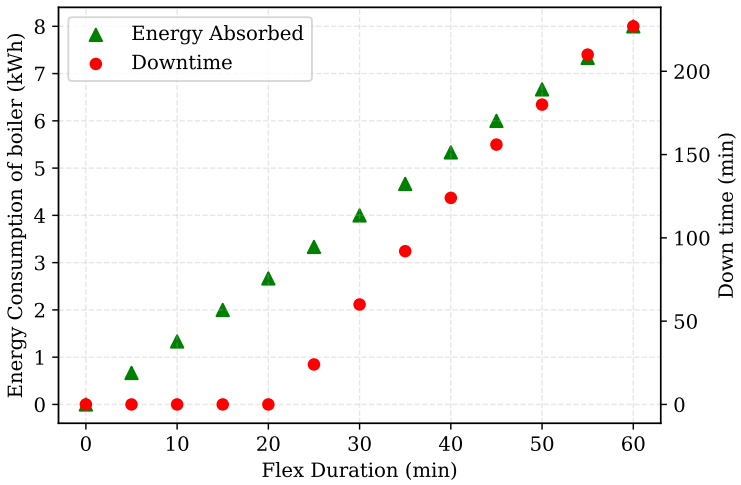

Figure 2.13: Analyzing the downtime and the energy absorbed as a function of the duration for which the EBST provides flexibility. Zero downtime depends highly on various factors such as the instance of flexibility activation, the amount of energy absorbed by the EBST, etc. These factors have been listed and discussed in the text.

- ambient temperature, for example, ambient thermal losses will be higher in winter than summer, and finally,
- control strategy, for example, a more sophisticated and advanced control scheme such as model predictive control, can control the boiler's operation to be more flexible compared to a simple rule-based control scheme used in the presented case study.

A similar collaborative study was also undertaken on thermal inertia in district heating networks to provide flexibility to the electrical power grid in [31]. Here, a detailed operational model of a district heating network was developed, including subsystem models for heat exchangers and network transport delays (standard components in large heating networks). Using a model predictive control with the developed detailed heat network model, we assessed the impact of network delays on the flexibility of the heat network to mitigate wind power forecast imbalance. We found that heat network delays due to thermal inertia played a significant role in determining the flexibility available to the electrical grid from the heat network. This insight further supports the argument for a need for detailed modeling.

In summary, in this section, I showed the use of a detailed thermal storage tank and electric boiler system model to determine factors such as downtime and

rebound effect. I showed the value of using detailed models to understand phenomena such as thermal stratification, which impacts the assessment of large thermal systems. Using simplified first-order models to represent a thermal system for large storage systems is therefore inaccurate.

2.3.2. EVALUATING ELECTROLYZER HEALTH

Detailed models can also be used to evaluate the health of the P2X system. Using the detailed electrolyzer model from Section 2.2 (Eqs. (2.2) to (2.6) and (2.8) to (2.11)), in this section, I examine the impact that provision of power system services has on the device. V-I curves are used in a laboratory setup to measure the health of an electrolyzer cell. The aim here is also to use the detailed model to generate V-I curves before and after experiments on the electrolyzer to test its health and viability as a flexibility service provider. The individual cells are assumed to be controlled quickly within 0-100% of their power range. I again assume, for simplification purposes, that the behavior and output of a single cell are not affected by other cells, and the gaseous output of a single cell and its behavior can be multiplied by the number of cells to represent a large-scale system.

For this example, nominal power of the electrolyzer is set at 10 MW, with the ability to sustain up to 150% of its rated power (15 MW) for short durations. Though a PEM electrolyzer can easily be switched OFF and ON quickly, to avoid cold-start, I set the minimum power consumption to 5 MW. This setting is due to two reasons: firstly, avoiding cold-start avoids the cell degradation caused by repetitive cycling of the electrolyzer between ON and OFF states, and secondly, a minimum power set-point maintains a minimum gas production. Such a constraint is useful for an industrial electrolyzer system where the main objective is to fulfill a gas demand. The existing model is extended by adding a power ramp rate limiter with maximum and minimum ramp rate set at $\pm 500 kW/s$, a typical standard for PEM electrolyzers [15]. Three cases are developed to assess the electrolyzer performance for three power system services and analyze the impact this has on the electrolyzer.

C2.1.1: FREQUENCY REGULATION

In this case, the performance of the electrolyzer system as a frequency regulation device is evaluated. The electrolyzer control system regulates its operation. The electrolyzer can also be operated temporarily at elevated current densities up to 150% of rated current density [32]. In this use case, I provide the electrolyzer system with a continuous 40-minute regulation signal (Reg-D) obtained from PJM [33] and observe the system response. The regulation signal is given in per unit (pu) values, which ranges between -1.0 and 1.0. This signal is multiplied by the regulation capacity R MW (= 5 MW) and added to the regulation baseline B MW

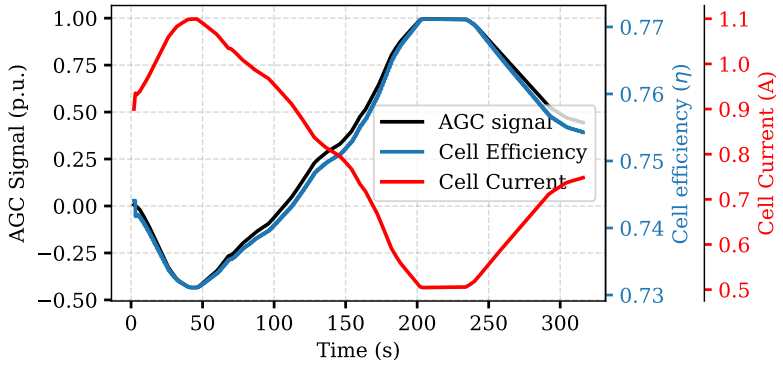

Figure 2.14: Electrolyzer cell performance for the given AGC signal. The electrolyzer can follow the AGC signal accurately, making it an excellent candidate for providing frequency regulation services to the power system. This result also shows that a constant power load model adequately represents electrolyzer systems in frequency support assessment studies.

=(10 MW) to obtain the power reference. The $R+B$ MW is then the input power for the electrolyzer system.

To measure the performance of the cell, the correlation between electrolyzer cell current and efficiency versus the AGC signal is observed. The response is shown in Fig. 2.14. The electrolyzer system can continuously follow the AGC signal accurately over the 40-minute duration. This implies that the cell dynamic response is adequate for using it as a frequency regulation device since it responds quickly to changes in the AGC signal. To analyze the electrolyzer degradation, the cell V-I plot is compared between the detailed model before and after the experiment (shown in Fig. 2.16). Since both curves are almost identical, it can be concluded that no significant cell degradation has occurred by providing this service over 40 minutes. Thus, a static power load model in frequency regulation studies is sufficient to represent an electrolyzer system.

C2.1.2: FLEXIBILITY PROVISION

In this case, the electrolyzer system's ability to correct wind forecast errors throughout the day to help the wind power producer maintain its day ahead positions and avoid imbalance costs is evaluated. The performance of the electrolyzer to respond within seconds to regulate frequency was analyzed in the last section; hence, in this case, I assume that the wind power forecast is constant over the 15-minute Program Time Unit (PTU) to focus on the ability of the electrolyzer to correct errors. To absorb the wind forecast errors, I need to control the electrolyzer power set-point such that operational constraints for the electrolyzer system and the grid are not violated.

As is shown in Fig. 2.15, the actual power exchange at the bus where the

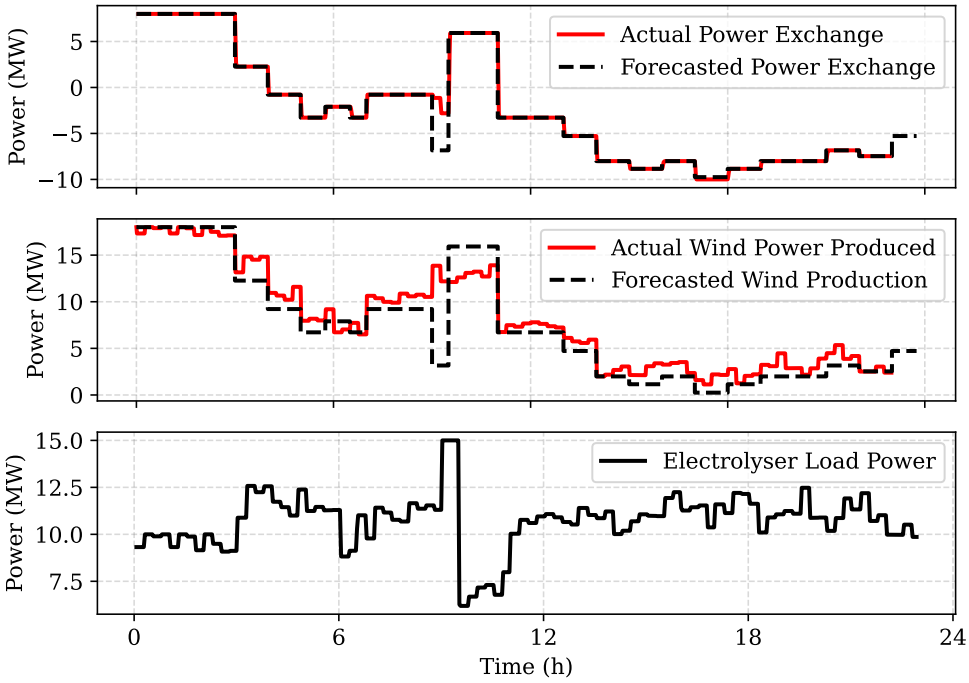

Figure 2.15: The top figure shows forecasted power and actual bus power exchange at the electrolyzer bus. The middle figure shows the actual wind and forecasted wind generated by the WTO. The bottom figure shows load set-points for the electrolyzer as it receives continuous updates about forecasting errors from the WTO. This operation allows the electrolyzer to mitigate imbalances of VRES when such a system is operated in tandem.

electrolyzer is connected is maintained equal to the forecasted power exchange (derived from the wind power forecasts). This behavior is achieved despite the wind power fluctuating from its forecasted value by controlling the flexible electrolyzer. The electrolyzer power set-points are shown at the bottom of Fig. 2.15, highlighting dynamic operation throughout the day. At the end of the day, the total energy in the fluctuations absorbed by the electrolyzer with its flexible operation is calculated. This value can then be used to remunerate the electrolyzer operator. In this case, the total energy in fluctuations absorbed by the electrolyzer during the day is calculated to 12.91 MWh.

To observe the device health, I construct the V-I curve as is shown in Fig. 2.16. Comparing the V-I curve before and after a full day simulation shows that the difference between the two curves is still negligible, similar to C2.1.1. This implies that the dynamic operation of the cell does not degrade the cell, even when operated dynamically throughout the day.

C2.1.3: LONG TERM IMPACT ANALYSIS

Most energy system planning tools that optimize system operation over longer time use models of energy conversion systems that do not exhibit any dynamic behavior. Examples of these tools includes PLEXOS, TIMES, etc. Even the tools that take care of short-term variations into long-term planning models, like OESMOSYS, do not consider the impact of the variable operation on the resource health itself (such as the impact of efficiency, degradation, etc.). Thus, the valuation of demand response flexibility from the said resource can be under- or over-estimated. In this case, changes to the electrolyzer's ability to provide flexibility are investigated using V-I curves generated from the detailed electrolyzer model.

C2.1.1 and C2.1.2 showed little correlation between cell degradation and dynamic operation. Nonetheless, degradation also comes from continuous operation of the electrolyzer and regular wear-and-tear, which may affect the device's ability to provide flexibility. To analyze the wear and tear, electrolyzer is operated in a constant current mode for a duration of 1 year. Figure 2.16 shows a shift of the V-I curve from the original curve for C2.1.3, signaling cell degradation. With the input current of 1.2 A, the new cell voltage is 1.6 V, increased from 1.58 V. The efficiency of the cell, as calculated by Eq. (2.7), now becomes 73.6 % compared to 74.4% of the new cell. Therefore, the current and the power required will increase to produce the same amount of hydrogen. Since the flexibility band remains fixed around the original nominal power of 10 MW, the flexibility available will also change. The efficiency drop in cell performance is more pronounced over a longer duration (for example, over a 5-year duration, the cell efficiency drops by almost 3.5%) than for a shorter duration. Since the amount of flexibility provided by the electrolyzer is determined by the range within which the power set-point can be varied, this drop in efficiency will impact the amount of flexibility that the electrolyzer can offer for frequency regulation service as well as forecast error correction service in the long term as well.

In summary, in this section, I showed the use of the detailed model to assess the health of the electrolyzer when it is used for providing power system services. The ability to extract V-I plots from such a model and the inability of a simplified constant power load model to do so again highlights the use of detailed modeling.

2.4. DISCUSSION

In the current energy landscape, the first step in adopting a technology is conducting a simulation-based assessment. The choice of models used in these studies, whether simple or detailed, will influence the study's outcome. In many studies on assessments and optimization of energy system configuration and

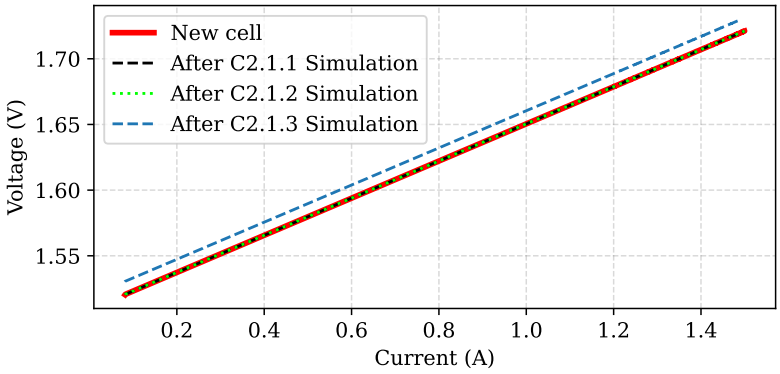

Figure 2.16: Effect of providing power system flexibility services on the electrolyzer itself, visualized and assessed using V-I curve for the three cases. The V-I curve for C2.1.3, which models the electrolyzer operation's long-term behavior, is shifted upwards, indicating that cell degradation has occurred. This degradation implies the reduced efficiency of the electrolyzer system, which must be accounted for when assessing flexibility from such systems over longer periods.

P2X operation, the components' models are frequently represented in simplified linear forms. A false representation of the technical models used in these assessments will impact the understanding of the applicability and feasibility of a particular technology in the future energy system.

Although model detail is necessary, it is essential to simultaneously consider the complexity that accompanies it in both the designing of the model to an appropriate level of detail and then complexity in the computation of the model itself. The question "how detailed is too detailed?" must be asked constantly. There are apparent trade-offs that need to be made between insight obtained from the model and the efforts in modeling and simulation of the said model.

In Section 2.2, the value of using detailed models over simplified models was immediately visible. The dependence of device characteristics such as efficiency and coefficient of performance on ambient temperatures causes deviations between results obtained from simple and detailed models. Since these characteristics are used extensively to represent P2X devices in technical assessments, due consideration must be given to deviations in the values of these characteristics. Knowledge of accurate device response provides economic benefits for power system services whose remuneration depends on the precise amount of energy exchange (such as frequency regulation, intraday imbalance correction, etc.).

For the sake of discussion, it is essential to point out that neither of the models developed is validated with real-world data leading to questions on the accuracy of model outputs. However, since Model B is built on top of Model A, the differences shown in model outputs are relative. If real-world data is avail-

able and model validation can be performed, then the differences in the model outputs would follow similar trends as obtained in this study. A more comprehensive parameter uncertainty assessment can be done further to understand the importance of tuned parameters on model output differences.

Detailed models of P2X systems help us understand the dependency between device physics and the power system. In Section 2.3.1, the load shifting capability of a large thermal storage tank coupled with an electric boiler was evaluated. Critical phenomena such as thermal stratification are not present in the simplified first-order model. Modeling these phenomena is critical to fully understanding the factors that impact flexibility available from resources utilizing their thermal inertia, such as the considered thermal storage tank. Modeling these phenomena requires discretization of the fluid volume, and the more the model is discretized, the closer its behavior is to reality. However, this leads us back to the question of "how detailed is too detailed?" since modeling detail has computational costs, as shown. To determine appropriate detail within reasonable computational costs, an iterative approach should be taken. When the incremental improvement in model outputs is lower than the effort required to compute (as well as design) the model, the model can be considered sufficiently detailed. Deciding on acceptable improvements in model detail relies on the modeler.

In Section 2.3.2, I looked at another application of a detailed model of P2X systems by comparing the V-I curves of the constituent electrolyzer cell. These curves help evaluate the electrolyzer's health and provide quantifiable information on the ability of the electrolyzer cell to operate flexibly. While the V-I curves obtained from detailed models provide valuable insights, these models are too detailed for all technical assessment studies conducted in time frames of seconds to days. However, insights from these models have a significant role in any flexibility assessment studies conducted within time frames of years, typically energy outlook scenarios and economic viability studies. These insights should be integrated into such assessments.

As more P2X devices are introduced into our energy system, and their intelligent operation allows us to use them in power system supporting services, attention must be paid to the modeling of these devices. Accurate insights from the detailed models will help better estimate the support these devices can offer to power system operations in the future. As was the practice during the early days of PV adoption, where distributed VRES were modeled as "negative loads," using simple model representations (such as constant power loads) as the go-to option is not viable anymore. Appropriate attention must be paid to the time frame of analysis, the device being used, and the size of the system considered. This consideration is valid, especially for large systems relying on thermal inertia, where it becomes essential to use detailed models to properly assess the impact

of phenomena such as rebound effect, thermal stratification, etc.

2.5. CONCLUSION

In this chapter, I have shown the important role that modeling P2X devices play in energy system analysis. In Section 2.2, the need for detailed modeling was established by showing conclusively that differences exist between simplistic and detailed model representations of P2X devices. Using examples of electric heat pumps and electrolyzer systems, I investigated these devices' coefficient of performance and efficiency metrics. The dependence of these metrics on ambient and operational temperature was highlighted. I showed that using detailed models of these devices leads to better insights into the operation of these systems. The electrolyzer considered in this example showed a difference of almost 0.6% in efficiency curves between simple and detailed models. The maximum difference in COP values for the considered heat pump was 1.4. These metrics influence not only the products produced by these devices but are also important to appropriately size the system. Inaccuracies stemming from the use of inadequate models can impact not only the contribution of these devices to power system services but also the amount of product they produce, which directly impacts the sizing and economic viability studies.

In Section 2.3, I investigated further the use of detailed models. In the first subsection, I developed a detailed model of an electric boiler and a thermal storage tank. Using a highly detailed model, a common phenomenon in flexibility analysis known as the demand response rebound effect was explored. It was concluded that using these detailed models, insights into underlying complex dynamics of large systems relying on thermal inertia can be obtained and subsequently be used to model them into flexibility assessment strategies.

Another example was explored to assess the value of detailed models in Section 2.3. In this subsection, technical analysis to evaluate the ability of a large-scale PEM electrolyzer to provide power system services was undertaken. I reused the electrolyzer model from Section 2.2. Three use cases were designed to assess the PEM electrolyzer under various operating conditions, and the impact on the electrolyzer was measured by studying the V-I curves of the electrolysis cell. It was seen that the PEM electrolyzer is an excellent candidate to provide various kinds of flexibility services to the power grid. Its fast dynamic response helps in providing frequency regulation services, while its efficient and safe part-load operation can be used to correct renewable forecast errors throughout the day. It is shown that dynamic operation has a negligible impact on degradation based on the model detail considered. The wear-and-tear of the cell was noticeable in the third case, where the cell was operated for an entire year. The drop in cell efficiency, as well as cell current, was noted. It was concluded that this

efficiency drop needs to be incorporated into the electrolyzer's long-term operational strategy, economic assessment, and business model. This insight also concludes that detailed models are integral in providing insights into the operation of P2X devices as power system flexibility resources.

In conclusion, it was determined that modeling any P2X device and its subsystem must always be done by assessing the use case. In the current changing energy landscape, where the development of new and improved technology is rapid, it is critical to include insights from detailed models in any technical and non-technical assessment studies.

BIBLIOGRAPHY

[1] Digvijay Gusain, Miloš Cvetković, and Peter Palensky. "Energy Flexibility Analysis Using FMUWorld". In: *2019 IEEE Milan PowerTech*. June 2019, pp. 1–6. DOI: 10.1109/PTC.2019.8810433.

[2] Digvijay Gusain et al. "Technical Assessment of Large Scale PEM Electrolyzers as Flexibility Service Providers". In: *2020 IEEE 29th International Symposium on Industrial Electronics (ISIE)*. June 2020, pp. 1074–1078. DOI: 10.1109/ISIE45063.2020.9152462.

[3] Peter D. Lund et al. "Review of Energy System Flexibility Measures to Enable High Levels of Variable Renewable Electricity". In: *Renewable and Sustainable Energy Reviews* 45 (May 2015), pp. 785–807. ISSN: 1364-0321. DOI: 10.1016/j.rser.2015.01.057.

[4] Selina Byfield and Dirk Vetter. *Flexibility concepts for the German power supply in 2050. Ensuring stability in the age of renewable energies*. Tech. rep. 978-3-8047-3549-1. Munchen: acatech – National Academy of Science and Engineering.

[5] Jyri Salpakari, Jani Mikkola, and Peter D. Lund. "Improved Flexibility with Large-Scale Variable Renewable Power in Cities through Optimal Demand Side Management and Power-to-Heat Conversion". In: *Energy Conversion and Management* 126 (Oct. 2016), pp. 649–661. ISSN: 0196-8904. DOI: 10.1016/j.enconman.2016.08.041.

[6] Georgios Papaefthymiou, Bernhard Hasche, and Christian Nabe. "Potential of Heat Pumps for Demand Side Management and Wind Power Integration in the German Electricity Market". In: *IEEE Transactions on Sustainable Energy* 3.4 (Oct. 2012), pp. 636–642. ISSN: 1949-3037. DOI: 10.1109/TSTE.2012.2202132.

[7] Prabha Kundur. "Power System Stability". In: *Power system stability and control* (2007), pp. 7–1.

[8] V. Garcia Suarez et al. "Integration of Power-to-gas Conversion into Dutch Electrical Ancillary Services Markets". In: *Proceedings of ENERDAY 2018-12th International Conference on Energy Economics and Technology*. 2018.

[9] Ramchandra Bhosale and Vivek Agarwal. “Control of Fuel Cell and Electrolyzer Based Hydrogen Storage System with Ultra-Capacitor for Voltage Stability and Enhanced Transient Stability of a DC Micro Grid”. In: *2018 International Conference on Power, Instrumentation, Control and Computing (PICC)*. Jan. 2018, pp. 1–6. DOI: 10.1109/PICC.2018.8384788.

[10] Meng Ni, Michael K. H. Leung, and Dennis Y. C. Leung. “Energy and Exergy Analysis of Hydrogen Production by a Proton Exchange Membrane (PEM) Electrolyzer Plant”. In: *Energy Conversion and Management* 49.10 (Oct. 2008), pp. 2748–2756. ISSN: 0196-8904. DOI: 10.1016/j.enconman.2008.03.018.

[11] Martin Geidl et al. “The Energy Hub–A Powerful Concept for Future Energy Systems”. In: *Third Annual Carnegie Mellon Conference on the Electricity Industry*. Vol. 13. 2007, p. 14.

[12] R. Morales González et al. “Optimizing Electricity Consumption of Buildings in a Microgrid through Demand Response”. In: *2017 IEEE Manchester PowerTech*. IEEE, 2017, pp. 1–6.

[13] Huiyong Kim, Mikyoung Park, and Kwang Soon Lee. “One-Dimensional Dynamic Modeling of a High-Pressure Water Electrolysis System for Hydrogen Production”. In: *International Journal of Hydrogen Energy* 38.6 (Feb. 2013), pp. 2596–2609. ISSN: 0360-3199. DOI: 10.1016/j.ijhydene.2012.12.006.

[14] Kazuo Onda et al. “Performance Analysis of Polymer-Electrolyte Water Electrolysis Cell at a Small-Unit Test Cell and Performance Prediction of Large Stacked Cell”. In: *Journal of The Electrochemical Society* 149.8 (June 2002), A1069. ISSN: 1945-7111. DOI: 10.1149/1.1492287.

[15] Bart W. Tuinema et al. “Modelling of Large-Sized Electrolysers for Real-Time Simulation and Study of the Possibility of Frequency Support by Electrolysers”. In: *IET Generation, Transmission & Distribution* 14.10 (Feb. 2020), pp. 1985–1992. ISSN: 1751-8695. DOI: 10.1049/iet-gtd.2019.1364.

[16] Marwan Chamoun et al. “Dynamic Model of an Industrial Heat Pump Using Water as Refrigerant”. In: *International Journal of Refrigeration* 35.4 (June 2012), pp. 1080–1091. ISSN: 0140-7007. DOI: 10.1016/j.ijrefrig.2011.12.007.

[17] Francisco da Costa Lopes and Edson H. Watanabe. “Experimental and Theoretical Development of a PEM Electrolyzer Model Applied to Energy Storage Systems”. In: *2009 Brazilian Power Electronics Conference*. Sept. 2009, pp. 775–782. DOI: 10.1109/COBEP.2009.5347619.

[18] Paul Schott et al. “A Generic Data Model for Describing Flexibility in Power Markets”. In: *Energies* 12.10 (Jan. 2019), p. 1893. DOI: 10.3390/en12101893.

[19] Manuel Espinosa-López et al. “Modelling and Experimental Validation of a 46 kW PEM High Pressure Water Electrolyzer”. In: *Renewable Energy* 119 (Apr. 2018), pp. 160–173. ISSN: 0960-1481. DOI: 10.1016/j.renene.2017.11.081.

[20] R. García-Valverde, N. Espinosa, and A. Urbina. “Simple PEM Water Electrolyser Model and Experimental Validation”. In: *International Journal of Hydrogen Energy*. 10th International Conference on Clean Energy 2010 37.2 (Jan. 2012), pp. 1927–1938. ISSN: 0360-3199. DOI: 10.1016/j.ijhydene.2011.09.027.

[21] Alexander Buttler and Hartmut Spliethoff. “Current Status of Water Electrolysis for Energy Storage, Grid Balancing and Sector Coupling via Power-to-Gas and Power-to-Liquids: A Review”. In: *Renewable and Sustainable Energy Reviews* 82 (Feb. 2018), pp. 2440–2454. ISSN: 1364-0321. DOI: 10.1016/j.rser.2017.09.003.

[22] John Webster and Carsten Bode. “Implementation of a Non-Discretized Multiphysics PEM Electrolyzer Model in Modelica”. In: *The 13th International Modelica Conference, Regensburg, Germany, March 4–6, 2019*. Feb. 2019, pp. 833–840. DOI: 10.3384/ecp19157833.

[23] Caner Yağci. “Investigating Hidden Flexibilities Provided by Power-to-X Considering Grid Support Strategies”. PhD thesis. Delft University of Technology, 2020.

[24] *Numpy.Polyfit — NumPy v1.22 Manual*. https://numpy.org/doc/stable/reference/generate

[25] Friedrich Kunz et al. *Electricity, Heat, and Gas Sector Data for Modeling the German System*. DIW Data Documentation 92. Berlin: Deutsches Institut für Wirtschaftsforschung (DIW), 2017.

[26] Björn Felten, Jan Paul Baginski, and Christoph Weber. *KWK-Mindest- Und Maximaleinspeisung - Die Erzeugung von Zeitreihen Für Die Energiesystemmodellierung (Restrictions of the Electricity Generation from CHP Plants - Producing Time Series for Energy System Modeling)*. SSRN Scholarly Paper 3082858. Rochester, NY: Social Science Research Network, Dec. 2017. DOI: 10.2139/ssrn.3082858.

[27] Andreas Bloess, Wolf-Peter Schill, and Alexander Zerrahn. “Power-to-Heat for Renewable Energy Integration: A Review of Technologies, Modeling Approaches, and Flexibility Potentials”. In: *Applied Energy* 212 (Feb. 2018), pp. 1611–1626. ISSN: 0306-2619. DOI: 10.1016/j.apenergy.2017.12.073.

[28] Tobias Gybel Hovgaard et al. “Energy Efficient Refrigeration and Flexible Power Consumption in a Smart Grid”. In: *Energy Systems and Technologies for the Coming Century*. Technical University of Denmark, 2011, pp. 164–175. ISBN: 978-87-550-3903-2.

[29] Wei Zhang et al. “Aggregated Modeling and Control of Air Conditioning Loads for Demand Response”. In: *IEEE Transactions on Power Systems* 28.4 (Nov. 2013), pp. 4655–4664. ISSN: 1558-0679. DOI: 10.1109/TPWRS.2013.2266121.

[30] Marcus Fuchs et al. “Structuring the Building Performance Modelica Library AixLib for Open Collaborative Development”. In: *14th International Conference of the International Building Performance Simulation Association, Hyderabad, India. And See: https://github. Com/RWTH-EBC/AixLib*. 2015.

[31] Thomas Spruit. “Operating Power-to-Heat in Thermal Grids: Mitigating Wind Power Intermittency through the Electrification of a Heat Network”. MSc Thesis. Delft: TU Delft, 2020.

[32] A. Villagra and P. Millet. “An Analysis of PEM Water Electrolysis Cells Operating at Elevated Current Densities”. In: *International Journal of Hydrogen Energy*. 9th International Conference on Hydrogen Production (ICH2P-2018) 44.20 (Apr. 2019), pp. 9708–9717. ISSN: 0360-3199. DOI: 10.1016/j.ijhydene.2018.11.179.

[33] *PJM - Ancillary Services*. https://www.pjm.com/markets-and-operations/ancillary-services.aspx.

3

Cosimulation of Multi Energy Systems

3.1. Motivation and Significance

The coupling of energy systems is essential for a sustainable energy system. This recent trend in coupling various energy sectors has been driven primarily by the effort to decarbonize the energy system [2, 3]. As an added benefit, the energy conversion devices enabling this coupling, such as power-to-heat, power-to-gas, and power-to-mobility, can also serve as sources of flexibility to the highly renewable future power systems [4, 5]. As previously mentioned, such coupled systems are known as multi-energy systems or MES.

To assess MES correctly, a holistic analysis of the system is required. It has been well noted in [6] that before an economic analysis can be conducted to determine a business case based on an MES, it is essential to evaluate its technical feasibility. This assessment involves evaluating various control strategies, assessing the operation and reliability of components and associated networks, determining operational bottlenecks, etc. Therefore, modeling and simulation-based analysis form the first step toward assessing such integrated energy systems.

Simulation-based assessments are not new in energy system analysis. The dynamic and steady-state characteristics of different energy domains are unique. For example, the system dynamics for different energy carriers evolve at different time scales. For an electricity network, the changes in active power and frequency are immediately visible throughout the network. This is not the case for a heat network: while pressure changes in the heat network are reflected throughout the network in seconds, the temperature dynamics across the network can

Contents of this chapter have been published in Elsevier's SoftwareX [1].

take minutes and hours to reach a steady state. Consequently, to accurately consider these characteristics in analyzing a particular energy sector, state-of-the-art tools and solvers have been used. These tools have been developed using years of research and development to accurately model the aforementioned unique characteristics of the energy domain in focus. Examples of such tools include POWERFACTORY for modeling electrical power system, DYMOLA/OPENMODELICA for modeling fluid system, MATLAB and PYTHON-based APMONITOR [7] for developing model-based control and PYTORCH [8] for developing data-driven controls.

When it comes to conducting a combined system study for an MES, there are two natural pathways. The first pathway is modeling the entire system in a single modeling environment, such as MATLAB, and then simulating it using a general-purpose solver. This process is a time-consuming approach: it requires extensive knowledge on the modeler's part to design different MES components. Moreover, the solver used to simulate the MES needs to be a general-purpose one that can handle the characteristics of various components of the MES as described previously. Finally, because the MES is modeled in a single environment, the problem size for the computer to solve increases, which can require significant computing resources [9].

The second pathway is dividing the MES into smaller subsystems (such as electrical, heat, gas, etc.) and leveraging software techniques to couple these subsystems. The subsystems can then be modeled using domain-specific modeling environments and solved with dedicated solvers to obtain high accuracy results. This method is known as co-simulation, or coupled simulation [10]. Co-simulation is a method that allows the coupling of models developed in various modeling environments by managing the time progression of the simulation and coordinating the data flow between subsystem models. Dynamic interaction between subsystem models can be facilitated by exchanging data (values of interest), such as process outputs, sensor measurements, etc. Even though any data value can be shared, when creating an MES model, the exchanged variables usually lay on the boundary of two energy carriers. For example, mechanical power of steam turbine obtained from the thermo-mechanical model (process output) of generator given as input to the rotor of the synchronous generator in the electrical power system model, or temperature of room obtained from a building's thermal model (sensor measurement) given as input to a control system model, etc. Enabling this dynamic interaction allows for a holistic system analysis, where domain-specific characteristics are preserved while interacting with other energy domains. As is noted in [11, 12], operational model details have significant impact on results. Thus, using domain-specific accurate models removes potentially misleading simplifying assumptions. It is interesting to point

out that by using co-simulation, large complex systems can be broken down into smaller subsystems and simulated in a coupled fashion using techniques such as parallel and distributed simulation [13]. Although, it must be noted that splitting larger systems into subsystems and using co-simulation introduces some numerical challenges of its own, such as algebraic loops [10].

The main challenge in achieving this goal is developing a modular framework that allows the coupling of various subsystem models and an algorithm that manages overall simulation time progression and data exchange. This is where ENERGYSIM steps in. ENERGYSIM allows users to easily couple subsystem models and focus on high-level tasks in MES technical assessment studies such as subsystem model development, control algorithm development, and case study definition, among others, rather than focusing on co-simulation-specific tasks such as time progression management and data exchange. The availability of a simplified energy system co-simulator will allow increased insights into an MES setting by enabling a more collaborative modeling and simulation environment.

Previously, I used ENERGYSIM in [14] and [15]. In [14], I demonstrated how complex the model of the closed-cycle gas turbine was combined with the dynamic model of the electricity network for analyzing the impact of fuel supply change on electrical network frequency. In [15] I demonstrated how ENERGYSIM can facilitate a multi-stakeholder analysis that involved concurrent simulation of detailed models of the electricity grid, electrolyzer, and control systems to correct forecasting errors of a nearby wind turbine. The version of ENERGYSIM used for simulating use cases in the aforementioned articles has been updated. The current version (ENERGYSIM (v2.1)) provides more simulation adapters (explained in the next subsection) to couple other widely used energy modeling tools, allows access to the algorithm that coordinates time progression and data exchange which further allows users to implement non-energy applications, uses HDF data format to store results, making it useful for very-high fidelity simulations generating considerable amounts of data.

ENERGYSIM is developed in Python and is tested for compatibility with Python version after v3.6. ENERGYSIM is installable via the Python Package Index (PYPI). An example case is available in the main repository to illustrate the usage. A working example of the use case described in this chapter has also been uploaded to the Code Ocean platform for reproducibility of results (available as a link on Github).

COMPARISON WITH OTHER TOOLS

At the heart of any co-simulation tool lies an algorithm that manages time progression and data exchange. There already exist a few tools in literature such as MOSAIK [16], MASTERSIM [17], MESCOS [18], PTOLEMY II [19] to set up co-

simulation. However, I believe ENERGYSIM offers several advantages to its users compared to the tools mentioned above. The first and foremost advantage is that it is developed in Python. Python is the most widely used language for scientific and general-purpose computing and has developed a huge user base, especially in the energy system community. Proprietary tools also frequently provide bindings to Python, which makes accessing them easy. This familiarity with the programming language allows ENERGYSIM to be easily understandable and accessible to large audiences compared to tools which are developed in languages such as JAVA (PTOLEMY II), C, C++ (MASTERSIM, MESCOS). Secondly, the structure of ENERGYSIM is modular. This modularity means that access to time progression and message exchange algorithm can be done via what I refer to as *simulation adapters*. Simulation adapters interface the simulation entity to ENERGYSIM by defining four key function: `init()`, `set_value()`, `get_value()`, and `step()`. These functions enable ENERGYSIM to initialize the simulator, set and get variable values at any time, and control the progress of the simulator in time, respectively. To put it simply, these adapters provide a way for ENERGYSIM to "talk to simulators." The tool already provides ready-made adapters to couple the most common tools used in the energy system modeling and simulation domain. Additionally, creating new adapters can also be done easily. This ease-of-use is in contrast to other tools which require complex setup configurations (such as setting up Scenario API and Component API for each simulator with MOSAIK) or can support only a single type of simulation entities (for ex. MASTERSIM supports only Functional Mock-up Units (FMUs)).

3.2. SOFTWARE DESCRIPTION

3.2.1. SOFTWARE ARCHITECTURE

ENERGYSIM is classified as a "hybrid-simulator". It supports both quasi-static and continuous-time dynamic simulation (CTDS). I have not classified ENERGYSIM as a discrete-time simulator because the term encompasses a broad range of simulation techniques, some of which ENERGYSIM does not support, for example, event-based simulations, such as those involving communication network simulation.

TIME PROGRESSION AND DATA EXCHANGE MANAGEMENT

In ENERGYSIM, there are two primary time variables to define: macro-time step (which is a global variable) and micro-time step (which is a local variable). The data exchange between simulators occurs at fixed time intervals, known as the macro-time step. Individual simulators use an optional and unique micro-time step between each macro-time step for solving their own model equations. This

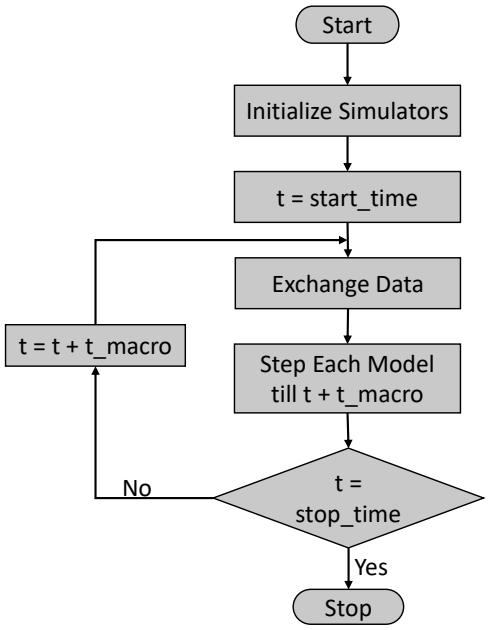

Figure 3.1: Flowchart depicting the co-simulation process. To start, the simulators are initialized, and then, at each macro time step data is exchanged between the simulators. Each simulator can use an individual micro-time step between the macro-time steps for simulation.

differentiation is essential for CTDS models to perform time integration for solving their model equations. The co-simulation flowchart is shown in Fig. 3.1.

In between the macro-time steps, when no input data is available to the CTDS model, an interpolation method needs to be applied. Although there are quite a few techniques to implement the interpolation (constant, linear, polynomial [20]), within ENERGYSIM, I have opted for a constant interpolation method. In this method, the inputs to the CTDS model are held constant at the value obtained at the last macro-time step.

SOFTWARE COMPONENTS

The core component of the ENERGYSIM package is the `world` object. Once the `world` object is imported from ENERGYSIM package, the user can instantiate it as shown in Listing 3.1.

Listing 3.1: Instantiating world

```
from energysim import world
my_world = world(start_time=0, stop_time=23*3600, logging=True, t_macro
    =60)
```

`my_world` is the canvas on which simulators, simulator connections, and simulation options can be specified. The main parameters to be specified here are `start_time`, `stop_time`, `logging`, and `t_macro`. The parameter `t_macro` specifies the macro-time step and has a default value of 60 seconds.

Once `my_world` object is created, users can add simulators to it via the `add_simulator()` method as shown in Listing 3.2.

Listing 3.2: Adding simulators

```
my_world.add_simulator(sim_type = 'fmu', sim_name = 'fmu1', sim_loc = '/
    path/to/fmu', step_size = 1, inputs = [], outputs = ['var', 'obj1.var1'
    ])
```

The `add_simulator()` method requires specification of `sim_type`, `sim_name`, `sim_loc`, and `step_size`. The parameter `step_size` specifies the micro-time step, unique to each simulator. These six parameters are shared for the specification of any simulator and are enough to execute a basic co-simulation. However, users can also do so if additional parameters need to be specified. For example, the electric network added as a PANDAPOWER [21] model in ENERGYSIM, by default, uses the AC power flow functionality of PANDAPOWER to solve the model (ENERGYSIM does not contain a solver of its own). Therefore, an additional argument `pf` is provided, so users can specify a different power flow option if required. These include "pf" (default), "dcpf", "opf", and "dcopf". This is useful when, for example, an optimal controller based on electrical network power flow is needed. The example in the GitHub repository uses this functionality. There exist other similar simulator-specific options within ENERGYSIM. The software documentation provides a detailed list and description of these options.

As mentioned in Section 3.1, I have developed simulation adapters to couple simulators to ENERGYSIM. Through an extensive literature search, I identified the languages that are most commonly used to develop models for energy domains of interest: Modelica [22–26], MATLAB [6], Python [27, 28] are typically used to model thermal and heat systems. Python [28, 29], DigSILENT PowerFactory [23, 30, 31], Modelica [32, 33], and MATLAB [34] are used for electricity network simulations. For gas systems, Modelica [32, 33, 35] is a common choice of software for many, whereas, for analysis of electric vehicle systems, Modelica [36], Python [27, 36, 37], and MATLAB [38] are used the most. These are summarized in Table 3.1.

Some modeling languages allow exporting models as Functional Mock-up Units (FMUs) according to the Functional Mock-up Interface (FMI) standard [39]. Models are packaged as a combination of XML files, binaries, and C-code and distributed as a ZIP file called FMU. The FMU contains model equations and

Energy Domain	Modeling Language
Heat Systems	Modelica, MATLAB/Simulink, Python, CSV, Others
Electricity Systems	Modelica, MATLAB/Simulink, Python, PowerFactory, Others
Gas Networks	Modelica, MATLAB/Simulink, Python, Others
Transportation	MATLAB, Python, CSV, Others

Table 3.1: List of common modeling languages used in energy system modeling and simulation community.

optionally an associated solver. Model exchange via FMU is gaining wider adoption across the modeling and simulation community, with currently more than 150 tools supporting exporting models to FMUs. Within ENERGYSIM, FMUs can be added by setting the value of the `sim_type` parameter as `'fmu'`.

To ensure wider operability and integration to other software/Python packages, I have also provided a way for users to interface their simulator of choice with ENERGYSIM by setting the `sim_type` parameter with `'external'`. To add a user-defined simulator to ENERGYSIM via a user-developed simulation adapter, the to-be-coupled simulator must offer a "play-and-pause" functionality. This means that ENERGYSIM must be able to:

- initialize the simulator,
- get inputs from simulator when requested,
- instruct the simulator to take one step forward,
- request output values from the simulator,
- pause the simulation while the simulator waits for instructions, and new inputs from ENERGYSIM.

A detailed description of this method is available in the documentation.

Once the simulators are specified and added to `my_world`, users can specify the connections between the simulators as a Python dictionary object, as shown in Listing 3.3. Then, the `my_world` object can then be simulated using the `simulate()` command. By default, the `record_all` parameter is set to *True* which instructs ENERGYSIM to record each simulator's output values at every micro-time step. *False* leads to output recording only at macro-time step intervals. The results can be obtained by calling the command `my_world.results()`,

which returns a Python dictionary object with keys as `sim_name` and value as a pandas dataframe with time-stamped output values. If the `to_csv` option is set to *True*, then results are also exported as CSV files. The parameter `record_all` toggles the simulation progress bar.

Listing 3.3: Finalizing simulation

```
connections = {'sim1.output_variable1' : 'sim2.input_variable1', 'sim3.output_variable2' : 'sim4.input_variable2', 'sim1.output_variable3' : 'sim2.input_variable3',}
my_world.add_connections(connections)
my_world.simulate(pbar=True, record_all=True)
results = my_world.results(to_csv=False)
```


3.2.2. SOFTWARE FUNCTIONALITIES

Apart from the basic functionality to add simulators and simulate them, ENERGYSIM offers a range of additional inbuilt functions to support the user in setting up multi-energy co-simulations.

ADDING SIGNALS

In many cases, users may require a simple external input to their model. For example, a control system simulator needs a constant input value of *True* to indicate that the simulator is active, or a wind power plant simulator which may require a random number generated from a continuously updated probability distribution function as an input to account for the randomness of wind power production, etc. These inputs can be added as CSV simulators, FMU simulators, or first, be modeled in another modeling language and interfaced to ENERGYSIM using the simulation adapters. However, such a process can be cumbersome. I developed dedicated functionality to add "signals" to simplify this process. Signals can provide the users with requested values and can be defined as Python functions. Signals can be added to ENERGYSIM using the `add_signal()` method. Examples of time-dependent and independent signals are shown in Listing 3.4.

Listing 3.4: Adding signal

```
def td_signal(t):
return [True]

def tid_signal(t):
return [np.sin(2*np.pi*omega*t)]

my_world.add_signal(sim_name='sine_wave_signal', signal = td_signal, step_size=1)
my_world.add_signal(sim_name='constant_signal', signal = tid_signal, step_size=1)
```

```
␣␣
```

INITIALIZATION

For CTDS models, correct initialization of system states is needed for accurate assessments. Different initial values will result in different dynamic behavior. To specify initial values to simulators, users can provide the initial values of parameters for the simulators as a dictionary with `'init'` keyword. This dictionary can then be passed onto the `my_world` object through `options` method.

MODIFYING DATA EXCHANGE

On many occasions, it becomes necessary to modify the output value of a particular simulator before it is provided to the other simulator. This situation is fairly common in multi-energy system simulations. Consider two simulators: a thermo-mechanical model of a combined heat and power system (CHP) and a steady-state power flow model of an electric network (EN). The power output from the CHP simulator is obtained in Watts (W). This power output of the CHP needs to be provided to the corresponding generator model in the EN. However, the generator in the EN accepts values only in megawatts (MW). One way to address the problem is to change the output values of the CHP in the model itself and recompile the model. However, this may not always be possible or doable (the model may require a toolchain for compilation that may not be available at that moment). Therefore, ENERGYSIM allows users to apply modifications simulator outputs by specifying a Python function that defines the modification. A dictionary entry listing all modification functions can then be provided to the `options` dictionary using `'modify_signal'` keyword. Both initialization and output modification is shown in Listing 3.5.

Listing 3.5: Initialization and Output Modifications

```
␣␣ini = {'sim1':(['sim_vars'], [vals]),
␣␣␣␣'sim2':(['sim_vars'], [vals])}
␣␣
␣␣def mod1(x):
␣␣return a1 * x + b1
␣␣
␣␣def mod2(x):
␣␣return np.log(x) + a1
␣␣
␣␣mdf = {'sim1.var1':mod1,
␣␣␣␣'sim2.var1':mod2}
␣␣
␣␣options = {'init' : ini,
␣␣␣␣'modify_signal': mdf}
```

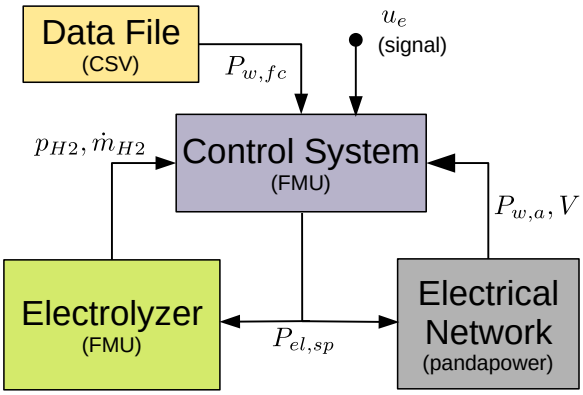

Figure 3.2: The co-simulation setup for the described case. Data File (as CSV) provide forecasted wind power to the control system. Electrolyzer FMU sends internal pressure and mass flow rates to the control system. The Electrical Network sends voltage values at each bus node and the actual power output from the wind plant to the control system. The Control System uses this input to determine the operational power set point for the electrolyzer, which it sends to both Electrical Network and Electrolyzer models.

```
    
    my_world.options(options)
```

PARAMETER SWEEP

Understanding the sensitivity of results on various simulation variables is an integral part of technical assessments of MES. To perform repeated simulations with different initial conditions for the co-simulation in focus, users can use the `init` option shown in Section 3.2.2. Using a for-loop and providing different values of initial conditions, the sensitivity of results from the co-simulation can be obtained.

TOPOLOGY PLOT

Using `plot()` method on `my_world` object, users can obtain a graph plot of the simulators, and connections between them. ENERGYSIM uses Python's NetworkX package to generate the topological plot of the multi-energy system based on the specified connections' dictionary.

3.3. ILLUSTRATIVE EXAMPLE

In this section, I illustrate the application of ENERGYSIM by showing a multi-stakeholder analysis. This is an extension of the study conducted in C2.1.2 in Section 2.3.2 (shown in Fig. 3.2). In C2.1.2, I investigated the impact on the electrolyzer of providing forecasting error correction service to the wind turbine op-

Stakeholder	Objective	Model Inputs	Model Outputs
Grid Manager	• Monitoring network imbalances • Monitoring network voltages • Monitoring line congestion	Electrolyzer power set-point & wind power production	Grid voltage and line congestion
Device Operator	• Device wear/tear • Primary production constraints	Electolyzer power set-point	Mass flow rates, cell temperature
Wind Turbine Operator	• Minimize imbalance and curtailment		Actual and forecasted power generation

Table 3.2: Objectives, inputs, and outputs of the three stakeholders considered in this study.

erator (WTO) throughout the day. Let us consider stakeholder 1 to be the WTO which operates an 18 MW rated wind turbine, and stakeholder 2 to be the electrolyzer operator. Additionally, the electrical grid operator needs to ensure that any changes in load and generation set-points coming from electrolyzer and wind turbine, respectively, due to flexibility arrangement does not affect voltage stability significantly in its distribution grid. Let us take the grid operator to be stakeholder 3. A recap of each stakeholder's objectives, inputs, and outputs is listed in Table 3.2.

The control system in Fig. 3.2 is tasked with assessing the full system using models provided by each stakeholder. The control system continuously receives information from the models of the three stakeholders. This information is: i) wind power forecast ($P_{\mathrm{w,fc}}$) and actual wind power production ($P_{\mathrm{w,a}}$) from WTO

(added as combination of `csv` simulator and `signal` simulator), ii) hydrogen pressure and mass flow rate ($p_{H2}, \dot{m}_{H2}$) from electrolyzer (added as a `fmu` simulator), and bus voltage at point of connection of wind turbine and electrolyzer (V) from grid operator (added as `powerflow` simulator). Based on the received values, it calculates the electrolyzer power set-point ($P_{el,sp}$) and dispatches those values to the electrolyzer model and grid. This set-point is used by 1) the electrical grid to evaluate bus voltage based on the AC power flow solution and 2) by the electrolyzer to calculate hydrogen production rates. It also generates an imbalance signal which is dispatched to the WTO to indicate if there was any imbalance.

Listing 3.6 shows the co-simulation setup in Python using ENERGYSIM.

Listing 3.6: A code snippet to illustrate setting up and simulating a co-simulation-based multi-stakeholder analysis using ENERGYSIM.

```
from energysim import world

mw = world(stop_time=3600*5., logging = True, t_macro = 120)

simulators_dir = ''   # setup a simultor directory containing all models

controller_loc = os.path.join(simulators_dir, 'controller.fmu')
grid_loc = os.path.join(simulators_dir, 'gridModel.p')
electrolyser_loc = os.path.join(simulators_dir, 'electrolyser.fmu')

mw.add_simulator(sim_type = 'powerflow', sim_name = 'grid', sim_loc =
    grid_loc, inputs = ['wind12.P', 'Electrolyser.P'], outputs=['Bus 0.V', '
    Bus 1.V', 'Bus 12.V', 'wind1.P', 'wind12.P', 'Electrolyser.P'],
    step_size=3)

mw.add_simulator(sim_type = 'fmu', sim_name = 'controller', sim_loc =
    controller_loc, step_size = 3, inputs = ['v', 'P', 'E_c'], outputs=['y',
     'gain1.y', 'load_should_be', 'new_load_should_be', 'p_forecasted', '
    power_delta'])

mw.add_simulator(sim_type = 'fmu', sim_name = 'electrolyser', sim_loc =
    electrolyser_loc, step_size = 3, inputs = ['p'], outputs=['y1', 'y2', 'p
    ', 'integrator1.y'], variable=True)

mw.add_simulator(sim_type = 'csv', sim_name = 'wind_data', sim_loc= os.path.
    join(simulators_dir, 'diff_win.csv'), step_size=60, outputs=['speed', '
    power', 'power2'])

def emergency(time):
return [1]

mw.add_signal(sim_name = 'Emergency', signal = emergency)
```

```
options = {'init':{'controller':(['v', 'E_c', 'P', 'C_max'], [14, 1, -18,
    -100]),
    'electrolyser':(['p'], [10])},
}

mw.options(options)

connections = {'wind_data.speed': 'controller.v',
    'wind_data.power': 'grid.wind12.P',
    'wind_data.power2': 'grid.wind1.P',
    'controller.y':'grid.Electrolyser.P',
    'Emergency.y':'controller.E_c',
    'grid.wind12.P':'controller.P',
    'grid.Electrolyser.P':'electrolyser.p',
}

mw.add_connections(connections)

res = mw.simulate(pbar=True)
```

Here, the co-simulation macro time-step is 120 seconds, meaning the simulators exchange data between themselves every 2 minutes. Additionally, each simulator has a unique micro time-step. The grid, control system, and electrolyzer system have a micro time-step of 3 sec, whereas the CSV simulator has a micro time-step of 60 seconds. The simulation takes precisely 6 minutes to execute on a dual-core Intel i5-6300U CPU @ 2.4GHz running Ubuntu 20.04. Figures 3.3 to 3.5 shows the electrical network bus voltage, the hydrogen production rate obtained from the detailed electrolyzer model simulator, and the electrolyzer operating power set-points determined by the control system simulator, respectively.

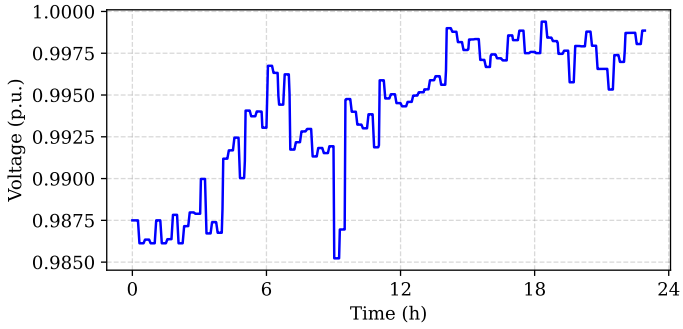

Figure 3.3: Voltage at the bus where the electrolyzer is connected to the electrical grid. This output comes from the electrical network simulator.

ENERGYSIM allows such analyses to take shape. A non-co-simulation ap-

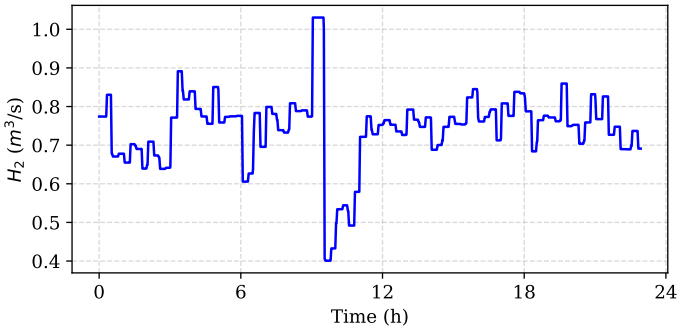

Figure 3.4: Production of hydrogen gas from the variable operation of the electrolyzer. This output comes from the detailed electrolyzer model simulator.

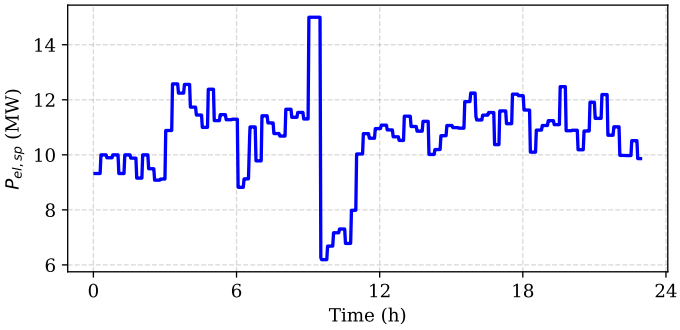

Figure 3.5: Electrolyzer operating power set point obtained. This output comes from the control system simulator.

proach would have required the entire system to be developed in a single monolithic simulation environment, which is time-consuming and requires expert knowledge of modeled subsystems (such as electrolyzer or electrical grid). With ENERGYSIM, models developed in various software domains can be put together. Because I have already developed adapters to the most commonly used energy system modeling and simulation software, ENERGYSIM provides an easy entry for users to integrate different models and expert knowledge. Additionally, with the availability of a simple method to connect any external simulator, ENERGYSIM ticks all boxes for multi-energy system analysis with multi-fidelity models.

3.4. DISCUSSION

The need to take the proposed approach of coupled simulation toward energy system technical analyses is highlighted by the widespread blackouts in Texas in 2021. Although the impact of extreme weather on power systems was assessed, the impact on natural gas supply and its equipment, which acts as a fuel source

for backup gas-powered peak power generation, was not considered jointly. This led to inaccurate assessments, leading to a catastrophic situation whereby millions lost access to electricity and heat. [40].

Using ENERGYSIM, a combined assessment of energy sectors is possible, allowing users of the tool to better understand technical limitations in an interconnected system. The availability of such a tool facilitates interdisciplinary research efforts by bringing together models developed by experts in modeling tools of their choice. By making the technical assessment model agnostic, all subsystems can be modeled in desired detail, solved using dedicated solvers, and brought together to create a system model closer to reality and, consequently, an analysis that presents better solutions. This approach contrasts existing modeling and simulation tools, simplifying or completely ignoring the interactions and dependence between energy sectors.

In Chapter 2, several models of various P2X resources are developed. For an FSP utilizing multiple such resources, it is essential to assess the operational flexibility extractable jointly from all the resources in this portfolio. It must consider that these resources are embedded in a network that its own limits can constrain, and therefore the operation of these resources must abide by these network constraints. As is shown in the example in Section 3.3 and Chapter 2, models available for P2X resources can have different levels of detail and be developed in different software packages or even different programming languages. ENERGYSIM will enable a simulation-based assessment of models of various P2X resources in the FSP's portfolio. Results obtained from this simulation-based assessment will help the FSP to evaluate the portfolio's operational behavior and, consequently, its flexibility. Furthermore, this will allow the FSP to derive critical insights and knowledge of their integrated system operation, identify operational bottlenecks, test control strategies, and evaluate sensitivities of various parameters on portfolio behavior.

3.5. FUTURE WORK

ENERGYSIM is a versatile tool for researchers to integrate various energy subsystem models to conduct holistic and comprehensive technical assessments. However, despite a range of available functionality, a few functionalities are still lacking, which are being actively worked on. These tasks have been identified to increase the adoption of ENERGYSIM and its capabilities as a multi-energy system co-simulator. Among these are the ability to specify different interpolations for data exchange between simulators, an inbuilt capability to parallelize the execution of individual simulators to enhance computational efficiency and enable large-scale co-simulations, and the development of simulation adapters for other common software tools such as DigSILENT PowerFactory.

3.6. CONCLUSIONS

In this chapter, I presented ENERGYSIM, a multi-energy system co-simulation tool for coupling energy system models developed in different software tools. I have described in detail the main features and functionalities of the proposed software, illustrating its ease of use and versatility. I provided code listings to highlight the important features of the proposed tool: such as adding user-defined signals, initialization for conducting parameter sweeps, the ability to perform output data modification, and generating topology plots for complex and simple MES. In the end, I demonstrated the use of ENERGYSIM in a case study where detailed models of an electrolyzer, the electricity network, and a control system are used to assess the ability of the electrolyzer to act as a flexibility service provider to the wind plant generator. The provided case study showed how various stakeholders could come together to perform a holistic study and use preferred modeling tools and solvers in doing so, which is not possible with traditional monolithic simulation tools.

BIBLIOGRAPHY

[1] Digvijay Gusain, Milos Cvetkovic, and Peter Palensky. "Simplifying Multi-Energy System Co-Simulations Using Energysim". In: *SoftwareX* 18 (June 2022), p. 101021. ISSN: 2352-7110. DOI: 10.1016/j.softx.2022.101021.

[2] C. Müller et al. "Integrated Planning and Evaluation of Multi-Modal Energy Systems for Decarbonization of Germany". In: *Energy Procedia*. Innovative Solutions for Energy Transitions 158 (Feb. 2019), pp. 3482–3487. ISSN: 1876-6102. DOI: 10.1016/j.egypro.2019.01.923.

[3] Thorsten Burandt et al. "Decarbonizing China's Energy System – Modeling the Transformation of the Electricity, Transportation, Heat, and Industrial Sectors". In: *Applied Energy* 255 (Dec. 2019), p. 113820. ISSN: 0306-2619. DOI: 10.1016/j.apenergy.2019.113820.

[4] Emiliano Dall'Anese, Pierluigi Mancarella, and Antonello Monti. "Unlocking Flexibility: Integrated Optimization and Control of Multienergy Systems". In: *IEEE Power and Energy Magazine* 15.1 (Jan. 2017), pp. 43–52. ISSN: 1558-4216. DOI: 10.1109/MPE.2016.2625218.

[5] Vahid Arabzadeh et al. "Deep Decarbonization of Urban Energy Systems through Renewable Energy and Sector-Coupling Flexibility Strategies". In: *Journal of Environmental Management* 260 (Apr. 2020), p. 110090. ISSN: 0301-4797. DOI: 10.1016/j.jenvman.2020.110090.

[6] Torben Ommen, Wiebke Brix Markussen, and Brian Elmegaard. "Comparison of Linear, Mixed Integer and Non-Linear Programming Methods in Energy System Dispatch Modelling". In: *Energy* 74 (Sept. 2014), pp. 109–118. ISSN: 0360-5442. DOI: 10.1016/j.energy.2014.04.023.

[7] *APMonitor Optimization Suite*. http://apmonitor.com/.

[8] Adam Paszke et al. "PyTorch: An Imperative Style, High-Performance Deep Learning Library". In: *Advances in Neural Information Processing Systems*. Ed. by H. Wallach et al. Vol. 32. Curran Associates, Inc., 2019.

[9] Petr Novák, Manuel Wimmer, and Petr Kadera. "Slicing Simulation Models into Co-simulations". In: *Industrial Applications of Holonic and Multi-Agent Systems*. Ed. by Vladimír Mařík et al. Lecture Notes in Computer Science. Cham: Springer International Publishing, 2017, pp. 111–124. ISBN: 978-3-319-64635-0. DOI: 10.1007/978-3-319-64635-0_9.

[10] Peter Palensky et al. “Cosimulation of Intelligent Power Systems: Fundamentals, Software Architecture, Numerics, and Coupling”. In: *IEEE Industrial Electronics Magazine* 11.1 (Mar. 2017), pp. 34–50. ISSN: 1941-0115. DOI: 10.1109/MIE.2016.2639825.

[11] Germán Morales-España, Laura Ramírez-Elizondo, and Benjamin F. Hobbs. “Hidden Power System Inflexibilities Imposed by Traditional Unit Commitment Formulations”. In: *Applied Energy* 191 (Apr. 2017), pp. 223–238. ISSN: 0306-2619. DOI: 10.1016/j.apenergy.2017.01.089.

[12] Niina Helistö et al. “Impact of Operational Details and Temporal Representations on Investment Planning in Energy Systems Dominated by Wind and Solar”. In: *Applied Energy* 290 (May 2021), p. 116712. ISSN: 0306-2619. DOI: 10.1016/j.apenergy.2021.116712.

[13] Jan Kraft, Tobias Meyer, and Bernhard Schweizer. “Reduction of the Computation Time of Large Multibody Systems with Co-simulation Methods”. In: *IUTAM Symposium on Solver-Coupling and Co-Simulation*. Ed. by Bernhard Schweizer. IUTAM Bookseries. Cham: Springer International Publishing, 2019, pp. 131–152. ISBN: 978-3-030-14883-6. DOI: 10.1007/978-3-030-14883-6_8.

[14] Digvijay Gusain, Miloš Cvetković, and Peter Palensky. “Energy Flexibility Analysis Using FMUWorld”. In: *2019 IEEE Milan PowerTech*. June 2019, pp. 1–6. DOI: 10.1109/PTC.2019.8810433.

[15] Digvijay Gusain et al. “Technical Assessment of Large Scale PEM Electrolyzers as Flexibility Service Providers”. In: *2020 IEEE 29th International Symposium on Industrial Electronics (ISIE)*. June 2020, pp. 1074–1078. DOI: 10.1109/ISIE45063.2020.9152462.

[16] Steffen Schütte, Stefan Scherfke, and Martin Tröschel. “Mosaik: A Framework for Modular Simulation of Active Components in Smart Grids”. In: *2011 IEEE First International Workshop on Smart Grid Modeling and Simulation (SGMS)*. Oct. 2011, pp. 55–60. DOI: 10.1109/SGMS.2011.6089027.

[17] Jose Evora Gomez, José Juan Hernández Cabrera, and Jean-Philippe Tavella. “Semantic Interoperability in Co-Simulation: Use Cases and Requirements”. In: *30th European Simulation and Modelling Conference · ESM 2016, octubre, Las Palmas de Gran Canaria, Spain, p. 5-9* (2016).

[18] Christoph Molitor et al. “MESCOS—A Multienergy System Cosimulator for City District Energy Systems”. In: *IEEE Transactions on Industrial Informatics* 10.4 (Nov. 2014), pp. 2247–2256. ISSN: 1941-0050. DOI: 10.1109/TII.2014.2334058.

[19] Michael Wetter. “Co-Simulation of Building Energy and Control Systems with the Building Controls Virtual Test Bed”. In: *Journal of Building Performance Simulation* 4.3 (Sept. 2011), pp. 185–203. ISSN: 1940-1493. DOI: 10.1080/19401493.2010.518631.

[20] Bernhard Schweizer, Daixing Lu, and Pu Li. “Co-Simulation Method for Solver Coupling with Algebraic Constraints Incorporating Relaxation Techniques”. In: *Multibody System Dynamics* 36.1 (Jan. 2016), pp. 1–36. ISSN: 1384-5640, 1573-272X. DOI: 10.1007/s11044-015-9464-9.

[21] Leon Thurner et al. “Pandapower—An Open-Source Python Tool for Convenient Modeling, Analysis, and Optimization of Electric Power Systems”. In: *IEEE Transactions on Power Systems* 33.6 (Nov. 2018), pp. 6510–6521. ISSN: 1558-0679. DOI: 10.1109/TPWRS.2018.2829021.

[22] Chang Liu et al. “A Wind Power Plant with Thermal Energy Storage for Improving the Utilization of Wind Energy”. In: *Energies* 10.12 (Dec. 2017), p. 2126. DOI: 10.3390/en10122126.

[23] Benedikt Leitner et al. “A Method for Technical Assessment of Power-to-Heat Use Cases to Couple Local District Heating and Electrical Distribution Grids”. In: *Energy* 182 (Sept. 2019), pp. 729–738. ISSN: 0360-5442. DOI: 10.1016/j.energy.2019.06.016.

[24] Edmund Widl et al. “Combined Optimal Design and Control of Hybrid Thermal-Electrical Distribution Grids Using Co-Simulation”. In: *Energies* 13.8 (Jan. 2020), p. 1945. DOI: 10.3390/en13081945.

[25] Francesco Neirotti et al. “Analysis of Different Strategies for Lowering the Operation Temperature in Existing District Heating Networks”. In: *Energies* 12.2 (2019), pp. 1–17.

[26] Stephane Vialle et al. “Scaling FMI-CS Based Multi-Simulation Beyond Thousand FMUs on Infiniband Cluster”. In: *The 12th International Modelica Conference, Prague, Czech Republic, May 15-17, 2017*. July 2017, pp. 673–682. DOI: 10.3384/ecp17132673.

[27] Stian Backe, Magnus Korpås, and Asgeir Tomasgard. “Heat and Electric Vehicle Flexibility in the European Power System: A Case Study of Norwegian Energy Communities”. In: *International Journal of Electrical Power & Energy Systems* 125 (Feb. 2021), p. 106479. ISSN: 0142-0615. DOI: 10.1016/j.ijepes.2020.106479.

[28] Daniel Lohmeier et al. “Pandapipes: An Open-Source Piping Grid Calculation Package for Multi-Energy Grid Simulations”. In: *Sustainability* 12.23 (Jan. 2020), p. 9899. DOI: 10.3390/su12239899.

[29] N. Bogunović et al. “Application of PandaPower Tool in Evaluating the Potential of Using PV Distributed Generation for Voltage Regulation in Electrical Power Networks”. In: *2020 43rd International Convention on Information, Communication and Electronic Technology (MIPRO)*. Sept. 2020, pp. 912–917. DOI: 10.23919/MIPRO48935.2020.9245182.

[30] Claudio David López, Miloš Cvetković, and Peter Palensky. “Distributed Co-Simulation for Collaborative Analysis of Power System Dynamic Behavior”. In: *Mediterranean Conference on Power Generation, Transmission, Distribution and Energy Conversion (MEDPOWER 2018)*. Nov. 2018, pp. 1–5. DOI: 10.1049/cp.2018.1876.

[31] Claudio David López et al. “A Variable-Rate Co-Simulation Environment for the Dynamic Analysis of Multi-Area Power Systems”. In: *2017 IEEE Manchester PowerTech*. June 2017, pp. 1–6. DOI: 10.1109/PTC.2017.7981117.

[32] Miguel Aguilera et al. “Coalesced Gas Turbine and Power System Modeling and Simulation using Modelica”. In: (Feb. 2019).

[33] Jan-Peter Heckel and Christian Becker. “Advanced Modeling of Electric Components in Integrated Energy Systems with the TransiEnt Library”. In: *The 13th International Modelica Conference, Regensburg, Germany, March 4–6, 2019*. Feb. 2019, pp. 759–768. DOI: 10.3384/ecp19157759.

[34] Merkebu Z. Degefa, Hanne Sæle, and Christian Andresen. “Analysis of Future Loading Scenarios in a Norwegian LV Network”. In: *2019 International Conference on Smart Energy Systems and Technologies (SEST)*. Sept. 2019, pp. 1–6. DOI: 10.1109/SEST.2019.8849081.

[35] Bin Chen et al. “Integration of Reversible Solid Oxide Cells with Methane Synthesis (ReSOC-MS) in Grid Stabilization: A Dynamic Investigation”. In: *Applied Energy* 250 (Sept. 2019), pp. 558–567. ISSN: 0306-2619. DOI: 10.1016/j.apenergy.2019.04.162.

[36] Moritz Stûber. “Simulating a Variable-structure Model of an Electric Vehicle for Battery Life Estimation Using Modelica/Dymola and Python”. In: *The 12th International Modelica Conference, Prague, Czech Republic, May 15-17, 2017*. July 2017, pp. 291–298. DOI: 10.3384/ecp17132291.

[37] Niklas Wulff. “Emobility in Python (Emobpy) and Vehicle Energy Consumption in Python (VencoPy). Demonstration of Two Open Source Tools Describing Electric Vehicle Energy Demand”. In: *DLR Knowledge Exchange Workshop*. Germany (online), May 2020.

[38] Jorge Varela Barreras et al. “An Advanced HIL Simulation Battery Model for Battery Management System Testing”. In: *IEEE Transactions on Industry Applications* 52.6 (Nov. 2016), pp. 5086–5099. ISSN: 1939-9367. DOI: 10.1109/TIA.2016.2585539.

[39] Torsten Blochwitz et al. “The Functional Mockup Interface for Tool Independent Exchange of Simulation Models”. In: *Proceedings of the 8th International Modelica Conference*. Ed. by Christoph Clauß. Dresden: Linköping University Press, Mar. 2011, pp. 105–114. ISBN: 978-91-7393-096-3.

[40] “2021 Texas Power Crisis”. In: *Wikipedia* (Sept. 2021).

4

QUANTIFICATION OF FLEXIBILITY IN MULTI ENERGY SYSTEMS

4.1. INTRODUCTION

The increased flexibility needs in power systems have created an attractive opportunity for actors such as aggregators to act as Flexibility Service Providers (FSPs). The FSPs find customers in entities such as Virtual Power Plants (VPPs), Balance Responsible Parties (BRP), Transmission System Operators (TSO), Distribution System Operators (DSO) who require flexibility to alleviate problems such as congestion management, feeder voltage management, forecast error correction, uncertain net-load ramps management, balancing problems, etc. Of particular interest are the flexibility needs arising specifically from the forecasting of power generation of variable renewable energy sources (VRES) present at various levels in the grid. Since weather cannot be forecasted much ahead of time, the actual power generation varies from the forecasted power generation, leading to requirements for correction of forecasting errors.

The BRP holds the responsibility to manage its imbalance before the system operator (SO) takes over the responsibility of management and settlement of imbalances (typically 3-4 Program Time Units (PTU) before the time of delivery. 1 PTU = 15 mins). The penalties for causing system imbalances are already large, and expected to increase even further in the future [2]. As such, it is of interest to the BRP to arrange the required flexibility beforehand to avoid any imbalance penalties. Enabled by a growing communication infrastructure, the FSPs utilize advanced control and coordination techniques to control a pool of

Parts of this chapter have been published in Elsevier's International Journal of Electric Power and Energy Systems [1].

flexible resources which can provide valuable flexibility to the BRPs [3, 4]. Typically, these resources consist of distributed generators (DG), thermostatically controlled loads (TCLs) (refrigeration systems, thermal storage, buildings, etc.), power-to-gas (P2G) systems, electric vehicles (EVs), etc. This flexibility from the FSP can be purchased by the BRP from short-term markets such as the intraday markets [5], be contracted by the BRP as a bilateral agreement, or from some form of a demand response market (DRX) [6]. Alternatively, the FSP can operate in close cooperation with the BRP, by controlling the resources in the BRP portfolio to fulfill the BRP's flexibility needs. The advantage of this idea is that the internal imbalances caused by the activation of flexibility are known to the BRP, and are managed as part of the flexibility provision scheme [7]. Such a model is already used by energy suppliers in the Netherlands [8].

In either case, it is crucial for the FSP to accurately assess and quantify the flexibility of its portfolio in order to provide reliable service. Estimating the flexibility of a pool of resources, however, is a challenging task. A pool of resources can have a diverse set of characteristics such as ramp rates, up/downtimes, power ratings, etc. If the characteristics of each of the resources are represented as a set of static time-invariant values such as power deviations, ramp rates, etc., then methods derived from set theory can be used to represent the aggregated flexibility. This is referred to as the *available flexibility*. The amount of flexibility that can be dispatched, however, can be different. It can be constrained by factors such as device inter-temporal constraints, network capacity constraints, the geospatial spread of the flexible resources on the network, and even the operational strategy employed. Furthermore, the uncertainty of the flexible load demand and the VRES generation can lend additional complexity to the problem of quantification. This much more constrained form of flexibility is referred to as the *operational flexibility*. In this thesis, I propose three metrics to quantify operational flexibility.

In [9], the authors formulate an optimal policy for energy-constrained battery systems. In this reference, flexibility is defined as the maximum time a set of battery systems can follow a power reference signal before exhausting its energy. However, the authors do not consider ramp constraints, the network constraints, and are limited to consideration of upward flexibility, i.e., the battery systems that can only discharge. In [10], the authors investigate the flexibility of a flexible resource from its location in the grid. The proposed methodology, however, does not indicate the aggregated flexibility from all such resources in the grid and does not take into account the operational strategy of the FSP. An interesting take on flexibility is seen in [11] where the authors propose a flexibility metric that does account for transmission limits. The flexibility of the system is quantified as a tuple of lower and upper bounds of the largest uncertainty under which the system

can remain operationally feasible.

The metric introduced in [11] is a deterministic one, derived from solving a robust optimization problem. Although robust optimization guarantees the feasibility and optimality of the solution even against the worst-case scenario, it does not provide an expected solution, which is more relevant for studies on the short-term markets, especially the intraday markets [12, 13]. In [14], the authors introduce the Normalized Flexibility Index as a metric to quantify flexibility in individual generating resources and the power system as a whole. The authors use deployable range, the summation of total power deviation, and the average ramp rate, to calculate the contribution of each resource to system flexibility. This approach is developed only for generation-side flexibility. Authors in [15] provide insights on the quantification of flexibility in the context of supply adequacy and reserve requirement in power systems. The quantification metric is derived from a process control paradigm, where three-dimensional polyhedra are used to represent available flexibility. The authors use this notion to assess the balancing reserves and flexibility in supply to meet the demand. However, the measure does not include flexibility from responsive demand or sector coupling.

More recently, authors in [16] have proposed two tools: Flexibility Solution Modulation Stack and Flexibility Solution Contribution Distribution to quantify flexibility from the perspective of the entity providing it, i.e. the FSP. Their focus in quantifying flexibility is limited to only power system components, and cannot take into account the flexibility from sector coupling. The authors in [17–19] have proposed flexibility envelopes. The primary application of the envelopes is for flexibility adequacy planning from a generation viewpoint. The authors account for sub-hourly dynamics by using dynamic models of the power system generators, providing flexibility to the power systems. The method proposed by the authors does not account for flexibility from sector coupling. Additionally, since the models are included within the economic dispatch framework that the authors propose, the models are simplistic linear time-invariant systems. This limits the representation of more complex, flexibility providing resources such as TCLs which have flexibility rebound effects. A rebound effect occurs when the changes in power consumption of a flexible resource from activation of flexibility at a particular time restrict its ability to do so again in subsequent time steps [20, 21].

To summarize, a useful flexibility metric must:

1. provide an assessment of portfolio-level aggregated flexibility considering operational characteristics of diverse resources in the portfolio,

2. account for resource and network constraints,

3. account for uncertainty in VRES power production, flexible load demand, and flexibility requests,

4. account for the strategy of control and coordination of resources, and finally,

5. be intuitive to understand.

In this thesis, I propose three new metrics to quantify operational flexibility. The proposed flexibility metrics are the first, to the best of the authors' knowledge, to jointly satisfy all the above requirements. The key characteristic of the newly proposed metrics is in their ability to quantify the portfolio response to uncertain flexibility requests while accounting for the network, resource, and spatio-temporal constraints and the operational strategy employed to dispatch flexibility. I use a scenario-based simulation method to achieve this.

This chapter is further divided into the following sections. Section 4.2 introduces the need for short-term flexibility planning to the FSP. Section 4.3 dives into the current flexibility quantification techniques and their limitations. Finally, it introduces the proposed metrics.

4.2. SHORT TERM FLEXIBILITY PLANNING

The increasing levels of sector integration between electricity, gas, heat, transportation, etc. have created ample opportunities for the FSP to include flexible demand in its portfolio. The demand response programs (DRP) designed by the FSP, therefore, play a crucial role in determining the amount of operational flexibility that can be extracted from its portfolio. As was previously stated, a DRP defines the conditions under which participating resources will be controlled to provide demand response. This includes setting parameters between which device will be asked to operate (such as defining temperature range for heating system in buildings), setting times and durations during which device will be asked to modulate its consumption pattern, etc. The FSP needs short-term flexibility planning to design suitable demand response policies that maximize the flexibility from its portfolio. Just as the transmission system operator (TSO) requires metrics such as EUE, LOLE, etc. to evaluate and compare long term flexibility measures (such as network expansion, generation planning, etc.), the FSP also requires metrics to evaluate short term flexibility measures (such as designing DRPs, selecting an operational strategy, comparing the value of flexibility from different products, etc.).

Figure 4.1 shows a typical scenario-based flexibility planning procedure for an FSP. The planning process is conducted well ahead of actual time of delivery of flexible energy. The FSP generates a time series of flexibility requests (called

FR signal) it expects to receive from the Flexibility Requesting Party (FRP). Since this time series is an uncertain quantity for the FSP to determine, multiple forecasts of FR signals are generated by the FSP (i.e. a scenario set consisting of FR signals is created). For each FR signal, the FSP executes an operational simulation to assess the flexibility of its portfolio. This operational simulation is conducted subject to constraints of resources in its portfolio. The bounds of these constraints are set by the FSP's DRP. Examples of such constraints can be the minimum duration for flexibility provision, the maximum number of flexibility activation requests received, temperature limits in thermal loads etc. The FSP always looks to maximize its ability to service any flexibility request it expects to receive. The results of these simulations are then quantified into flexibility metrics. These metrics help the FSP to quantify the effectiveness of DRP in use to extract flexibility from the portfolio. If flexibility in the portfolio is sufficient for the forecasted FR signals in each scenario, then the process ends. If however, for the evaluated DRP, the flexibility in portfolio is not sufficient to fulfill the forecasted FR signals, the FSP can update the DRP. When changes in DRP do not lead to any improvement in the value of metrics (i.e. do not increase the ability of portfolio to fulfill the forecasted FR signals) compared to previous iterations, then most appropriate DRP is selected. Additionally in such a case, the FSP can procure additional flexibility (for example, from intraday or demand response market or through bilateral contracts) to cover for insufficient flexibility.

The inclusion of operational simulation in Fig. 4.1 serves an important purpose in this quantification process. An important determinant of flexibility is the possible rebound effect [21, 22] that occurs after its activation. I believe that it is imperative that any flexibility quantification metric must be inclusive of this information. By executing an operational simulation, such effects are inherently captured through resource operational constraints.

4.3. FLEXIBILITY QUANTIFICATION

4.3.1. STATE OF THE ART

Some efforts have been made to quantify and represent short-term flexibility from a portfolio using static resource characteristics. For example, in the case of thermostatically controlled loads, temperature bands around the nominal operating point are used to represent flexibility [23]. Set notations have also been employed to represent the flexibility of a resource. In reference [24], the authors quantify flexibility from a single resource with a set of power, ramp rate, and energy deviations from the nominal operating point, and represent it as a polytope. When considering flexibility from a portfolio of resources, total flexibility is proposed to be calculated by applying set-theory methods. One such well-known

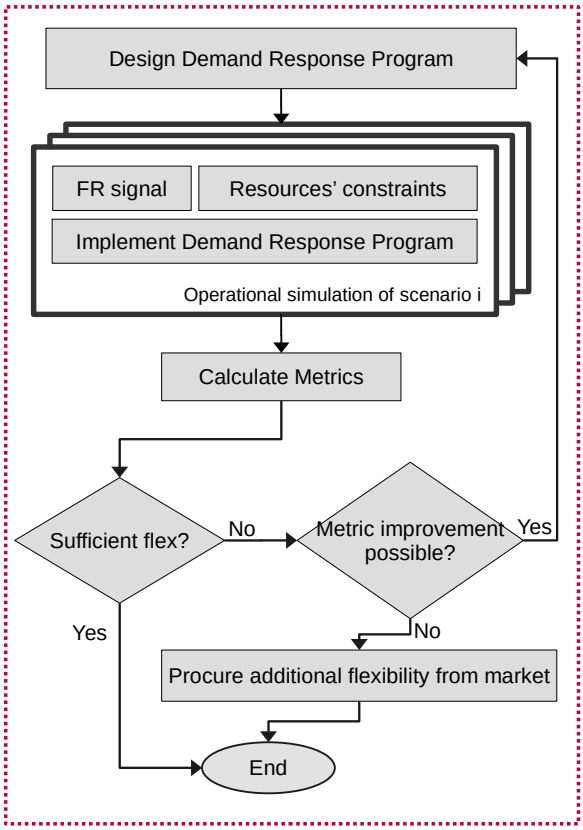

Figure 4.1: Planning for short term flexibility by the FSP. Metrics help the FSP to assess and quantify the flexibility available from its portfolio when using a particular DRP.

and ubiquitously used method is the *Minkowski Summation* as proposed in [24, 25]. However, as shown next, this is not an accurate representation of flexibility.

Consider a pool I consisting of N_i flexible resources. The flexibility of resource i at PTU (Program Time Unit) k is denoted with the set $\nu^{\uparrow,\downarrow}_{i,k} = (\Delta P^{\uparrow,\downarrow}_{i,k}, r^{\uparrow,\downarrow}_{i})$. Here, $\Delta P^{\uparrow}_{i,k}$ is the available power deviation $(\overline{P}_i - P_{i,k})$ in the upward direction and $\Delta P^{\downarrow}_{i,k}$ is the available power deviation $(P_{i,k} - \underline{P}_i)$ in the downward direction. $r^{\uparrow}_{i,k}$ and $r^{\downarrow}_{i,k}$ are the available ramp rate in upward and downward direction respectively. $P_{i,k}$ is the scheduled operating state at start of PTU k, whereas $\overline{P}_i$ and $\underline{P}_i$ are the maximum and minimum allowable power limits of resource i. The Minkowski Summation method for representing the aggregated flexibility available from this pool of N_i total resources in PTU k is given by Eq. (4.1).

$$\begin{aligned} \nu^{\uparrow}_{ms,k} &= \left(\sum_{i=1}^{I} \Delta P^{\uparrow}_{i,k}, \sum_{i=1}^{N_i} r^{\uparrow}_{i,k} \right) \\ \nu^{\downarrow}_{ms,k} &= \left(\sum_{i=1}^{I} \Delta P^{\downarrow}_{i,k}, \sum_{i=1}^{N_i} r^{\downarrow}_{i,k} \right) \end{aligned} \tag{4.1}$$

For the sake of simplicity, I focus on the case of ramping up of a resource without losing generality and drop the $\uparrow,\downarrow$ notations. Then, $\nu_{\mathrm{ms},k}$ represents the aggregated flexibility (in the upward direction) at PTU k calculated using the Minkowski summation method (denoted by subscript ms). However, since the Minkowski summation is a set summation method and is calculated for an interval of time, in this case for a PTU, it ignores the sub-hourly and sub-PTU resource inter-temporal dynamics important for flexibility assessment. To specifically account for these peculiarities in flexibility assessment, it is necessary to conduct an operational simulation.

Consider in the same PTU k, when a resource starts ramping at $t = 0$ (assuming the start of PTU corresponds to start of global time t), depending on its ramp rate, time to reach the required power level can be more or less than the PTU duration ($\tau_{\mathrm{PTU}} = 15$ mins). Here, I define *Time to Ramp*, denoted by $\tau_{i,k}$ (Eq. (4.2)), as the time taken by the resource i in PTU k to change its operating power by $\Delta P_{i,k}$ units.

$$\tau_{i,k} = \frac{\Delta P_{i,k}}{r_{i,k}} \tag{4.2}$$

If $\tau_{i,k}$ is less than the duration of a PTU, then the resource will ramp up and stay at the new power level for the remainder of the duration of the PTU as shown in Fig. 4.2. When flexibility from multiple resources is activated in PTU k, the aggregated continuous-time power profile of the portfolio will naturally be the

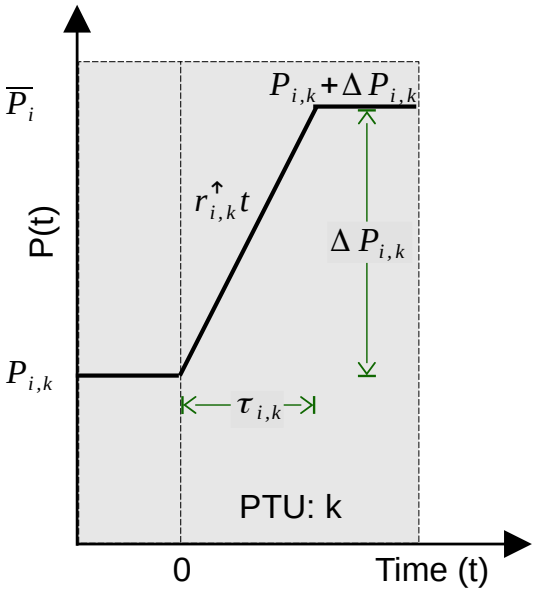

Figure 4.2: The sub-PTU power profile for resources with short time to ramp $\tau_{i,k}$.

sum of individual continuous-time power profiles (considering a copperplate network). I refer to this as an Individual Power Profile (IPP) Summation method. If all the resources have the same $\tau_{i,k}$, the ramp rate of the portfolio will be given by Eq. (4.1). Consequently, the time to ramp for the portfolio will be given by Eq. (4.3).

$$\tau_{\text{ms},k} = \frac{\sum_{i=1}^{I} \Delta P_{i,k}}{\sum_{i=1}^{I} r_{i,k}} \tag{4.3}$$

In the case where at least two resources have different $\tau_{i,k}$, the ramp rate of the aggregated power profile will decrease at each $\tau_{i,k}$, making the aggregated ramp rate of the portfolio, a piecewise linear function. This decrease occurs because at each $\tau_{i,k}$, the resource i will reach the specified power set-point and can no longer contribute to the aggregated ramp of the portfolio. Therefore, Eq. (4.4) gives the time to ramp for the portfolio.

$$\tau_{\text{agg},k} = \min(\max\{\tau_{i,k} : \forall i \in I\}, \tau_{PTU}) \tag{4.4}$$

Although it seems logical to conclude that $\tau_{\text{agg},k} = \tau_{\text{ms},k}$, it can be proved that $\tau_{\text{ms},k} \leq \tau_{\text{agg},k}$. The basis for the proof lies in *Mediant inequality*.

Proposition 4.3.1 (Mediant Inequality)**.** *For positive real numbers a, b, c, d such that $a/c \leq b/d$ then the following holds:*

$$\frac{a}{c} \leq \frac{a}{c} \oplus \frac{b}{d} \leq \frac{b}{d}$$

$$\text{where} \quad \frac{a}{c} \oplus \frac{b}{d} = \frac{a+b}{c+d}$$

Corollary 4.3.1.1. *For any PTU k, let $\Xi_k = \{\tau_{i,k} : \forall\, i \in I\}$ be the set of time to ramp for each resource in the portfolio, then,*

$$\max(\Xi_k) \geq \frac{\sum_{i=1}^{N_i} \Delta P_{i,k}}{\sum_{i=1}^{N_i} r_{i,k}}$$

Proof. In the set Ξ_k, let j be the resource with the largest $\tau_{j,k} = \frac{\Delta P_j}{r_j} = \max(\Xi_k)$. Therefore,

$$\frac{\Delta P_j}{r_j} \geq \frac{\Delta P_i}{r_i} \iff \Delta P_j \cdot r_i \geq \Delta P_i \cdot r_j \quad \forall\, i \in I$$

Then, from Proposition 4.3.1, the following holds.

$$\frac{\Delta P_j}{r_j} \geq \frac{\Delta P_1 + \cdots + \Delta P_I}{r_1 + \cdots + r_I}$$

$$\iff \Delta P_j r_1 + \ldots \Delta P_j r_I \geq \Delta P_1 r_j + \ldots \Delta P_I r_j$$

□

Since the $\tau_{\text{ms},k} \neq \tau_{\text{agg},k}$, there exists a difference between the continuous-time aggregated power profile generated using the Minkowski Summation method and that generated using the IPP Summation method. I refer to this gap as the *Flexibility Gap*.

To illustrate the flexibility gap, let us consider a small example. A portfolio of three flexible resources (R1, R2, R3), at a randomly chosen PTU k, is selected. Each of the three resources can increase their power consumption by 1 MW with ramp rates of 1.5, 2, 8 MW/PTU. The flexibility set ν of the portfolio is given by $\{(1, 1.5), (1, 2), (1, 8)\}$. Following Eq. (4.1), the total ramp, and power deviation available from the portfolio in this PTU is $\nu_{\text{ms},k} = [(3, 11.5)]$. I will drop the PTU notation (k) henceforth in this example since I consider a single PTU. I take $\Delta_t = 1$ min and $N_t = 15$, such that total time of interest is $T = \Delta_t \cdot N_t = 15$ min.

Next, consider a flexibility request $\nu_{\text{req}} = [(2.5, 11.5)]$, implying a flexibility request for $\Delta P = 2.5$ MW at 11.5 MW/PTU ramp rate. When all the resources in the

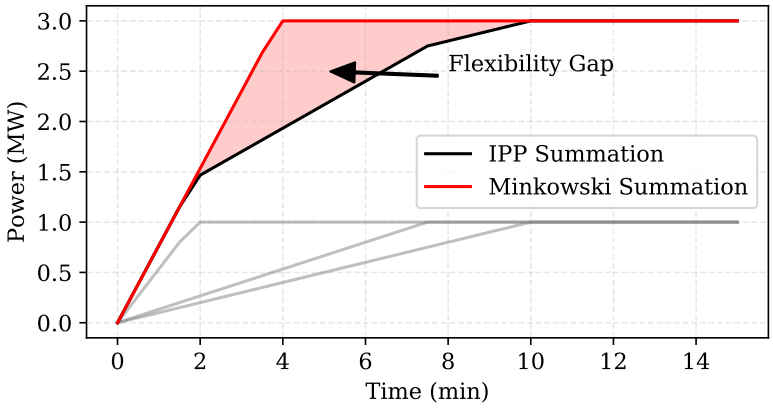

Figure 4.3: Aggregated portfolio power profile generated using Minkowski Summation method and IPP Summation method. The shaded region is the Flexibility Gap. The gray lines indicate IPP for R1, R2, and R3.

portfolio are activated simultaneously to fulfill the request, the ramp rate of the aggregated profile trajectory is $\sum r_i = 11.5$ MW/PTU. Among the three resources, the one with the lowest τ_i is R3 ($\tau_3 = 0.125$ PTU $= 2$ min). When ΔP reaches 1 MW, R3 will stop contributing to the total ramp at $t = 2$. With only R1 and R2 now contributing, the total ramp decreases to $\sum r_i = 3.5$ MW/PTU. This process will continue as R2 ($t = 7.5$ min), and then finally R1 reach their respective $\Delta P = 1$ MW ($t = 10$ min). The continuous-time power profile of the aggregated portfolio (in red) and individual resources (in gray) within the PTU is shown in Fig. 4.3. It is seen that the total portfolio ramp changes at each τ_i. In the same figure, the black line represents the power profile generated using the Minkowski Summation method. It can be seen here that $\tau_{\text{agg}} = \tau_1 \geq \tau_{\text{ms}}$, where τ_1 is the time to ramp for R1. The shaded region between the two curves is the flexibility gap.

4.3.2. INSPIRATION FROM SYSTEM ADEQUACY METRICS

In this section, I seek to be inspired by the metrics used by transmission system operators (TSO) to ensure adequacy in power systems. These will serve as an inspiration for the metrics this thesis proposes. As mentioned in Section 1.7, the TSO uses power system adequacy metrics such as LOLE and EUE to make appropriate investment and policy decisions such that system reliability is maintained. The TSO uses these metrics extensively in generation planning, network expansion planning, etc.

Since, the power system adequacy metrics were created for a system that was based on the concept of "generation must always follow demand", this concept is no longer "always" applicable to the renewable-rich power system. This limits

their applicability in future power system planning. To overcome this challenge, several authors suggested modifications to existing adequacy metrics that can assist the traditional generation adequacy studies with VRES. The Insufficient Ramp Resource Expectation (IRRE) metric proposed in [26] is a power system flexibility metric that takes into account the operational schedules of generators in the portfolio and provides the expected number of observations when the system will face ramping shortages arising from the variations in netload. Another metric introduced in [27] is called Periods of Flexibility Deficit (PFD). The PFD measures the frequency of flexibility shortfalls of specified time duration for each hour. The flexibility needs are derived from netload ramps, similar to those in IRRE. The calculation of IRRE and PFD follows that of LOLE and helps the TSO in generation planning considering challenges from VRES. These metrics quantify the system inflexibility based on which generation planning decisions (such as investments in a more high-ramping generation like gas turbines) can be formulated.

Due to this lack of metrics to quantify short-term flexibility, many studies employ power system adequacy metrics in some form to the short-term flexibility planning. Reference [28] incorporates the Expected Energy Not Served Supplied (EENS) metric with its Conditional Value at Risk (CVaR) to determine optimal sizing and location of the DER units in the distribution system using a risk-based optimization framework. In [29], the authors employ Expected Unserved Energy (EUE) and Loss of Load Probability (LOLP) to formulate a reliability constrained unit commitment problem. Other adequacy metrics such as SAIDI and SAIFI [30, 31], etc. are also employed to conduct operational studies to evaluate the impact of flexibility from DER and flexible loads in a microgrid. While the metrics IRRE and PFD overcome some challenges posed by VRES, they are still primarily focused on generation planning in the long term.

The disadvantage of using power system adequacy metrics for short-term flexibility studies stems directly from their calculation methodology, and consequently, their interpretation. Firstly, these metrics are calculated by aggregation of yearly data, which implies that sub-hourly dynamics are unaccounted for. This is important since, in operational time scales, such dynamics can constrain the amount of flexibility [32]. Secondly, the impacts stemming from activation of flexibility, such as previously mentioned flexibility rebound effects cannot be captured through these metrics. Thirdly, since these metrics are designed to evaluate the power system's ability to meet demand in the long term [33], they do not consider any network-related constraints or uncertainty in demand and VRES generation.

Despite the disadvantages, the methodology used for calculating these metrics is noteworthy because it condenses complex relationships between various

variables (such as those defined in AC and DC power flow equations) available as time-series data (yearly load, generation profiles) into a single numerical value that conveys useful information to the TSO about adequacy of generation in the power system. To the best of the authors' knowledge, metrics specifically addressing the requirements for short-term flexibility quantification highlighted in Section 4.1 do not exist. Few metrics that do quantify short term flexibility are furthermore shown to be inaccurate (Section 4.3.1).

In Section 4.3.3, I therefore propose three new flexibility quantification metrics. These metrics take inspiration from the methodology used in the calculation of system adequacy metrics, and use a simulation-based approach to address the requirements listed in Section 4.1 for a useful flexibility metric.

4.3.3. PROPOSED METRICS

Revisiting the requirements for a useful flexibility metric from Section 4.1, I propose three flexibility quantification metrics derived from scenario-based simulations. The proposed metrics provide a comprehensive overview of the operational flexibility available to the FSP from its portfolio. However, to understand and derive the metrics, it is first important to define the following terms:

- Flexibility Request (FR) signal: The FR signal (denoted by π) is a time series of power set-points that the FSP receives from the FRP.
- Unserved Flexibility (UF) signal: The UF signal (denoted by P^{π}_{UF}) is determined after running an operational simulation using the FR signal. The FSP aims to follow the FR signal as closely as possible by controlling and coordinating the resources in its portfolio. Therefore, any non-zero values of P^{π}_{UF} will imply the FSP is unable to fulfill some part of the flexibility request. Technically, if P_{sh} is the power signal that represents the power shifted by FSP to fulfill the FR signal, then, I can define P^{π}_{UF} as UF signal with Eq. (4.5).

$$P^{\pi}_{\text{UF}}(t) = |\pi(t) - P_{\text{sh}}(t)| \tag{4.5}$$

Here, the value of UF signal P^{π}_{UF} at each time step t is the absolute value of the difference between value of FR signal and P_{sh} at time step t. Now, I can now define the three metrics:

EXPECTED UNSERVED FLEXIBLE ENERGY (EUFE)

The energy in the UF signal (P^{π}_{UF}) after serving a flexibility request π is the unserved flexible energy (UFE). However, the FR signal is an uncertain quantity for

the FSP to determine. To address uncertainty in the flexibility evaluation, the FSP considers a range of FR signals ($\pi_1, \pi_2 \ldots \pi_n \in \Pi$) to obtain the expected value of the UFE. This expected value is termed as Expected Unserved Flexible Energy (EUFE) and calculated using Eq. (4.6). The EUFE metric is similar to the calculation of the power system reliability metric Expected Unserved Energy.

$$\text{EUFE} = \frac{1}{N_\pi} \cdot \sum_{\pi_i=1}^{N_\pi} (\Delta_t \cdot \sum_{t=0}^{T} P_{\text{UF}}^{\pi_i}[t]) \tag{4.6}$$

Here, $P_{UF}^{\pi_i}$ is the UF signal corresponding to the FR signal π_i and defined in MW, Δ_t is the time resolution of UF signal in *hours* and N_t is the total time steps in the UF and FR signals, and N_π is the total number of FR signal scenarios.

4

EXPECTED DURATIONS OF INSUFFICIENT FLEXIBILITY (EDIF)

The Expected Duration of Insufficient Flexibility (EDIF) is a graphical measure of flexibility. It aggregates the UF signal calculated after analyzing all the N_π number of UF signals to generate an overview of the time periods of insufficient flexibility in the portfolio and its direction and presents it as a heatmap. Each cell (m, n) in the m^{th} row and n^{th} column of the heatmap is value of $P_{\text{UF}}^{\pi_i}$ signal at in the m^{th} scenario and n^{th} time interval.

EXPECTED FLEXIBILITY INDEX (EFI)

Expected Flexibility Index or EFI provides a more general and intuitive indication of the flexibility of a portfolio. EFI is a unitless measure of the operational flexibility of the portfolio. It is the expected value of $\hat{F}_\pi(0)$ calculated over the set of FR signals ($\pi_1, \pi_2 \ldots \pi_n \in \Pi$). Here, $\hat{F}_\pi$ is the Empirical Cumulative Distribution Function (ECDF) (shown in A.1) of the UF signal P_{UF}^{π}. $\hat{F}_\pi(0)$ denotes the fraction of the UF signal π that is zero. The FSP's ability to fulfill the FR signal is indicated by $\hat{F}_\pi(0)$, which is the fraction of the total time steps where the value of P_{UF}^{π} is 0. The FSP is completely flexible to fully service the FR signal π when $\hat{F}_\pi(0) = 1$. Conversely, the FSP is completely incapable of servicing any FR signal when $\hat{F}_\pi(0) = 0$. While no particular value is a reference for EFI, the FSP should desire a value as close to 1 as possible.

4.3.4. APPLYING THE PROPOSED METRICS

Increasing distributed VRES, especially utility-scale wind and solar PV, has led to the emergence of entities such as virtual power plant operators (VPP), which aggregate these power-generating sources for trading their electricity on markets such as the day-ahead market. However, as with any VRES, which depends on unpredictable weather conditions for power generation, generation surpluses and deficits are common. Mitigating these imbalances is essential for the VPP to

avoid penalties. FSPs with a portfolio of flexible energy resources find an essential role to play in this scenario. The FR signals, in this case, will be defined with forecasts of deviation in scheduled power generation from the VRES in the VPP portfolio. The FSP can use these forecasts of FR signals to assess flexibility in its portfolio to service the VPP.

Similarly, congestion is an issue commonly encountered in electricity distribution networks. Many factors contribute to the issue of congestion within the distribution network. These include increased adoption of solar rooftop PV, higher peak loads due to electrification of heating, mobility, etc. Until DSO can upgrade its network capacity, it uses market-based solutions such as flexibility markets, day-ahead dynamic pricing, and non-market-based solutions such as bilateral contracts for demand response with industrial loads. If this does not work, it must use direct control methods such as network reconfiguration, transformer tap changing, and active and reactive power control of loads [34]. Direct load control measures can be undesirable for customers. An FSP can provide flexibility to the DSO to alleviate its congestion problems. As with the previous example, the FSP finds an essential role. FSPs can intelligently modulate the operation of the flexible resources in their portfolio and provide this flexibility to the DSO. The FSP can use the introduced metrics to assess operational flexibility in its portfolio. In this thesis, I focus on the two aforementioned power system challenges.

For these power system challenges, the FSP uses proposed metrics as part of the flexibility assessment of its portfolio (as shown in Fig. 4.1). The FSP calculates EUFE and EFI along with the EDIF heatmap and uses these to update and tune its DRP such that the portfolio is as flexible as possible to service the forecasted FR signals. The calculated metrics, therefore, allow the FSP to quantify the impact of modifying DRP in use on available flexibility from the portfolio. If the portfolio has sufficient flexibility to fulfill the forecasted FR signals, there is no need to update the DRP or procure additional flexibility. However, if the operational simulation results in insufficient flexibility, then the FSP has an option to update its DRP. As will be shown using examples in the following chapter, by modifying the parameters of the DRP, a portfolio can be made more flexible. If changes in DRP do not lead to any improvement in the value of the metrics, i.e., there still exist instances of insufficient flexibility after an operational simulation is conducted, then the FSP can procure additional flexibility from external sources itself (such as intraday market, or contracting additional flexible units).

It must be noted here that both the FR signal and the UF signal (input to the operational simulation and the output generated from it) are time series characterized by signal time resolution Δ_t and the total number of time steps N_t. The resolution of this time series depends on the type of service FSP provides. For ex-

ample, an FSP provides flexibility to address challenges such as congestion management, VRES power forecast error balancing, and others where the FR signals are specified in sub-hourly intervals (1 min, 5 min, 15 min, etc.), Δ_t will be in the same time scale. However, for an FSP providing frequency support service (where the FR signal would be the AGC signal), Δ_t will be in seconds. In either case, once these signals are known, the proposed metrics can be calculated. It is also helpful to note here that in planning for operational flexibility of its portfolio, the FSP always looks to maximize its ability to service any flexibility request it expects to receive.

4.4. DISCUSSION

Flexibility is an unavoidable necessity of the future power system, and FSPs will play a significant role in ensuring its availability. Therefore, the ability to quantify flexibility is necessary for the FSP to operate. In this chapter, I started with evaluating existing methods for flexibility quantification and assessment. The focus was on accurate quantification of short-term operational flexibility considering peculiarities arising from activation of flexibility, particularly demand response. It was shown, analytically, that the Minkowski Summation method was insufficient for estimating and assessing flexibility from a portfolio of resources with diverse characteristics. A simulation-based approach was therefore proposed. Additionally, I proposed three metrics to quantify the flexibility of a portfolio of flexible energy resources. These metrics are designed to process the data generated from the proposed simulation-based approach and provide a quantifiable way to gain insights into the flexibility of a portfolio of flexible energy resources.

However, there are a few limitations to the proposed simulation-based approach and the metrics introduced. The first one is computational complexity. The metrics are computed using scenario-based simulations, which involve executing FSP's operational policy subject to individual resource dynamics and constraints. Firstly, I assume that a model accurately represents the real-world physical system. Any approach suffers from modeling assumptions and inaccuracies when compared to reality. Secondly, if additional model complexity is included for more realistic representation (for example, including network constraints such as heat network transport delays, electric network voltage violations, etc.), the simulation problem can be hard to solve and become time-consuming. To overcome this, scenario simulations must be well formulated.

A second limitation of the method is that the quantification process depends on the accuracy of scenarios of the FR signals. While the forecasted signals will never be 100% accurate and will introduce uncertainties in the results, advanced scenario generation and reduction techniques can partially offset these limitations. Finally, the metrics EUFE and EFI provides a single expected value of the

UFE, which is generated from scenario simulations. This can be deceiving if not properly used. Since this is an expected value, extreme values are usually masked. This can lead to issues if the FSP is looking for robust solutions. In Chapter 5, these challenges are highlighted with illustrative examples.

4.5. CONCLUSIONS

The chapter focused on the problem of quantification of operational flexibility from a portfolio of flexible resources. Firstly, available and operational flexibility in power systems was clearly defined and differentiated. Next, existing methods to quantify flexibility were shown to be inadequate. I then proposed three new metrics: EUFE, EDIF, and EFI, to measure portfolio flexibility. The metrics are shown to be calculated analytically using scenario-based simulations.

BIBLIOGRAPHY

[1] Digvijay Gusain, Milos Cvetkovic, and Peter Palensky. "Quantification of Operational Flexibility from a Portfolio of Flexible Energy Resources". In: *International Journal of Electrical Power & Energy Systems* 141 (Oct. 2022), p. 107466. ISSN: 0142-0615. DOI: 10.1016/j.ijepes.2021.107466.

[2] Maria Derks. *Annual Market Update 2018*. 2018.

[3] He Hao et al. "Aggregate Flexibility of Thermostatically Controlled Loads". In: *IEEE Transactions on Power Systems* 30.1 (Jan. 2015), pp. 189–198. ISSN: 1558-0679. DOI: 10.1109/TPWRS.2014.2328865.

[4] Anna Lewandowska-Bernat and Umberto Desideri. "Opportunities of Power-to-Gas Technology". In: *Energy Procedia* 105 (May 2017), pp. 4569–4574. ISSN: 18766102. DOI: 10.1016/j.egypro.2017.03.982.

[5] José Pablo Chaves-Ávila, Rudi A. Hakvoort, and Andrés Ramos. "Short-Term Strategies for Dutch Wind Power Producers to Reduce Imbalance Costs". In: *Energy Policy*. Special Section: Transition Pathways to a Low Carbon Economy 52 (Jan. 2013), pp. 573–582. ISSN: 0301-4215. DOI: 10.1016/j.enpol.2012.10.011.

[6] Hieu Trung Nguyen, Long Bao Le, and Zhaoyu Wang. "A Bidding Strategy for Virtual Power Plants With the Intraday Demand Response Exchange Market Using the Stochastic Programming". In: *IEEE Transactions on Industry Applications* 54.4 (July 2018), pp. 3044–3055. ISSN: 1939-9367. DOI: 10.1109/TIA.2018.2828379.

[7] Aliene van der Veen et al. *USEF Flexibility Value Chain*. Tech. rep. 2018, p. 17.

[8] *Peeeks - Eneco*. https://www.eneco.nl/over-ons/wat-we-doen/duurzame-bronnen/peeeks.

[9] Michael P. Evans, Simon H. Tindemans, and David Angeli. "A Graphical Measure of Aggregate Flexibility for Energy-Constrained Distributed Resources". In: *IEEE Transactions on Smart Grid* 11.1 (Jan. 2020), pp. 106–117. ISSN: 1949-3061. DOI: 10.1109/TSG.2019.2918058.

[10] Matthias A. Bucher et al. "On Quantification of Flexibility in Power Systems". In: *2015 IEEE Eindhoven PowerTech*. June 2015, pp. 1–6. DOI: 10.1109/PTC.2015.7232514.

[11] Jinye Zhao, Tongxin Zheng, and Eugene Litvinov. "A Unified Framework for Defining and Measuring Flexibility in Power System". In: *IEEE Transactions on Power Systems* 31.1 (Jan. 2016), pp. 339–347. ISSN: 1558-0679. DOI: 10.1109/TPWRS.2015.2390038.

[12] Zhi Chen, Lei Wu, and Yong Fu. "Real-Time Price-Based Demand Response Management for Residential Appliances via Stochastic Optimization and Robust Optimization". In: *IEEE Transactions on Smart Grid* 3.4 (Dec. 2012), pp. 1822–1831. ISSN: 1949-3061. DOI: 10.1109/TSG.2012.2212729.

[13] Ming Wei and Jin Zhong. "Optimal Bidding Strategy for Demand Response Aggregator in Day-Ahead Markets via Stochastic Programming and Robust Optimization". In: *2015 12th International Conference on the European Energy Market (EEM)*. May 2015, pp. 1–5. DOI: 10.1109/EEM.2015.7216732.

[14] Juan Ma et al. "Evaluating and Planning Flexibility in Sustainable Power Systems". In: *IEEE Transactions on Sustainable Energy* 4.1 (Jan. 2013), pp. 200–209. ISSN: 1949-3029, 1949-3037. DOI: 10.1109/TSTE.2012.2212471.

[15] N. Menemenlis, M. Huneault, and A. Robitaille. "Thoughts on Power System Flexibility Quantification for the Short-Term Horizon". In: *2011 IEEE Power and Energy Society General Meeting*. July 2011, pp. 1–8. DOI: 10.1109/PES.2011.6039617.

[16] Thomas Heggarty et al. "Quantifying Power System Flexibility Provision". In: *Applied Energy* 279 (Dec. 2020), p. 115852. ISSN: 0306-2619. DOI: 10.1016/j.apenergy.2020.115852.

[17] Hussam Nosair and Francois Bouffard. "Flexibility Envelopes for Power System Operational Planning". In: *IEEE Transactions on Sustainable Energy* 6.3 (July 2015), pp. 800–809. ISSN: 1949-3029, 1949-3037. DOI: 10.1109/TSTE.2015.2410760.

[18] Hussam Nosair and François Bouffard. "Economic Dispatch Under Uncertainty: The Probabilistic Envelopes Approach". In: *IEEE Transactions on Power Systems* 32.3 (May 2017), pp. 1701–1710. ISSN: 1558-0679. DOI: 10.1109/TPWRS.2016.2602942.

[19] Hussam Nosair and Franois Bouffard. "Reconstructing Operating Reserve: Flexibility for Sustainable Power Systems". In: *IEEE Transactions on Sustainable Energy* 6.4 (Oct. 2015), pp. 1624–1637. ISSN: 1949-3037. DOI: 10.1109/TSTE.2015.2462318.

[20] Philipp Lütolf et al. "Rebound Effects of Demand-Response Management for Frequency Restoration". In: *2018 IEEE International Energy Conference (ENERGYCON)*. June 2018, pp. 1–6. DOI: 10.1109/ENERGYCON.2018.8398849.

[21] Digvijay Gusain, Miloš Cvetković, and Peter Palensky. "Energy Flexibility Analysis Using FMUWorld". In: *2019 IEEE Milan PowerTech*. June 2019, pp. 1–6. DOI: 10.1109/PTC.2019.8810433.

[22] Peter Palensky and Dietmar Dietrich. "Demand Side Management: Demand Response, Intelligent Energy Systems, and Smart Loads". In: *IEEE Transactions on Industrial Informatics* 7.3 (Aug. 2011), pp. 381–388. ISSN: 1941-0050. DOI: 10.1109/TII.2011.2158841.

[23] Rongxin Yin et al. "Quantifying Flexibility of Commercial and Residential Loads for Demand Response Using Setpoint Changes". In: *Applied Energy* 177 (Sept. 2016), pp. 149–164. ISSN: 0306-2619. DOI: 10.1016/j.apenergy.2016.05.090.

[24] Andreas Ulbig and Göran Andersson. "Analyzing Operational Flexibility of Electric Power Systems". In: *International Journal of Electrical Power & Energy Systems*. The Special Issue for 18th Power Systems Computation Conference. 72 (Nov. 2015), pp. 155–164. ISSN: 0142-0615. DOI: 10.1016/j.ijepes.2015.02.028.

[25] Lin Zhao et al. "A Geometric Approach to Aggregate Flexibility Modeling of Thermostatically Controlled Loads". In: *IEEE Transactions on Power Systems* 32.6 (Nov. 2017), pp. 4721–4731. ISSN: 0885-8950, 1558-0679. DOI: 10.1109/TPWRS.2017.2674699.

[26] Eamonn Lannoye, Damian Flynn, and Mark O'Malley. "Evaluation of Power System Flexibility". In: *IEEE Transactions on Power Systems* 27.2 (May 2012), pp. 922–931. ISSN: 1558-0679. DOI: 10.1109/TPWRS.2011.2177280.

[27] Eamonn Lannoye et al. "Assessing Power System Flexibility for Variable Renewable Integration: A Flexibility Metric for Long-Term System Planning". In: *CIGRE Science and Engineering Journal* 3 (Oct. 2015), pp. 26–39. ISSN: 2426-1335.

[28] Rodrigo Mena et al. "A Risk-Based Simulation and Multi-Objective Optimization Framework for the Integration of Distributed Renewable Generation and Storage". In: *Renewable and Sustainable Energy Reviews* 37 (Sept. 2014), pp. 778–793. ISSN: 1364-0321. DOI: 10.1016/j.rser.2014.05.046.

[29] S. Goleijani et al. "Reliability Constrained Unit Commitment in Smart Grid Environment". In: *Electric Power Systems Research* 97 (Apr. 2013), pp. 100–108. ISSN: 0378-7796. DOI: 10.1016/j.epsr.2012.12.011.

[30] S. Talari and M.R. Haghifam. “The Impact of Load and Distributed Energy Resources Management on Microgrid Reliability”. In: *22nd International Conference and Exhibition on Electricity Distribution (CIRED 2013)*. Stockholm, Sweden: Institution of Engineering and Technology, 2013, pp. 1035–1035. ISBN: 978-1-84919-732-8. DOI: 10.1049/cp.2013.1045.

[31] I. Bae and J. Kim. “Reliability Evaluation of Customers in a Microgrid”. In: *IEEE Transactions on Power Systems* 23.3 (Aug. 2008), pp. 1416–1422. ISSN: 1558-0679. DOI: 10.1109/TPWRS.2008.926710.

[32] Carlos M. Correa-Posada et al. “Dynamic Ramping Model Including Intraperiod Ramp-Rate Changes in Unit Commitment”. In: *IEEE Transactions on Sustainable Energy* 8.1 (Jan. 2017), pp. 43–50. ISSN: 1949-3029, 1949-3037. DOI: 10.1109/TSTE.2016.2578302.

[33] Directorate-General for Mobility and Transport (European Commission) et al. *Identification of Appropriate Generation and System Adequacy Standards for the Internal Electricity Market: Final Report*. LU: Publications Office of the European Union, 2014. ISBN: 978-92-79-45126-3.

[34] Shaojun Huang et al. “Review of Congestion Management Methods for Distribution Networks with High Penetration of Distributed Energy Resources”. In: *IEEE PES Innovative Smart Grid Technologies, Europe*. Oct. 2014, pp. 1–6. DOI: 10.1109/ISGTEurope.2014.7028811.

5

USE CASES FOR THE PROPOSED METRICS

5.1. INTRODUCTION

In Chapter 1 I introduced power system challenges requiring flexibility, such as VRES forecasting errors, congestion management in both transmission and distribution networks, etc. To put it in the context of this work, these power system issues determine the flexibility request signals or FR signals introduced in Chapter 1. In this chapter, I present two use cases to illustrate the FSP's use of proposed metrics in addressing these challenges.

5.2. EXAMPLE STUDY 1

In this first example, I focus on the issue of flexibility caused by VRES forecasting errors. To illustrate this, consider a region's virtual power plant (VPP) aggregating distributed wind generators. The VPP optimizes its power exchange for each hour of day D with the external grid by executing a day-ahead scheduling program on D-1. The VPP is also a BRP; once the TSO confirms the schedule, it is solely responsible for any imbalance in its portfolio. Since the VPP is a collection of distributed VRES, forecasting errors and imbalances are inevitable. It, therefore, requires flexibility to avoid unforeseen costs arising from the resulting imbalance. The VPP contracts an FSP to obtain this flexibility. The FSP can use multiple electrical and thermal loads connected to the local electric and heat network and exploit their flexibility. Therefore, the FSP must evaluate its portfolio's flexibility to adequately assist the VPP in managing its imbalance.

Parts of this chapter have been published in Elsevier's International Journal of Electric Power and Energy Systems [1].

5.2.1. FSP'S PORTFOLIO DESCRIPTION

In this example, the portfolio of the FSP is a multi-energy system (as shown in Fig. 5.1). Selecting the FSP portfolio as a multi-energy case study instead of a pure power system is natural. As motivated in Chapter 1, the P2X resources are increasingly prevalent in our energy system and, consequently, lead to tighter integration between electricity and other energy sectors. Therefore, the flexibility of these resources requires the integrated system to be analyzed as a whole. The electric network interfaces to the higher voltage level via the main substation (here represented as an external grid (EG)). Two additional substations (SS1 and SS2) are servicing two feeders (F1 and F2). These substations are connected to EG via underground cables. SS1 connects a small-scale fuel cell (FC) to the electrical grid, while SS2 is connected to a large electrical boiler (EB). The EB interfaces the electrical grid to the local heat grid. The heat grid is responsible for supplying necessary heat to two nearby greenhouses (GH-A and GH-B). For emergencies, the heat grid also contains a gas boiler (GB) operated using natural gas. A thermal storage (TS) tank is available as a buffer to reduce the dependence on GB. A building load (B) is connected to SS2 via a heat pump (HP). The FSP controls F1, F2, FC, and EB. Additionally, it controls the temperatures inside the building (θ_{B}) and the greenhouses (θ_{GH}). The building temperature is controlled by modulating the HP power, while the temperatures inside GH-A and GH-B are controlled by modifying the thermal power demand of greenhouses. The FSP controls the EB and GB thermal power outputs to meet the thermal power demand. P_{FR} is a negative power systems load that represents the FR signals. The model of FR signals is explained in the next subsection. Table 5.1 lists the upper and lower limits of power and ramp rates of flexible resources in the given portfolio.

5.2.2. FR SIGNALS

In this case, the VPP is considered to have a significant amount of wind power in its portfolio. Due to the inherent uncertainty in wind speeds, there almost always exists a difference between the day-ahead committed power from the wind generator and the actual power generated, which gives rise to wind power forecasting errors. In this case, I assume that the VPP portfolio is dominated by wind power, and therefore, the VPP's flexibility requests comprise mainly of these wind power forecasting errors. The FSP receives this FR signal from the VPP to mitigate the forecast errors from its renewable-rich portfolio throughout the day. To plan for this, the FSP conducts an operational simulation of the portfolio using forecasts of FR signals. In [2], wind power forecasting errors can be modeled using a Gaussian distribution. The Gaussian model is parameterized by $\mathcal{N}(0, 0.1)$. This model generates forecasts of FR signals for $N_s = 10$ scenarios. A dummy power system load at the point of connection of VPP to the grid represents the

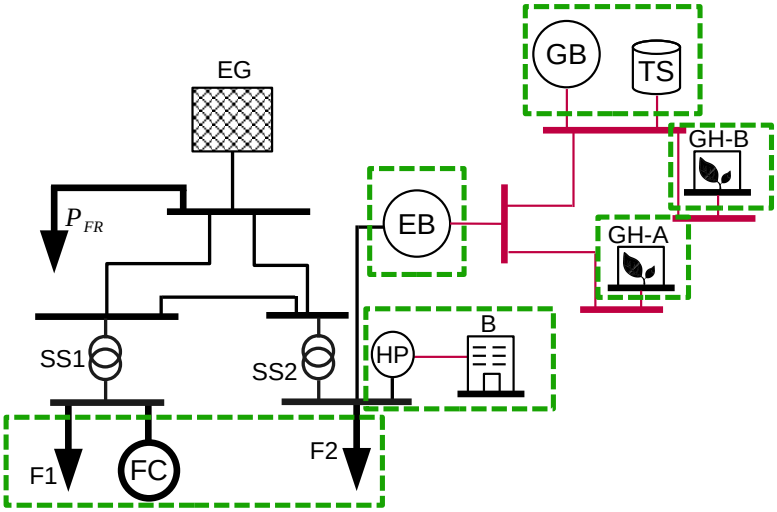

Figure 5.1: Proposed multi-energy system setup representing the FSP's portfolio. The red area represents the heat network, while the black part represents the electricity network. All the resources in FSP's portfolio are highlighted with green dashed lines. EG: External Grid, FC: Fuel Cell, HP: Heat Pump, B: Building, EB: Electric Boiler, GB: Gas Boiler (for peak demands), TS: Thermal Storage, GH: Greenhouse.

Resource	Parameter	Value	Unit
EB	$\underline{P}_{\text{EB}}, \overline{P}_{\text{EB}}$	0, 1	MW
F_i	$\underline{P}_{\text{F},i}, \overline{P}_{\text{F},i}$	0, 3	MW
F_i	$r^{\downarrow}_{\text{F},i}, r^{\uparrow}_{\text{F},i}$	-3, 3	MW/PTU
FC	$\underline{P}_{\text{FC}}, \overline{P}_{\text{FC}}$	0, 3	MW
FC	$r^{\downarrow}_{\text{FC}}, r^{\uparrow}_{\text{FC}}$	-3, 3	MW/PTU
HP	$\underline{P}_{\text{HP}}, \overline{P}_{\text{HP}}$	0, 2	MW
HP	$r^{\downarrow}_{\text{HP}}, r^{\uparrow}_{\text{HP}}$	-2, 2	MW/PTU
B	$\underline{\theta}_{\text{B}}, \overline{\theta}_{\text{B}}$	24, 25	$°C$
GH_i	$\underline{\theta}_{\text{GH}}, \overline{\theta}_{\text{GH}}$	33, 34	$°C$
GB	$\underline{P}_{\text{th,GB}}, \overline{P}_{\text{th,GB}}$	0, 0.5	MW_{th}
TS	$\underline{P}_{\text{th,TS}}, \overline{P}_{\text{th,TS}}$	-0.5, 0.5	MW_{th}
TS	$\underline{S}_{\text{TS}}, \overline{S}_{\text{TS}}$	0, 0.5	MWh_{th}

Table 5.1: Parameters for resources in the FSP's portfolio.

FR signals. For the use case defined here, since FR signals represent the VRES forecasting errors, which can be positive or negative, the value of P_{FR} can also be positive and negative depending on whether a surplus or deficit of VRES generation needs to be corrected respectively.

5.2.3. OPERATIONAL SIMULATION

As was mentioned in Section 4.2 and Section 4.3.4, the FSP looks to maximize its ability to service any flexibility request (π) it receives from the VPP. In other words, the FSP's operational policy minimizes the EUFE given by Eq. (4.6). In most markets, imbalance penalties are determined based on the magnitude and direction relative to the system imbalance position. If the BRP contributes to the system imbalance position, it is fined, while if its imbalance lies in the opposite direction relative to the system imbalance position, it is remunerated. Therefore, there is an opportunity for an entity to make money if it can ensure that its imbalance lies in a direction opposite to the system position. However, this depends on the accuracy of the forecast of system position, which can be tricky. Therefore, in this study, to simplify the matter, I minimize the absolute P^{π}_{UF} signal. This objective implies that the focus is on reducing the magnitude of imbalance regardless of its direction. The study is focused on understanding the impacts of the thermal temperature range of devices connected directly (B) and indirectly (GH-A, GH-B, TS) to the electricity grid on flexibility. In this example study, I set $\Delta_t = 15$ min and $N_t = 96$ to represent an optimal re-dispatch for an entire day. It must be noted, however, that it is also possible to consider finer resolution signals with $\Delta_t = 5$ min or $\Delta_t = 1$ min to quantify flexibility using the proposed method and metrics when resources such as electrolyzers and battery systems are included where the sub-PTU dynamics can be more relevant in the quantification process.

5.2.4. OVERVIEW OF CASE STUDIES

In total, in this example, I investigate five cases. These are divided into three subsections for easier understanding. The first subsection is *Flexibility Assessment using Minkowski Summation*. This assessment of portfolio flexibility is conducted using Minkowski summation. To compare and contrast the result of this method with the proposed method, flexibility in the portfolio is also assessed with the simulation-based approach. The simulation is modeled as an optimal dispatch problem with the objective to minimize UFE subject to equality and inequality constraints defined in A.2 and parameterized using Table 5.1. This is then taken as the base case C5.1.1. Each subsequent case builds on the results from the previous cases. The second subsection is *Flexibility Assessment for Designing DRP*. In this subsection, I formulate and investigate two cases (C5.1.2,

C5.1.3), built upon the results from C5.1.1 Herein, I show the use of proposed metrics and the heatmap to assist the FSP in updating and tuning its DRP as mentioned previously in Section 4.2 and making the portfolio more flexible. The third subsection is *Flexibility Assessment for Intraday Market Participation*. In this subsection, two more cases (C5.1.4 and C5.1.5) are formulated and investigated, further building on the results from C5.1.3. The idea here is to show the use of the proposed metrics and heatmap in assisting the VPP+FSP entity in planning and covering for flexibility shortages using the intraday market. The simulations take the form of a MILP problem, which is modeled in Python using pyomo [3] framework and solved using the Gurobi solver. All the simulations are carried out on a dual-core Intel i7-10510U CPU @ 1.80GHz running Ubuntu 20.04. The cases are further explained in the following subsections.

FLEXIBILITY ASSESSMENT USING MINKOWSKI SUMMATION

This method explicitly takes into account only the ramp rates (in MW/min) of the electrical assets of the FSP —F1, F2, FC, EB, and HP. In other words, the flexibility of resources connected to the heat grid —TS, GH-A, GH-B, GB, and the operational inter-dependencies resulting from sector coupling are not captured by this method.

As discussed previously, Minkowski Summation for flexibility assessment is not based on simulation but on set summation. The FSP using this method for flexibility assessment does so by calculating the aggregated power deviation and ramp rate available from the resources' planned operational state (the D-1 optimal power schedule) for each required interval of time and at each required time step using Eq. (4.1). This gives static upper and lower bounds on the power excursions that its portfolio can take at each time step interval. For this MES case, the Minkowski evaluated bounds are shown in Fig. 5.2.

Figure 5.2 can be interpreted as follows: the FSP is assured that there is enough flexibility in the portfolio to fulfill any received FR signal it receives at any time. In the rest of this section, I will use the metrics proposed in this paper to show that this characterization is invalid. A significant limitation here, in addition to previously mentioned issues, is that the assessment from this method does not inform the FSP of changes occurring in the event of the activation of flexibility in any resource. In such an event, the resources and, consequently, the portfolio's operational state change. The available power deviation and ramp rate from the resource change for a subsequent time step directly impact the flexibility available in subsequent periods. Therefore, a re-assessment of portfolio flexibility is needed every time flexibility in a resource is activated.

To compare with the method proposed in this paper, flexibility is evaluated by conducting a simulation-based assessment and then calculating the proposed

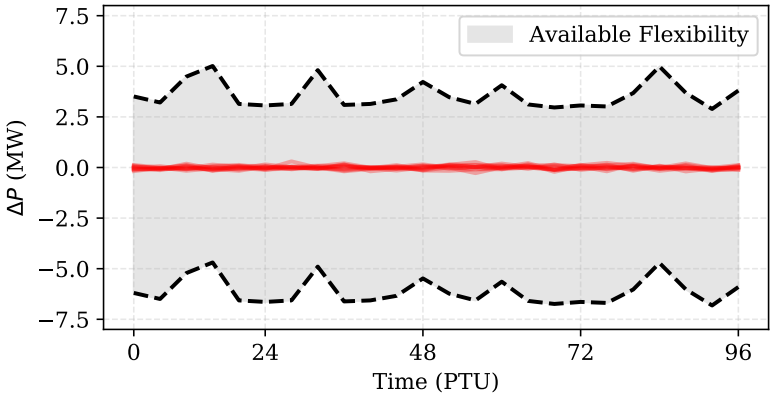

Figure 5.2: Assessing flexibility using Minkowski Summation. The red lines indicate the FR signal scenario set. The black dashed lines indicate the upper and lower levels of allowable power excursion calculated using the Minkowski method. The available flexibility bound is calculated in each PTU for the next PTU.

metrics for this case. In this baseline case C5.1.1, the parameters values in Table 5.1 for defining operational constraints given by Eqs. (A.3) to (A.15) form the DRP. The temperature in the office building is to be maintained between 24°C and 25°C. For the greenhouses, the temperature must be maintained between 33°C and 34°C. The total load on feeders F1 and F2 cannot be ramped by more than 3MW in either direction per PTU. The fuel cell generator's power rating is 3MW, which limits its flexible operation. The values for the parameters are summarized in Table 5.1.

For C5.1.1, the operational simulation results in a EUFE value of 1.858 MWh. Although the EFI is relatively high, a closer look at FR and UF signals in the worst-case scenario in Fig. 5.3 shows that while the FR signal is absorbed in most parts of the day ($P^{\pi}_{\text{UF}} = 0$), the UF signal still has significant and frequent variations in the remaining time steps. The presence of non-zero values in the UF signal (P^{π}_{UF}) highlights the insufficiency in flexibility in the portfolio to service the corresponding FR signal (π). Furthermore, the energy in the FR signal is 1.92 MWh, whereas the energy in the UF signal corresponding to this FR signal is 1.858 MWh. This result indicates that the DRP in use merely aggregates and shifts the energy in the FR signal, and there is little flexibility in the portfolio. Therefore, the current DRP is highly ineffective. As is visible in Fig. 5.4, the expected time instances (PTUs) where the FSP's portfolio flexibility is insufficient to service the FR signal scenario set Π are shown. Applying the ECDF function on the FR signal set (Π) and corresponding UF signal set (P^{Π}_{UF}) yields Fig. 5.5 which helps to visualize and calculate EFI. In C5.1.1, the EFI is 0.906.

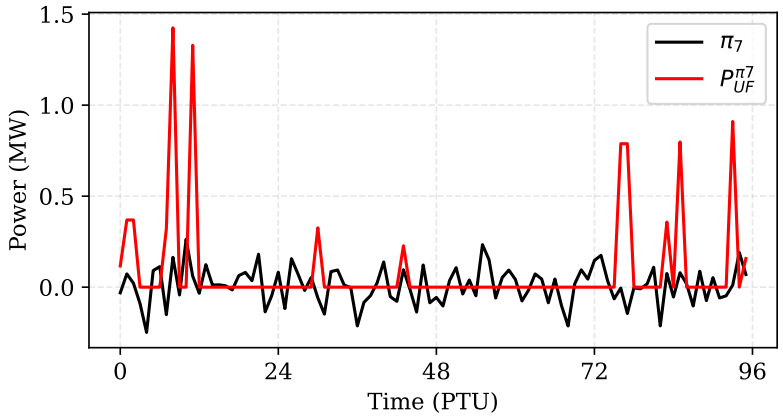

Figure 5.3: The FR signal π_7 for scenario 7 (black) and the corresponding $P^{\pi 7}_{\text{UF}}$ signal (red) in C5.1.1 which has the worst UFE. While the flexibility requests are serviced in most parts of the day ($P^{\pi 7}_{\text{UF}} = 0$), the UF signal still has large and frequent non-zero values in the other time instances, indicating that the DRP is ineffective.

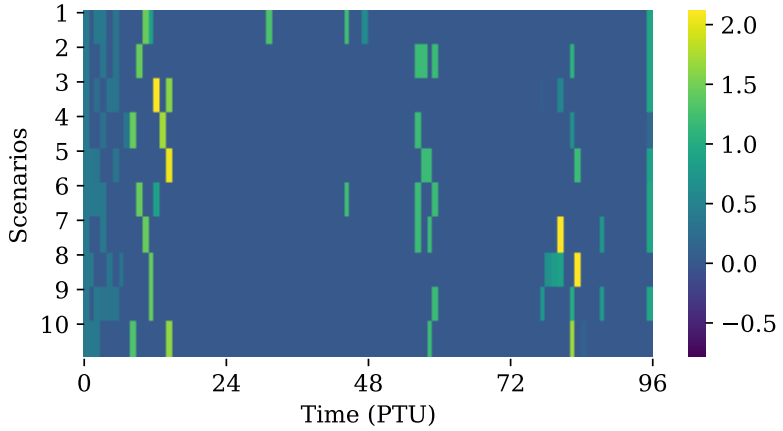

Figure 5.4: EDIF heatmap for C5.1.1. As mentioned in Section 4.3.3, each cell in a row represents the value of P^{π}_{UF}. Using the color bar as a legend, it is visible that in each scenario, there are instances of insufficient flexibility, or unserved flexibility, early in the morning, in the daytime, and then again at late night. The specific instances and magnitude of insufficient flexibility in each scenario are different, which is expected. P^{π}_{UF} in each scenario is a result of an operational simulation, a representation of system behavior if the forecast of FR signals was realized. Since the forecast in each scenario is different, the portfolio behavior, and consequently, P^{π}_{UF} is different.

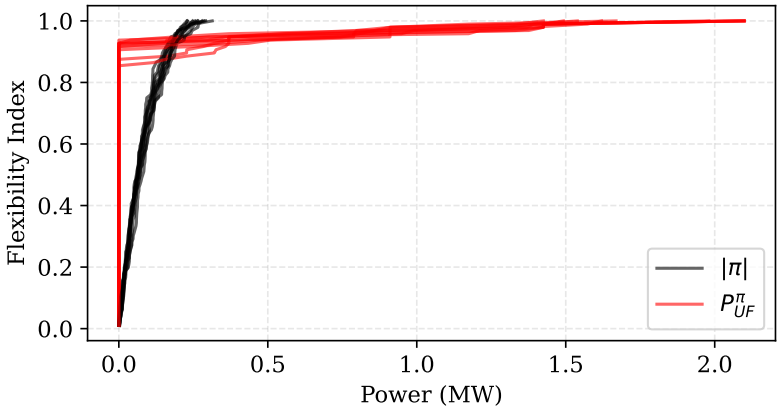

Figure 5.5: The ECDF of the FR signal set and UF signal set obtained from scenario simulations for C5.1.1 helps to visualize and calculate EFI. An *(x, y)* value on this curve indicates the ratio *y*, of values in the input signal less than or equal to value *x*. Here, vertical lines depicting P^{π}_{UF} in red indicate that over 85% of values in the UF signal for every scenario are serviced. This figure also shows that power values in the UF signal set are much larger than in the FR signal set.

5

FLEXIBILITY ASSESSMENT FOR DESIGNING DRP

It is visible from the calculated metrics, and the EDIF heatmap in C5.1.1 that used DRP on the portfolio is highly insufficient to service the FR signal set, despite the assessment made using the Minkowski Summation method. The largest magnitudes in the set of P^{π}_{UF} can be seen particularly in the early mornings, midday, and then late-night periods. The FSP will want to reduce the EUFE of its portfolio while also improving EFI. An obvious source of additional flexibility is temperature flexibility in thermal loads. An increased range for temperature variability will proportionally allow increased power variations (Eq. (A.6)) and, therefore, create greater flexibility in the portfolio. By modifying constraints in C5.1.1, two new case studies are designed: C5.1.2 and C5.1.3, representing two options for tuning the DRP.

- C5.1.2: The temperature bands are increased by $\pm 1°C$ across all three thermal loads (B, GH-A, GH-B). Since the modification is time-invariant, this is referred to as additional non-targeted DR.

- C5.1.3: The office building temperature bands are relaxed only for time intervals with low expected occupancy. The temperature limits in the building are set to $22-27°C$ between 0000h-0800h, and 1900h-0000h; to $24-25°C$ between 0800h-1900h. An additional constraint is added, which ensures that the building temperature is equal to $24°C$ at 0800h (typical start of work hour). The temperature bands for greenhouses are kept unchanged

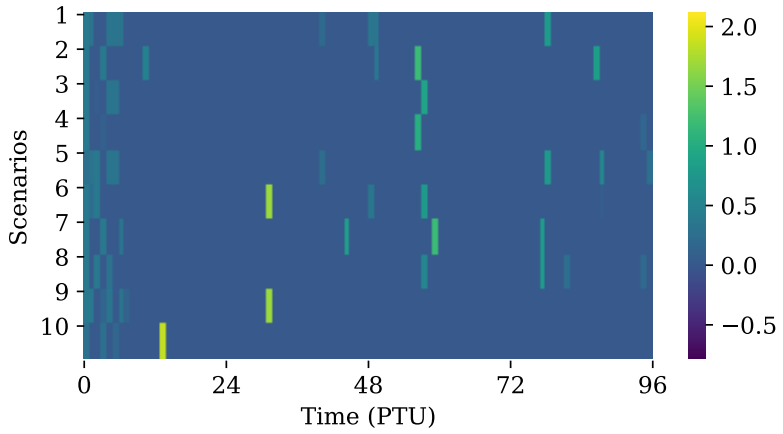

Figure 5.6: EDIF heatmap for C5.1.2. When compared with the EDIF heatmap of C5.1.1 in Fig. 5.4, it can be seen that the cells are reduced in intensity. This result implies that compared to C5.1.1, the portfolio can absorb FR signals more effectively. This reduction is made possible by increasing temperature bands on all thermal loads, which leads to significant reductions in durations of insufficient flexibility compared to C5.1.1.

from C5.1.1. The reason for this choice of DRP stems from the knowledge that crop yields are sensitive to ambient temperature variations, and therefore maintaining the greenhouse temperature will have greater priority than maintaining thermal comfort in the office temperature. Since this DR strategy has time variance, it is referred to as additional targeted DR.

The operational simulation of C5.1.2 with updated temperature ranges results in a EUFE of 0.746 MWh. This shows a reduction in EUFE of the portfolio by $\approx 60\%$ compared to C5.1.1. The EFI of 0.934 corroborates the result that increasing temperature bands by ± 1 degrees on all thermal loads can provide significant flexibility to the FSP. This is also visible with the EDIF heatmap in Fig. 5.6 where the individual cell values are reduced in intensity and frequency of occurrence across all scenarios. It can be observed that for the same PTUs with a high magnitude of unserved flexibility in C5.1.1, the corresponding values for C5.1.2 are lower, some even reduced to zero. Although the magnitude and frequency of occurrence of unserved flexibility are reduced to some extent, it exists prominently in most scenarios.

With C5.1.3, the operational simulation resulted in a EUFE value of 0.608 MWh, whereas the EFI is calculated to 0.948, which suggests that C5.1.3 offers an improvement over C5.1.2 and is, therefore, a more effective DRP. The decrease in EUFE values compared to C5.1.1 and C5.1.2 can be explained by the fact that the building heating load is directly connected to the electricity grid,

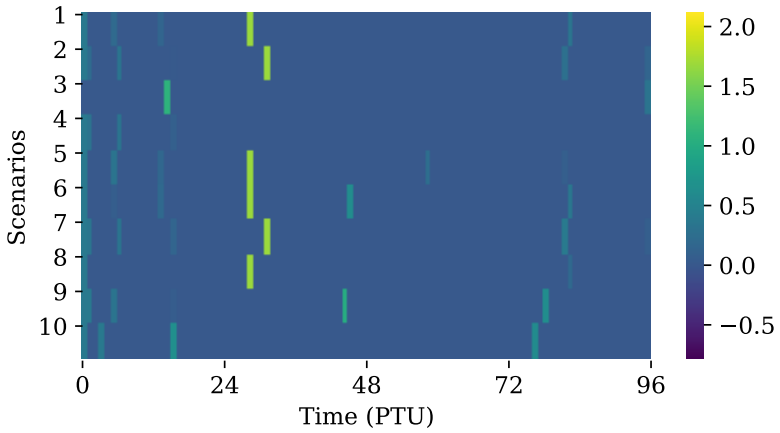

Figure 5.7: EDIF heatmap for C5.1.3. Compared to the EDIF heatmap in C5.1.2, in Fig. 5.6, it is seen that cells are further reduced in their intensity, and most cells are zero. This reduction is made possible by using targeted demand response from office building load by modifying temperature bands provides slightly more flexibility to the system than C5.1.2.

whereas the greenhouses are connected to the heat grid. While the heat storage tank, along with the peak boiler and the electric boiler, serves the loads in the heat grid, the heat load for the building is supplied only from the electricity grid. Thus, the flexibility of the building thermal load is directly available to the power system, whereas flexibility from greenhouses is indirectly available, also depending on the operating state of resources in the heat network. The EDIF heatmap for C5.1.3 shown in Fig. 5.7 shows the values of the unserved flexibility signal. Although there is not a significant difference, there seem to be lesser times of insufficient flexibility across all scenarios compared to C5.1.2.

The temperature of the office building and the greenhouses is also shown in Fig. 5.8. The larger temperature variation range in the early morning and night periods allows the building load to be more flexible with temperature variations, thus providing increased flexibility to the FSP.

As shown in these cases, the metrics EUFE, EFI, and EDIF heatmap help the FSP to compare flexibility from different DRPs and resources quantitatively. These results have been summarized in Table 5.2. It can be seen from improved EFI, and EUFE values that targeted DR actions will have a more significant impact on the operational flexibility of the FSP portfolio.

FLEXIBILITY ASSESSMENT FOR INTRADAY MARKET PARTICIPATION

Although many more combinations of DR actions can be evaluated, for brevity, I assume that this is the maximum flexibility that the FSP can obtain from its portfolio. This assumption implies that the EUFE of 0.608 MWh (value from C5.1.3)

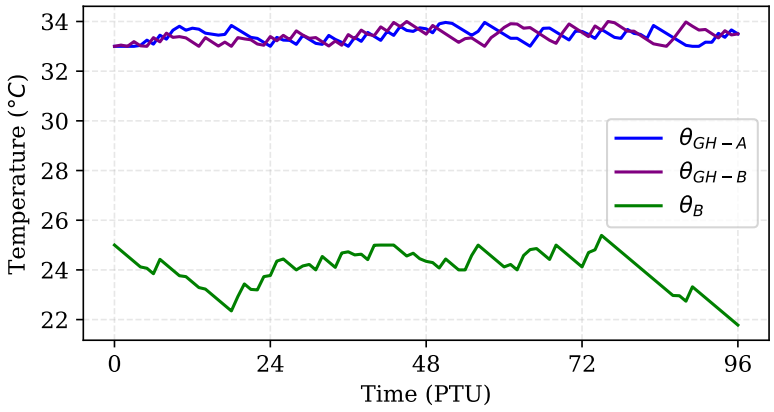

Figure 5.8: The temperatures (θ) profiles for greenhouses and office building in the FSP portfolio.

Case	EUFE	EFI	EDIF
C5.1.1	1.858	0.906	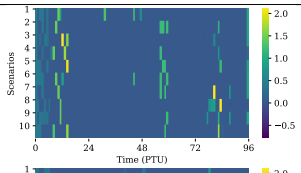
C5.1.2	0.746	0.934	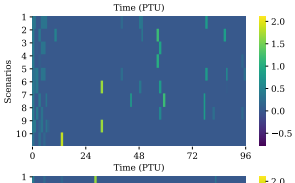
C5.1.3	0.608	0.948	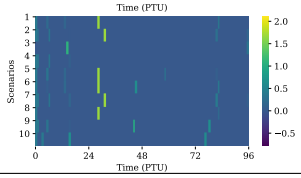

Table 5.2: Overview of results C5.1.1 to C5.1.3.

still needs to be procured from external sources, and therefore, the FSP relays this information to the VPP. In this example, the additional flexibility is procured by the VPP from the intraday market. Two strategies (and consequently, two new cases) for the VPP are envisioned:

- C5.1.4: VPP is a risk-neutral entity and buys energy equivalent to the average UFE in each PTU in C5.1.3.
- C5.1.4: VPP is a risk-averse entity and buys energy equivalent to UFE in the worst-performing scenario in C5.1.3.

In C5.1.3, the EFI value was 0.948, which implies that, on average, the portfolio was able to service flexibility requests for 94.8% of the 96 PTUs (leaving ≈ 6 PTUs to be filled) evaluated for each scenario. Therefore, on average, 0.608 MWh of energy needs to be procured for 6 PTUs per scenario. The location of these PTUs in the day can be approximated by analyzing the EDIF heatmap. Considering the EDIF heatmap for C5.1.3, the six periods of insufficient flexibility are PTUs 12, 28, 31, 45, 76, and 78. Therefore, 0.608 MWh/6 = 0.101 MWh of energy needs to be procured for each of the 6 PTUs.

In C5.1.4, I specify the power bought from the intraday market ($P_{\text{ID}}(k)$) at PTU k in Eq. (A.4) as 0.101 MWh/0.25h = 0.405 MW for each of the 6 PTUs listed. On executing the operational simulation, the EUFE value is calculated at 0.077 MWh, while the EFI is 0.987. The corresponding EDIF heatmap is shown in Fig. 5.9. The obtained values can be reasonably explained despite the expectation that procuring the calculated amount of energy will result in ideal EFI (=1) and EUFE (=0) values.

Investigating the EDIF heatmap for C5.1.3, it can be seen that inflexibility only occurs in a few scenarios at isolated PTUs, each of which is of different magnitudes. In C5.1.4, I calculated the power to be procured from the intraday market using expected values (EUFE and EFI). This approach masks a magnitude of insufficient flexibility in each PTU and scenario. For a risk-neutral VPP, this could be an acceptable solution since the EDIF heatmap suggests that most of the inflexibility is measured for some scenarios and only at a minimal number of PTUs. An EFI close to 1 (0.987) reaffirms that the small inflexibility is likely to occur in one or two PTUs in only a few scenarios.

In C5.1.4, the FSP is a risk-averse entity, which means it would analyze the worst-case scenario and plan its market participation accordingly. To achieve this position, more attention needs to be paid to the EDIF heatmap from C5.1.3. The scenario with the highest unserved flexible energy is selected, and intraday market participation is derived by analyzing this scenario. For C5.1.3, this is scenario 7. The unserved flexible energy in scenario 7 is 0.82 MWh and is seen in

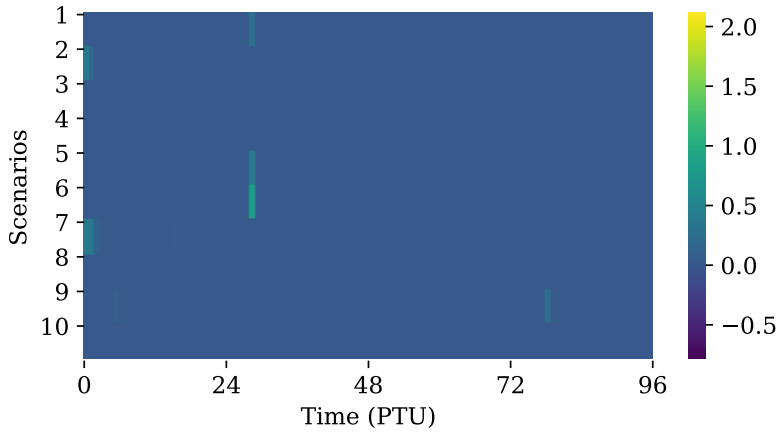

Figure 5.9: EDIF heatmap for C5.1.4. The energy to be procured from the intraday market is calculated based on the EFI and EUFE values, along with EDIF heatmap from C5.1.3.

Case	Characteristics	EUFE (MWh)	EFI	Cost (€)
C5.1.1	Baseline	1.858	0.906	38696
C5.1.2	Additional non-targeted DR	0.746	0.934	15536
C5.1.3	Additional targeted DR	0.608	0.948	12662
C5.1.4	IDM with risk-neutral VPP	0.077	0.987	1603
C5.1.4	IDM with risk-averse VPP	0.0	1.00	0

Table 5.3: Flexibility metric values for different cases

PTU 1, 2, 7, 16, 32, 82, and 96. This indicates an insufficient energy equivalent to 0.82 MWh/6 = 0.1171 MWh for each PTU that needs to be procured from the intraday market. The value of P_{ID} for these PTUs is set to 0.1171 MWh/0.25h = 0.4686 MW in Eq. (A.4). The operational simulation with the updated values of P_{ID} results in EUFE of 0, and EFI of 1. The EDIF heatmap for C5.1.4 is shown in Fig. 5.10, where it can be seen that there are no streaks, implying in all scenarios, flexibility requirements are fully met with the proposed intraday market participation. The FR and UF signals for the evaluated scenario seven are shown in Fig. 5.11. Figure 5.12 represents the ECDF chart for signals in C5.1.4. The results from the cases are summarized in Table 5.3 and plotted in Fig. 5.13.

5.2.5. ECONOMIC ANALYSIS

While EUFE indicates the volume of the flexible energy, the value for FSP in using the proposed method to design DRPs can be best motivated by analyzing the unforeseen costs it would incur due to inaccurate flexibility assessment. In the UK, according to ref. [4], the average imbalance price in 2019 was 57.06 €/MWh. The

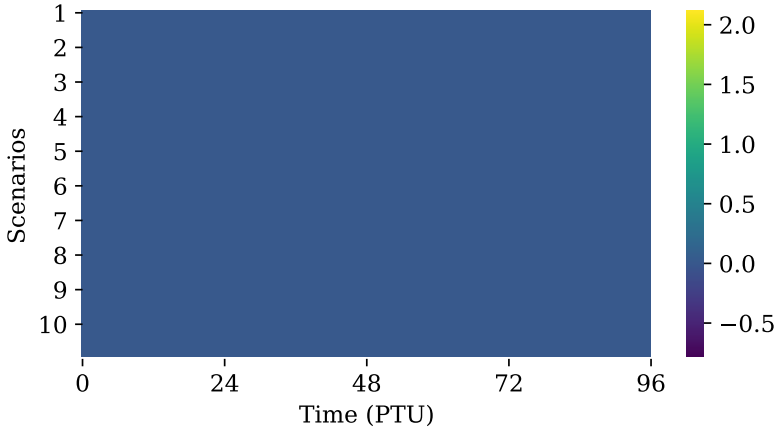

Figure 5.10: EDIF heatmap for C5.1.5. No streaks indicate that the expected procured energy from the intraday market will be sufficient to guarantee that any expected flexibility request from VPP can be accommodated.

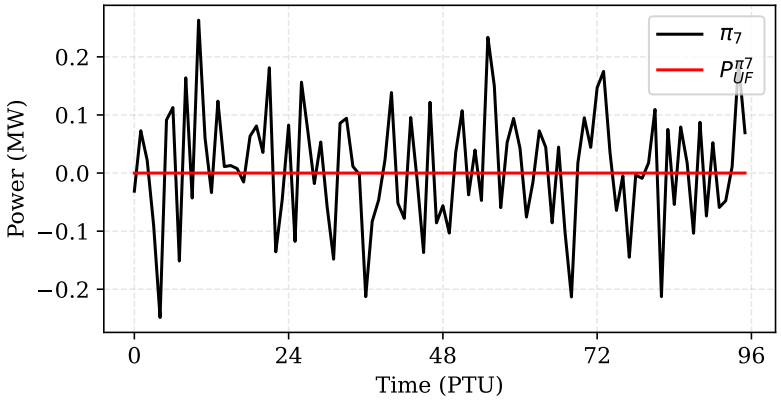

Figure 5.11: This figure shows the FR signal π_7 for scenario seven and the corresponding UF signal $P_{\text{UF}}^{\pi 7}$ for C5.1.5. The unserved flexibility is zero, implying the portfolio can fulfill the FR request.

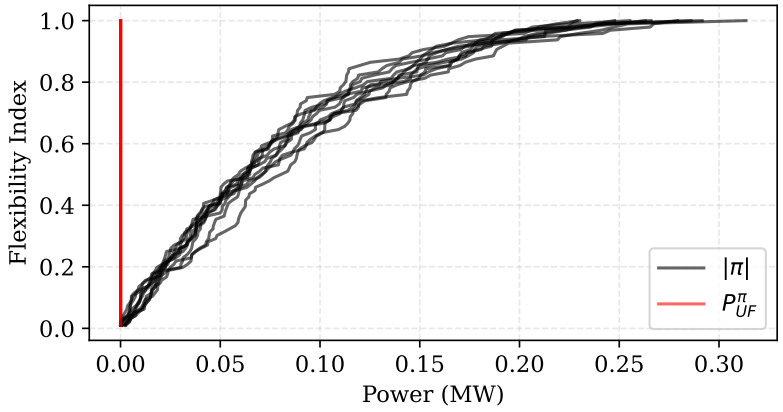

Figure 5.12: This figure shows the ECDF curves for FR and UF signals in C5.1.5. A vertical line of the UF signal at 0 shows that the flexibility index is 1, implying a fully flexible portfolio.

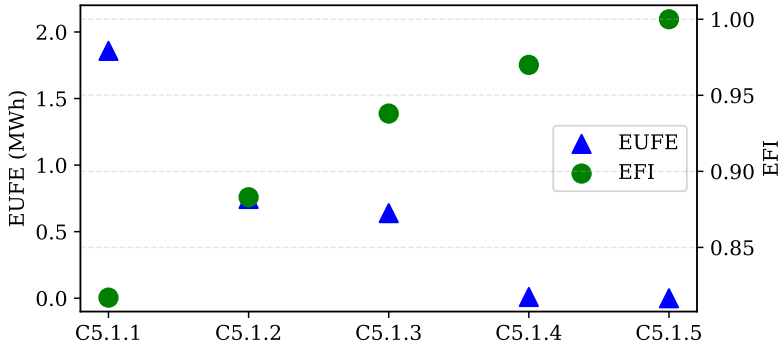

Figure 5.13: Comparison of EUFE and EFI for all 5 cases.

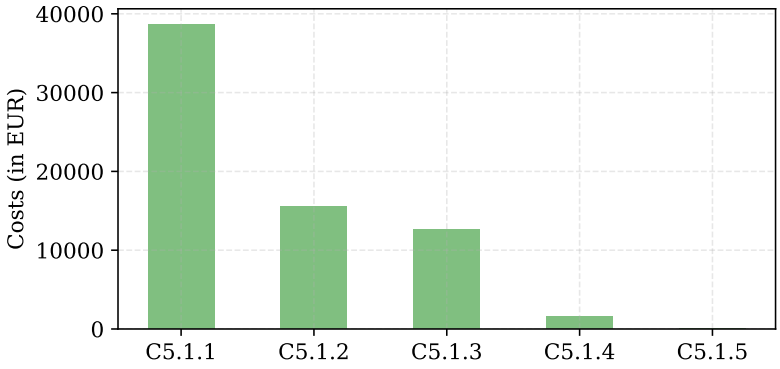

Figure 5.14: Comparison of imbalance penalties for the FSP when using the Minkowski Summation method (C5.1.1) and proposed method for flexibility assessment (C5.1.2, C5.1.3, C5.1.4, and C5.1.5). The costs are yearly cumulative imbalance costs faced by the considered FSP due to insufficient flexibility in the portfolio.

Minkowski summation method for flexibility quantification suggested that portfolio flexibility was sufficient to fulfill every FR signal request at each time step. However, using the simulation-based approach, I determined that the EUFE is 1.858 MWh. For the FSP, this directly translates to a yearly cost of € 38696. With tuning of DRP, as shown with C5.1.2 and C5.1.3, the FSP can reduce the EUFE to 0.746 MWh and 0.608 MWh, respectively. Consequently, its imbalance costs decrease to € 15536 and € 12662 respectively. When FSP engages in timely intraday or day-ahead market participation to correct this expected insufficiency in the flexibility calculated in C5.1.3, then, as shown in C5.1.4 and C5.1.4, the EUFE and consequently its costs are further reduced to € 1603 and € 0 respectively, a negligible amount compared to C5.1.1. The economic results are summarized in Fig. 5.14 and tabulated alongside the technical results in Table 5.3. This analysis shows that the proposed method offers the FSP a significant economic benefit, even in highly volatile balancing markets.

5.3. EXAMPLE STUDY 2

In this case study, I focus on the second application area of the proposed metrics – DSO congestion management. Here, the DSO is considered to contract an FSP controlling flexible units in the distribution grid to alleviate congestion issues.

5.3.1. FSP'S PORTFOLIO DESCRIPTION

The FSP's portfolio consists of $N_i = 2000$ units of integrated electric water boilers each with rated power of $P_{\text{rated}} = 15kW$ with electric boiler and storage tank (EBST). The EBST units service hot water requirements in buildings and residen-

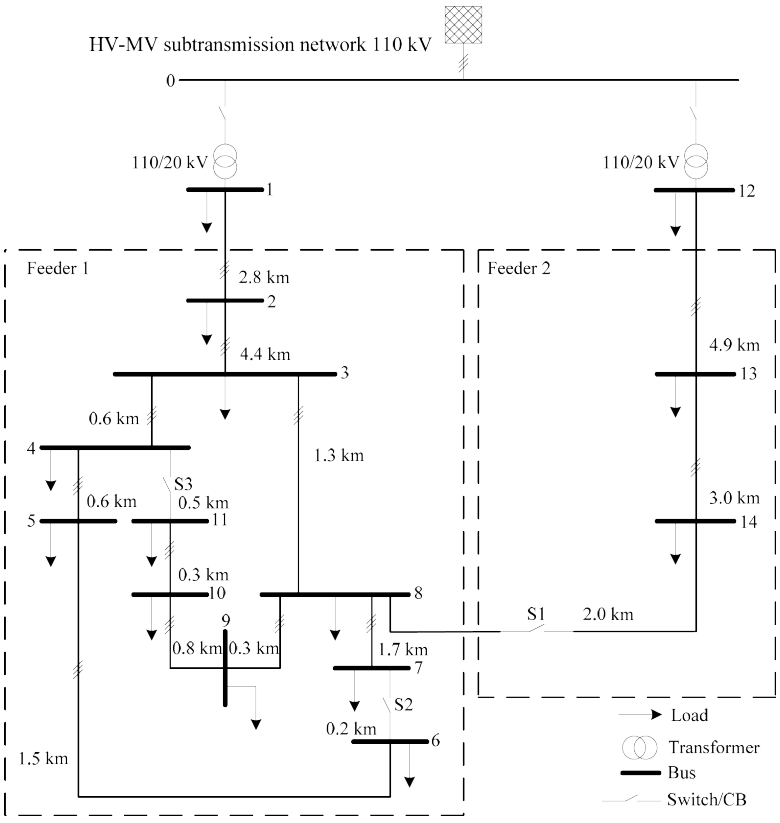

Figure 5.15: CIGRE medium voltage network used for deriving FR signals. The VRES in the network is assumed to be solar rooftop PV systems aggregated at the MV node.

tial households. These units are assumed to be scattered all over the distribution network. The FSP utilizes flexibility in the operation of these EBST units to keep the temperature in the integrated tank within the acceptable range, in this example, between 33° and 34° C. Thermal power consumption and losses to the ambient environment in the integrated thermal storage tank are taken to be a constant 7.5 kW.

5.3.2. FR SIGNALS

A CIGRE medium voltage network [5] is used to generate a realistic representation of FR signals. The network is shown in Fig. 5.15. For each load, a base load profile is generated using its nominal load value in the CIGRE model and scaled to a representative load profile that depicts a typical residential consumption pattern in the Netherlands. This representative load profile is obtained from NEDU (www.nedu.nl). Then, for each scenario, a gaussian model $\mathcal{N}(P_d[t], P_d[t]/10)$

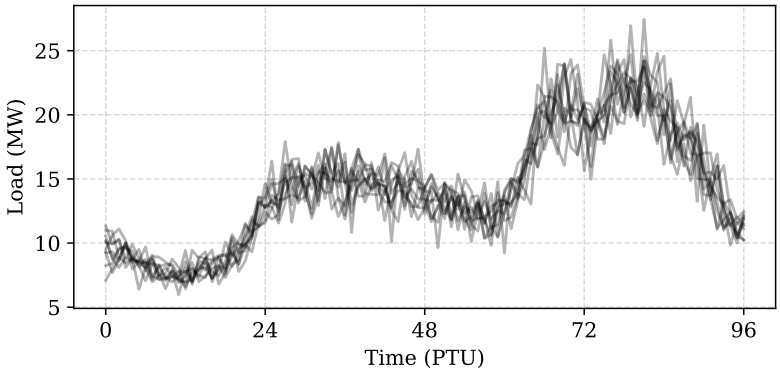

Figure 5.16: For each load in the network in Fig. 5.15, $N_s = 10$ scenarios are generated, with each scenario consisting of load profiles for each load. This figure illustrates the constructed load profile for load 1 for each scenario. Similar load profiles are constructed for every load in the network for each scenario.

is used to generate load profile for each load. Here, $P[t]$ is the value at time t for load d in its base load profile. This model is sampled at each time step t to generate the load profile for load d for that scenario. Power flow calculations are executed at every 15-minute interval for a full day to obtain approximate congestion magnitude and time. This is done for $N_s = 10$ scenarios. The heatmap in Fig. 5.17 shows that the congestion is most likely to occur during the evening time when the solar PV generation declines and the general load consumption increases.

Zooming in on the evening period, as shown in Fig. 5.18, it can be seen that loading at the transformer can reach up to 180% in specific scenarios. Assuming that the maximum loading at the transformer is allowed to be only 100% at any time (although in reality, it can momentarily be around 120%), the FR signal set is generated by Eq. (5.1), where P^{ss} is the active power through the transformer at the substation, and nom subscript stands for a nominal power of the transformer.

$$\pi = P^{\text{ss}} - P^{\text{ss}}_{\text{nom}} \tag{5.1}$$

The generated FR signal set Π is shown in Fig. 5.19.

5.3.3. OPERATIONAL SIMULATION

The FSP controls the operation of EBST to provide flexibility to the DSO. Firstly, based on the FR signal, the FSP determines the number of EBST units it requires to turn OFF such that the required reduction in demand is achieved (N_{req}). Once this is determined, the FSP takes stock of the number of EBST units available to

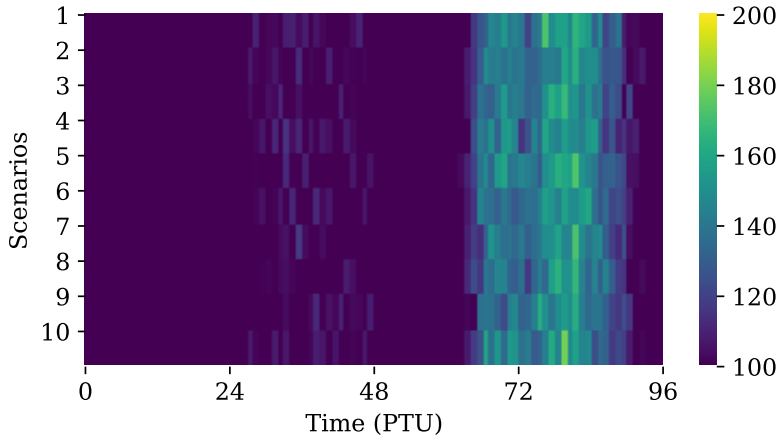

Figure 5.17: Loading at the substation transformers. The value is the average loading at the two transformer sites. The axis originates at 100% loading since values below 100% are not interesting to consider for congestion.

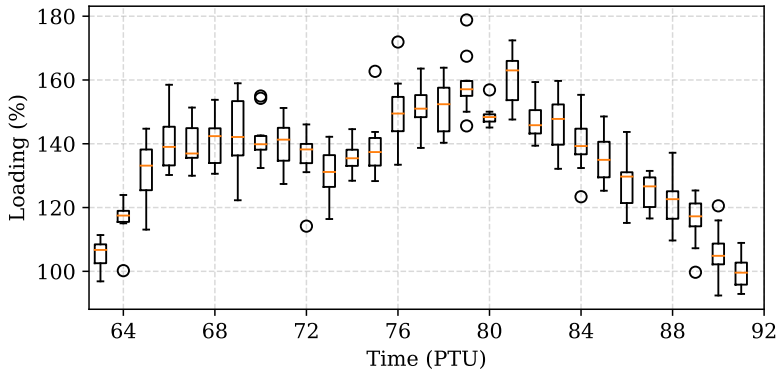

Figure 5.18: Box plot highlighting congestion in evening period. At every time instance, median loading (orange lines) at the substations is more than 100%. The box captures values from the data's first to the third quartile. Other aspects of the boxplot are explained in https://en.wikipedia.org/wiki/Box_plot.

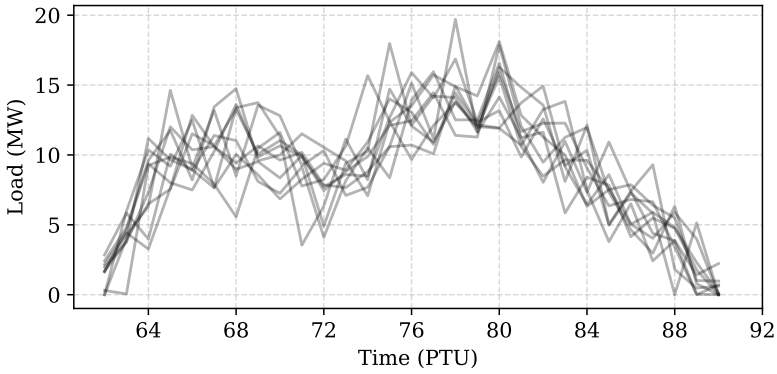

Figure 5.19: FR signals $\pi_1, \pi_2, ..\pi_{10} \in \Pi$ generated according to Eq. (5.1).

it for the demand reduction process (N_{ava}) from the pool of all units (N_{tot}). The following conditions must be met for an EBST unit to be available:

- The temperature of the water in the storage tank is between 33° and 34° C.
- The EBST must already be in ON state (i.e., it must be charging).

If the number of EBST units required N_{req} is less than the total number of units available for demand reduction N_{ava}, then N_{req} units are selected at random from pool of N_{ava} EBST units, otherwise, all N_{ava} units are selected. To add realism and complexity to this example, I have introduced a probabilistic variable p_a associated with the EBST unit. p_a denotes the EBST units' *probability of acceptance* to FSP's request to turn the unit OFF (for example, due to the user's comfort preference, it may not turn OFF the EBST unit). In today's world, privacy is of utmost importance. A non-intrusive control scheme, which allows participants a "master control" over their resources, will always have greater preference over direct control schemes where FSP controls the participants' resources outright. Providing this option also means that the FSP is now less certain about the amount of flexibility available in its portfolio. The introduction of this variable in the simulation helps to evaluate the proposed metrics' use of the FSP, which involves probabilistic resource availability.

In Section 2.3.1, I discussed the need for detailed models of thermal storage systems when considering their flexibility. I established that the small thermal storage units, such as those used in this example, can be sufficiently modeled using first-order thermal dynamics. Therefore, the thermal dynamics in EBST units used in this example are modeled using Eq. (2.17). Each EBST unit uses an internal rule-based control scheme to maintain the temperature between the

specified limits. For each scenario simulation, the EBST units use a uniform distribution function ($U(a,b)$) for initializing the EBST temperature ($U(33,34)$) and a binomial distribution function to initialize the starting ON/OFF state. Each operational simulation provides the UFE value, which can then be used to calculate EUFE.

5.3.4. OVERVIEW OF CASE STUDIES

To assess the flexibility of the portfolio, three test cases are designed C5.2.1, C5.2.2, and C5.2.3. These are categorized under two subsections for a clearer understanding. In Section 5.3.4 I explain Case 1, where I investigate the flexibility in the portfolio of 2000 EBST available to the FSP using the Minkowski Summation method. This static flexibility assessment method does not consider the impact of flexibility activation on flexibility available in subsequent time instances. In Section 5.3.4, I assess flexibility using the proposed simulation-based assessment and calculate the proposed metrics. In this subsection, I investigate two cases, C5.2.2 and C5.2.3. In C5.2.2, the *probability of acceptance*, $p_a = 1$. Therefore, the FSP assesses flexibility, in this case, knowing that all EBST units will accept the turn OFF signal. In C5.2.3, I examine the impact of the parameter *probability of acceptance* by using different values of $p_a \leq 1$. This sensitivity analysis assesses the parameter's influence on proposed metrics EUFE and EFI.

FLEXIBILITY ASSESSMENT USING MINKOWSKI SUMMATION

As in Section 5.2, in this case, C5.2.1, I conduct an assessment of flexibility based on the current state the EBSTs are in using the Minkowski summation method. Figure 5.20 shows the number of available EBST units in each time instant in ON and OFF states averaged over all scenarios. This is calculated by executing a simple simulation where the EBSTs are allowed to function as normal without any FR signals given as inputs. The number of EBSTs in the ON state at each time instant is added up to obtain the total units that the FSP can turn OFF in that time instant.

As seen in Fig. 5.21, all the FR signals lie below the available flexibility curve determined using the Minkowski summation method between PTU 76 and 82. The EDIF heatmap supports this assessment for C5.2.1 shown in Fig. 5.22. The EDIF heatmap is generated by simulating the portfolio for each scenario. At every time instant, depending on the state of the EBST unit, the amount of flexible power available to the FSP to turn OFF is determined and compared to the FR signal. It is important to note here that since this is a Minkowski summation-based method, the simulation does not include changes in the state of EBST units from activation of flexibility. In this case, the nominal states of EBST units are first calculated and then used to determine available flexibility at each time instant.

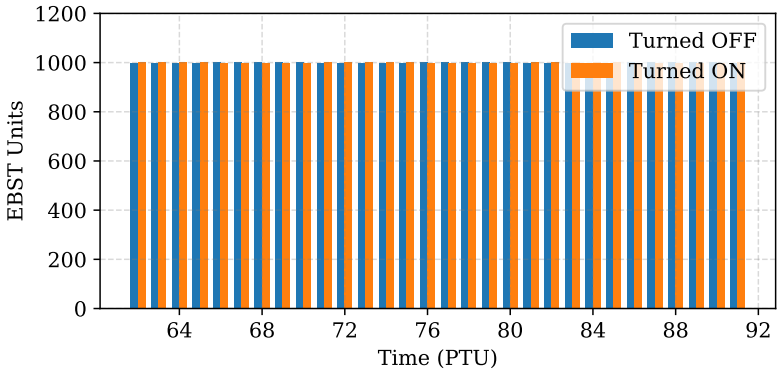

Figure 5.20: Availability of EBST units under nominal operating conditions averaged over all scenarios. Every EBST unit's temperature is initialized using a uniform distribution, while its ON/OFF status is initialized with a binomial distribution. Due to this initialization, there are an almost similar number of EBST units in ON and OFF states (1000) at each time instant.

From Fig. 5.22, it is visible that the portfolio can provide adequate flexibility since most cells have a zero value except for a few time instances between PTU 76 and 82, indicating insufficient flexibility in those time instances.

The EUFE for this case is calculated at 0.602 MWh, whereas the EFI is 0.9724. For comparison, the average energy in the FR signal set is 64.42 MWh. Therefore, the Minkowski method suggests that a portfolio of 2000 EBST units can provide the majority of flexibility the DSO needs, with a deficiency of only 0.602 MWh expected.

FLEXIBILITY ASSESSMENT USING PROPOSED METHOD

In C5.2.1, by not considering flexibility requests within the simulation, the flexibility in the system was calculated to be sufficient. However, as mentioned, changes in EBST unit states due to activation of flexibility at all time instants were not considered. This assumption impacts flexibility assessment from the portfolio. This section addresses this assumption by conducting a simulation where activation of flexibility from EBST units changes the subsequent ability of the EBST unit to be available for flexibility. Furthermore, in this case, $p_a = 1$; therefore, it is known with 100% certainty that flexibility signals given to selected EBST units are accepted. The EDIF heatmap for C5.2.2 is given in Fig. 5.23. This EDIF heatmap shows that the portfolio is not as flexible as determined in C5.2.1 using the Minkowski Summation method.

The EUFE value also corroborates this finding for this case, which comes to 30.69 MWh, whereas the EFI comes to 0.048, which indicates that, on average, the portfolio can only fully service 5% of the signals in the FR signal set. Therefore, the portfolio is not as flexible as it may seem. Figure 5.24 shows the power profiles

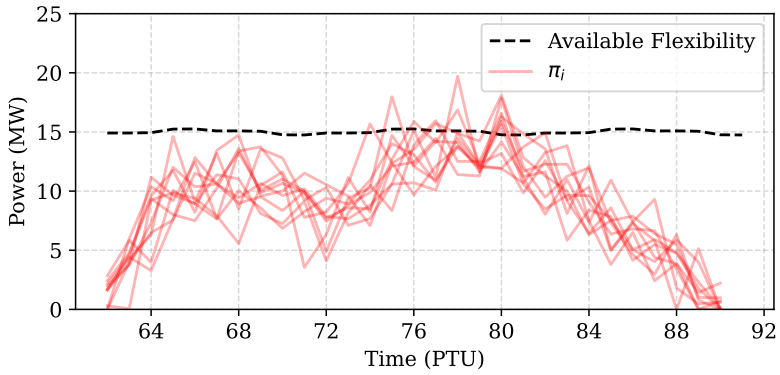

Figure 5.21: The available flexibility calculated from the average availability of EBST units over all scenarios using the Minkowski method is shown in the black dashed line. This corresponds to the total power available to be turned OFF at each time instant (obtained by assessing Fig. 5.20). The red curves correspond to the FR signal set.

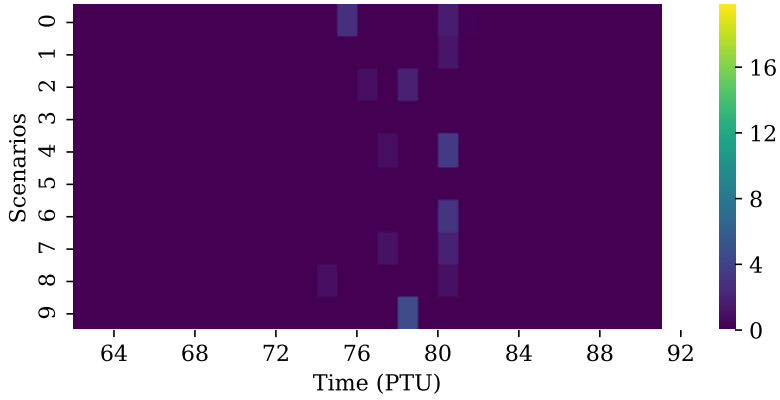

Figure 5.22: EDIF heatmap corresponding to C5.2.1. A few cells have non-zero values between PTUs 76 and 82, indicating insufficient flexibility in those instances. This result is also corroborated by Fig. 5.21 where part of the FR signal set lies above the Minkowski method's available flexibility curve.

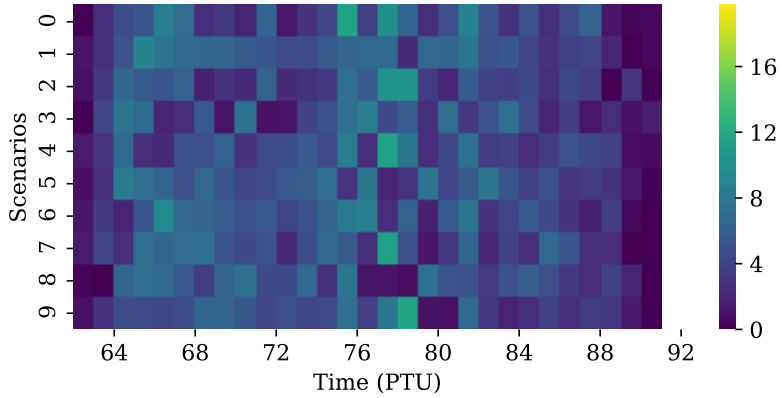

Figure 5.23: EDIF heatmap for C5.2.2. As opposed to EDIF heatmap from C5.2.1, which suggested that the portfolio was amply flexible, the simulation-based approach suggests that the portfolio is not as flexible. In each scenario, there are many time instances where the FSP portfolio does not fully service the FR signal.

of the ten considered scenarios of FR signal set (Π) and the corresponding UF signals (P_{Π}^{UF}) obtained from the simulation.

SENSITIVITY TO p_a

In C5.2.1, the EBSTs were assumed to always respond to the FSP signal. However, in reality, this may not always be the case. The individual EBST unit may decline to accept the FSP's request to turn it OFF. This stochastic nature of flexible resource operation is important for the FSP to assess flexibility. In this case, C5.2.3, I evaluate this very phenomenon. Table 5.4 tabulates the change in EUFE and EFI values for the same simulation setup as in C5.2.2 but with different probability of acceptance values used for the EBST units. This is also plotted in Fig. 5.25.

Probability of Acceptance	EUFE (MWh)	EFI
0.5	48.982	3.793
0.6	45.617	3.862
0.7	41.732	4
0.8	38.305	4.069
0.9	34.637	4.138
1	30.690	4.896

Table 5.4: Flexibility metric values for different values of p_a for case C5.2.3.

As can be seen, for lower values of p_a, the EUFE is closer to EUFE of C5.2.1, whereas for a $p_a = 1$, the EUFE is equal to that of C5.2.2. This is understandable since if there is only a 50% chance that the EBST unit accepts the flexibility re-

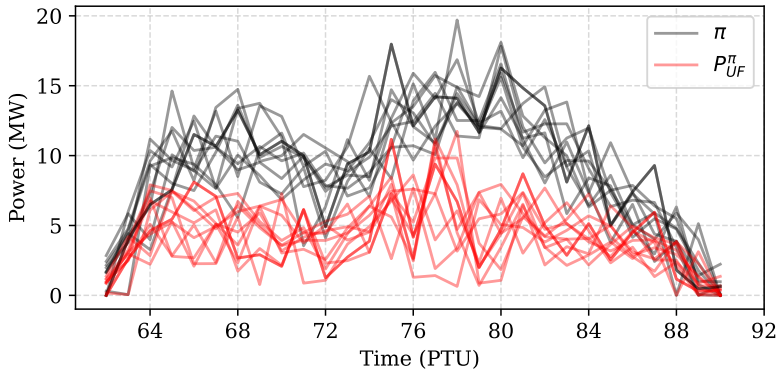

Figure 5.24: FR and UF signal sets are shown in black and red, respectively. A UF signal close to zero implies the FR signal is fully serviced. In this case, in almost all time instances, the UF signal is non-zero.

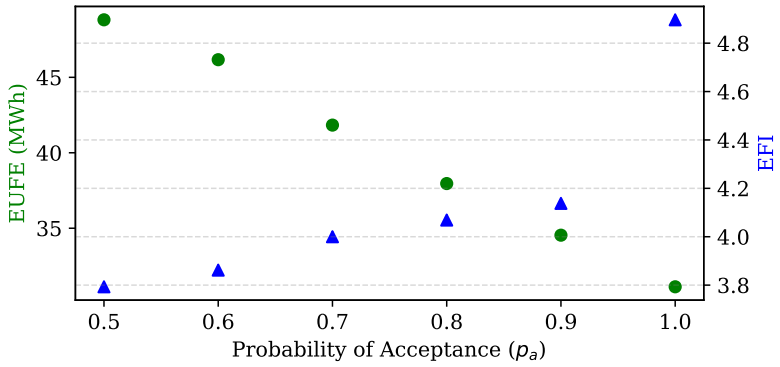

Figure 5.25: Change in EUFE and EFI for different values of p_a for case C5.2.3.

quest signal to turn OFF the EBST, then the amount of flexibility available from the n selected resources will be lower than the case when it is known with complete certainty that flexibility from all units is available. Using historical data, the FSP can estimate the participation factor from its portfolio and use that information to assess the amount of flexibility in the portfolio.

The DSO uses the information provided by the FSP to determine further actions on the grid to mitigate congestion issues. These actions are transformer tap-changes, network reconfiguration, and ultimately load shedding. An accurate and timely assessment of flexibility available to the FSP can help it support the DSO operation by avoiding untimely and undesirable mitigation actions such as load shedding.

5.4. DISCUSSION

A simulation-based approach enables a more accurate assessment of the flexibility of a portfolio of flexible resources. A unique advantage of the proposed metrics is their usefulness in comparing resource flexibility that is defined in unique ways. For example, in C5.1.2 and C5.1.3 from Section 5.2, the FSP can compare the value of flexibility provided by altering temperature bands for electricity grid-connected buildings compared to altering temperature bands for all thermal loads, two of which are connected to heat grid and therefore coupled to electricity grid indirectly. Such a comparison can also be conducted for comparing flexibility from resources with vastly different operational characteristics, such as heat pump operation in a heat grid and a battery system in the electric grid. The introduced metrics allow FSPs to assess the contributions of such varied forms of flexibility intuitively. This assessment is useful for the FSP to design appropriate DRPs as shown in Section 5.2 whereby flexibility derived from time-dependent and time-independent temperature bands for thermal loads are compared.

Another use for proposed metrics and approach has been shown in C5.1.4 and C5.1.5 in Section 5.2. The applicability of the three metrics to decide participation in intraday markets is illustrated. It is a well-known fact that prices of electricity closer to gate closure time can be highly unpredictable and in many cases, unusually high. The earlier a trade is made, the lower the uncertainty in price. Since the EUFE and EDIF heatmap is calculated offline, the information derived from these metrics can be used to procure any additional flexibility required well ahead of time.

An interesting point of discussion is the choice of the objective function for the operational simulation in Section 5.2. There, I have proposed to minimize the absolute value of the UF signal, which means I am aiming to minimize the absolute amount of energy in the UF signal, ignoring the direction component

of the UF signal. This choice is deliberately made for two reasons. One, the imbalance costs are associated with the magnitude of the imbalance. The type of payment to be made (either from system to BRP or BRP to system) depends on BRP's imbalance relative to the overall power system imbalance (which is a highly uncertain quantity). If the magnitude of imbalance is minimized, the payment (in either direction) can automatically be minimized. Two, consideration of direction appends additional complexity to the operational simulation. Although it was not examined here, the direction of the UF signal can be included in the objective formulation as required without affecting the quantification process.

Section 5.3, focuses on the use of proposed metrics by the FSP addressing network congestion challenges faced by the DSO using thermal flexibility in residential electric boiler and storage (EBST) systems. I again illustrated the benefit of using a simulation-based approach over the Minkowski Summation method for assessing flexibility. This example brings back findings from Section 2.3.1, which listed the factors which impact flexibility available from resources utilizing thermal inertia to support the electrical power system. One of the critical factors I named there was the rebound effect. The flexibility evaluated using the Minkowski method did not account for this since the method is a static measure. Utilizing a simulation-based approach, the FSP can accurately determine and quantify the impact of this phenomenon.

A key point of discussion in this example is the applicability of proposed metrics to quantify flexibility from a portfolio of P2X resources when the behavior of these devices is probabilistic. This probabilistic behaviour is realized by introducing parameter p_a or probability of acceptance associated with each EBST unit. The introduction of p_a adds realism to the example. In the example, I evaluate ten scenarios, each representing a different FR signal the FSP expects to receive from the DSO. However, since resource behavior is uncertain, in each scenario, multiple operational simulations executed with the same FR signal can generate different UF signals. It can be argued, therefore, that for each scenario, multiple simulations are required to accurately calculate the unserved flexible energy (energy in UF signal, mentioned in Section 4.3.3) and, consequently, to calculate the EUFE and EFI. However, increasing the number of simulations conducted increases the computation time for calculating the metrics. This leads us back into discussions on the need to strike a balance between computational time and result accuracy.

5.5. CONCLUSIONS

In this chapter, I introduced two examples to illustrate the usage of proposed metrics: the renewable error forecasting problem and the distribution grid congestion issue. Both the examples were formulated from the point of view of the

FSP who serves different FRP. In the first example, the flexibility requester is a BRP with large distributed VRES and controllable thermal loads, which requires flexibility to address the forecasting errors from its VRES power plants. In the second example, the FRP is a DSO that needs the flexibility to address congestion issues at its distribution transformers.

Within these two examples, different case studies are analyzed. In Section 5.2, I modeled simple resource dynamics and network constraints in an optimal dispatch problem. The nonlinearity in the objective formulation was reformulated to create a standard well-formulated MILP problem. Here, the metrics were shown to assist the FSPs in designing an appropriate DRP, comparing flexibility from various resources, formulating operational policies, and identifying potential insufficiency in flexibility provision from a portfolio. Flexibility is provided by resources that interface power and heat energy sectors, P2H systems. It is shown that flexibility can be extracted not only from resources directly coupled to the electricity grid but also from those that are indirectly linked to the electricity grid (in the presented example, these are the greenhouses connected to the heat grid). The simulation-based approach enables the assessment of this flexibility, and the proposed metrics allow this flexibility to be quantified. A short economic assessment is also conducted at the end to highlight the value of proposed metrics for the FSP.

In Section 5.3, I evaluated flexibility from electrical boiler and storage system (EBST) units to solve the congestion problem. Here, I showed the use of metrics and proposed a simulation-based approach to provide an accurate assessment of flexibility in the portfolio and compared it to the Minkowski Summation method. The FSP and DSO then used this information to mitigate congestion issues. Further complexity was introduced by defining a probability of acceptance parameter. This parameter dictated the probability of the EBST unit accepting the FSP's request to turn OFF. It was shown that the metrics can be used to assess the impact of uncertainty in resource availability on the flexibility available from the portfolio.

In both cases, I have shown the usefulness of the simulation-based approach compared to static approaches such as the Minkowski Sum method for assessing flexibility. The proposed metrics were shown to encapsulate the information generated from the simulation to provide valuable insights into the flexibility of a portfolio. Their usefulness to the FSP is shown in the examples presented.

BIBLIOGRAPHY

[1] Digvijay Gusain, Milos Cvetkovic, and Peter Palensky. "Quantification of Operational Flexibility from a Portfolio of Flexible Energy Resources". In: *International Journal of Electrical Power & Energy Systems* 141 (Oct. 2022), p. 107466. ISSN: 0142-0615. DOI: 10.1016/j.ijepes.2021.107466.

[2] Bri-Mathias Hodge et al. "Wind Power Forecasting Error Distributions : An International Comparison". In: *:* National Renewable Energy Laboratory, USA, 2012.

[3] William E. Hart et al. *Pyomo — Optimization Modeling in Python*. Second. Springer Optimization and Its Applications. Springer International Publishing, 2017. ISBN: 978-3-319-58819-3. DOI: 10.1007/978-3-319-58821-6.

[4] Desen Kirli, Maximilian Parzen, and Aristides Kiprakis. "Impact of the COVID-19 Lockdown on the Electricity System of Great Britain: A Study on Energy Demand, Generation, Pricing and Grid Stability". In: *Energies* 14.3 (Jan. 2021), p. 635. DOI: 10.3390/en14030635.

[5] Kai Strunz, N. Hatziargyriou, and C. Andrieu. "Benchmark Systems for Network Integration of Renewable and Distributed Energy Resources". In: *Cigre Task Force C* 6.04-02 (2009), p. 78.

6

CONCLUSION

I set out to conduct this research to understand, model, simulate, and quantify the flexibility available to future electrical power systems. In this future, the presence of flexible energy resources, such as electrolyzers, electric heat pumps, electric boilers, etc., is abundant, owing to increased electrification efforts in our society. My main objective was to quantify the flexibility available from the intelligent operation of these resources; to come up with metric(s) that are intuitive and simple yet encapsulate the complexity behind quantifying energy flexibility. To achieve the research objective, seven research questions (listed in Chapter 1) were formulated that methodically and systematically have led me to develop a better understanding of flexibility. In the subsequent sections, I answer these questions, discuss their applications and implications, and provide suggestions for future research.

6.1. ANSWERS TO RESEARCH QUESTIONS

In this section, I answer the research questions formulated in Chapter 1.

The amount of flexibility must be expressed with respect to the nature of flexibility requests. What are the flexibility requests of interest for an FSP?

In Section 1.2, I listed various power system challenges which require flexibility. These include frequency response, ramp requirements, VRES forecasting error mitigation, congestion management, etc. The FSP can address any of these challenges depending on the characteristics of its portfolio's flexible resources and business model. In this work, however, I have explicitly focused on power system challenges of VRES forecast error mitigation and congestion management, commonly faced by balance responsible parties (BRPs) and distribution

system operators (DSOs), respectively.

The level of detail in a model directly influences outputs obtained from that model. What impact does model detail have on the accurate assessment of operational behavior and, consequently, accurate assessment of flexibility available from P2X devices?

Chapter 2 tackles this question. In Section 2.2, I sought to establish the need to use detailed models over simplified models. Here, a power-to-heat electric heat pump and a power-to-gas electrolyzer system were modeled in two levels of detail. In the simplified models, the temperature dependencies within the model were ignored, as is the case in current literature. In the detailed models, I explicitly consider the temperature dependencies between different variables. Outputs from the two model representations are compared. I observed distinct differences between outputs from simple and detailed models. The significance of these differences is shown to be dependent on the application of these models. A slight difference between simple and detailed models of electrolyzers used in the example may seem insignificant, but it can be significant for purposes such as frequency response. Additionally, when considering a more significant number of these resources in a more extensive study (such as national energy transition scenarios), deviations in results from using the two models can become more significant. The insight generated from this research was beneficial; the impact of temperature dynamics on the operation of these devices should be considered when making operational and planning decisions.

Once the need for detailed models is established, I show, using two examples, the use of detailed models to extract relevant information in assessing flexibility from P2X devices. In Section 2.3.1, using a thermal storage system model, I highlight the influence of complex physical phenomena that dictates the resource's flexibility. Specifically, the impact of modeling and considering thermal stratification in thermal storage systems on its flexibility and the time taken to simulate the model is evaluated. It is noted that while greater detail in modeling does benefit flexibility assessment studies, it comes at the cost of computational time. It is noted that an incremental, iterative approach would suit well in determining appropriate model detail. In this approach, models could be made incrementally more detailed and be noted for the additional value they bring to the table. When this value becomes insignificant compared to computational costs, a model can be deemed to have the appropriate level of detail. The incremental significance associated with model outputs is tied to the application.

Next, in Section 2.3.2, a detailed model of the power-to-gas electrolyzer is developed to understand valuable information regarding the degradation of the device. Using this detailed model, I quantified the adjustments that would need to

be made in evaluating the resource's flexibility as time progresses. By conducting experiments on the applicability of P2X devices for different power system services spanning different time durations, I found that the impact of degradation on the flexibility offered by the device is more useful in long-term studies than in studies involving shorter time frames. This insight was possible only by studying the V-I curves obtained from a detailed model of the electrolyzer cell, which once again underlined the value of detailed models.

Evaluation of flexibility from P2X devices must be done by considering its operation in an integrated setting. How can this be achieved?

In Chapter 3, I highlighted that various components in a multi-energy system have different modeling and, consequently, model-solving and simulating characteristics. To bring together the models of these components, such as P2X resources, grid models etc., into a single modeling and simulation framework is challenging. Models of such components are best developed and solved in domain-specific modeling languages and tools. Accordingly, an open-source tool that enables assembling these models and executing a coupled simulation, or co-simulation, was introduced. Using an example case, it was shown how perspectives and objectives of different stakeholders could be addressed using ENERGYSIM in an integrated setting. The tool allows using models provided by the stakeholder themselves. A collaborative effort using co-simulation benefits the process of flexibility evaluation for a couple of reasons. Firstly, each stakeholder can model its asset/process in as much detail as needed, enabling access to only necessary variables while preserving any details about the model, essentially providing a black box system that allays any intellectual property-related concerns. Secondly, using these detailed models in an integrated setting allows assessment of operational dependencies between various models and obtaining a greater insight from the study.

For an FSP, assessing flexibility from a portfolio of various P2X technologies in an integrated setting, where each P2X device has unique operational characteristics, is essential. ENERGYSIM allows the FSP to conduct a model and simulation-based portfolio assessment whereby the available subsystem models of portfolio components are developed in different modeling environments, solved using different solvers, and may be fully encrypted black-box models. Since the specification of the time scale of integrated simulation and individual subsystem model simulation in ENERGYSIM can be freely defined from seconds to hours and days, a wide range of studies addressing different power system challenges pertinent to different time scales can be conducted. This includes flexibility assessment for frequency response (seconds), congestion management (minutes), and VRES forecast error correction (hours and day-ahead), among others. Therefore, EN-

ERGYSIM allows the FSP to simulate the behavior of its portfolio to assess its flexibility in addressing the power system challenge of interest.

The metric must convey information on the ability of a portfolio with flexible resources to fulfill flexibility requests. How can such metric(s) be formulated?

In Chapter 4, I have discussed the factors that characterize a useful flexibility metric at length. The notion of measuring "ability" of an asset, in this case, a portfolio of flexible resources, and associating a quantifiable value to it, is complex. In my view, quantifying ability requires defining an associated challenge that the asset must be able to address. In this case, I aimed to measure the "ability" of the portfolio of flexible resources to provide flexibility; the challenge takes the form of defining flexibility requests. Therefore, I measure this ability by quantifying the response of the portfolio when these flexibility requests are provided as input. When the portfolio is modeled, a simulation-based approach is used to measure this response and examine it against the input. I derived a quantity that I called unserved flexibility, which is the portfolio's response to flexibility requests. Assessing the unserved flexibility then allowed me to measure the "ability of the portfolio to be flexible" — flexible-ability — flexibility.

Activation of flexibility from a device at any time can lead to changes in the subsequent ability of devices to provide flexibility. How can the time-dependent behavior of P2X resources be accounted for in the formulation of the metric(s) describing flexibility?

As mentioned, a simulation-based approach is taken to evaluate the flexibility in the FSP's portfolio of flexible resources. A simulation-based approach has the benefit of inherently taking into account the individual constraints of the devices in the portfolio, including activation and subsequent unavailability constraints (such as due to rebound effect). A simulation-based approach ensures that the time-dependent operational states of the resources are dynamically updated as the simulation progresses; therefore, its behavior at any time is derived from not only the specified device and network level constraints but also the current and previous state of the resources. This was shown in Chapter 5, where the state of the thermal storage system at previous time steps was considered while evaluating flexibility available from the device at the current time step. Therefore, I could encapsulate the time-dependent behavior within the metric formulation with the proposed approach.

Flexibility requests and availability of P2X devices for providing flexibility are uncertain quantities to determine. How can the metric(s) capture this uncertainty?

Uncertainty is inherent in any simulation-based assessment. Uncertainty

can creep in from various sources: model parameterization, model solving, input data, prediction of future states, etc. A scenario simulation approach is proposed to address uncertainty in flexibility requests that the FSP will receive. By creating multiple scenarios of flexibility requests and assessing the unserved flexibility signal obtained by simulation of each scenario of the modeled flexibility request, the portfolio's behavior and ability to service flexibility requests are evaluated. This takes the form of the expected value (i.e., mean value) of energy in the unserved flexibility signal obtained from each scenario simulation. Besides uncertainty in formulating flexibility requests, resource availability is another form of uncertainty addressed in this thesis. With growing concerns around privacy and increasing research on non-intrusive load monitoring and control, this was an essential criterion to evaluate. The proposed simulation-based approach enables the FSP to assess the influence of uncertain operational behavior of the portfolio on the flexibility available to it. The introduced metrics can encapsulate this behavior into quantifiable information on operational flexibility in the portfolio, which the FSP can use to determine its operational strategy to service forecasted flexibility requests fully.

How will such metric(s) be helpful for an FSP?

One critical value of the proposed metrics and the scenario simulation-based approach is that metric calculation is independent of the type of flexibility requests it processes. As has been said previously in Section 4.3.4, the metrics can be calculated as long as an FR signal, and corresponding UF signal can be obtained. This is key since different approaches best represent flexibility requests representing different power system challenges. For example, to model flexibility requests for the FSP participating in the frequency response market, a time series modeling technique (such as Auto-Regressive Integrated Moving Average (ARIMA) models) may be better, whereas, for modeling wind power forecasting errors, a simple Gaussian/Cauchy model can be used. By separating the quantification process from flexibility request modeling, I ensure that the metric can measure the flexibility of a portfolio independent of which power system challenge FSP targets. In this thesis, I showed the applicability of the proposed metrics for two power system issues — VRES forecasting error mitigation and congestion management.

Further, in Chapter 5, I provide examples illustrating the use of proposed metrics to address realistic flexibility issues a representative FSP would target. These examples employed the proposed scenario simulation-based approach to quantify the flexibility in a portfolio of flexible resources by considering various real-world constraints which can influence the flexibility that an FSP can extract from its portfolio. These included 1) flexibility from resources indirectly

connected to the electric grid, 2) comparison of flexibility from time targeted demand response programs (DRPs) and non-targeted DRPs, and finally, 3) the probabilistic nature of individual flexible resources in adhering to flexibility activation signals received from the FSP. Additionally, I compared the benefits of using the proposed approach against the current method of flexibility evaluation extensively. I also presented an economic study highlighting the benefit of employing the proposed metrics for the FSP in avoiding unforeseen costs.

6.2. APPLICATION

There are two main contributions from this research that will have real-world applications. The first one is the rise of entities such as multi-energy system aggregators that combine flexible resources from the integrated energy system. The absence of metrics that can accurately quantify the flexibility of flexibly operable resources connected in different parts of the integrated grid is one of the reasons that such an entity does not yet exist. Most aggregators work by pooling resources of a single category, for example, thermal storage units, electric heat pumps, building HVAC systems, and others. The availability of proposed metrics that encapsulates flexibility from resources with diverse characteristics in an integrated way opens the doors for an entity such as an MES aggregator. Secondly, the open source tool ENERGYSIM provides a way to couple energy system simulators to come together to perform an integrated system assessment. Although catering to the energy systems community, ENERGYSIM provides a ready-to-use functionality to couple any Python-based simulator with another where a time-dependent behavior of the combined system needs to be assessed. Therefore, it can find non-energy uses where an assessment of the time evolution of subsystems is required in an integrated manner. Immediately, urban area planning comes to mind as a use case. Consider the availability of models of urban population growth, transportation systems, and water and waste management. These models can be combined to assess how an urban area develops over time and what policies could benefit the residents.

6.3. FUTURE RESEARCH

The area of flexibility assessment in energy systems still requires extensive research. Here, I list some of the areas that could serve as an extension to the presented work, as well as some topics that would be useful for the energy community in assessing flexibility. In this work, I have delved deep into modeling flexible energy resources. I have established that detailed models are of significant value since they help understand and quantify the impact of complex phenomena present in these resources, affecting the operation and, consequently,

the assessment of flexibility available. Assessing other P2X devices and identifying phenomena directly impacting the flexibility of P2X devices (such as electric vehicles) is needed. Here, an area of further interest is the inclusion of actors in the simulation of P2X devices, specifically the behavioral aspects. This can point to research on the quantification of uncertainty in their behavior, its impact on quantified flexibility in a portfolio of flexible resources with individual operational policies, etc.

Another meaningful research direction is investigating the uncertainty of model parameters and the accuracy of model outputs. In the absence of real-world data, validation of either Model A or Model B was not possible, which meant that both models are assumed to be accurate. However, an interesting comparison can be made between the value of a non-validated and non-tuned detailed model and a validated and tuned simplified model. In the case study I presented in Section 2.2, the detailed Model B is built by adding a thermal subsystem model to simplified Model A. Therefore, if the simplified Model A is validated and accurately represents reality, then what range of parameter uncertainty in the detailed model still adds value to the user over using validated simplified models?

Next, the quantification process uses a scenario simulation approach and advocates the use of detailed models therein. As is shown, this could be a potential issue when it is required by the application to use a highly detailed and complex model or use a large number of scenarios. To this end, computationally efficient methods need to be devised and researched. This includes replacing physical models with data-driven models such as those based on neural networks and using techniques such as Multi-level Monte Carlo to speed up computations. An exciting area within data-driven modeling efforts is physics-informed neural networks (PINN). PINNs have attracted much attention in the domain of ata-driven modeling of physical processes. Such techniques can allow high-speed computations and simulate hundreds of scenarios. This finds use in concepts such as in Digital Twin, where a faster than the real-time model could benefit users in devising mitigation and correction actions for various flexibility issues such as congestion in real-time.

The use of these metrics to assess the flexibility of P2X devices for frequency reserve services in power systems and the use of the proposed metrics for power system expansion and planning problems is also interesting area for future research. Planning for future power systems which consider the benefits of short-term operational flexibility quantified in this thesis can lead to a more efficiently designed and operated power system.

A

APPENDIX

A.1. EMPIRICAL CUMULATIVE DISTRIBUTION FUNCTION

Empirical Cumulative Distribution Function (ECDF) is a common non-parametric estimator used in exploratory data analysis. Traditionally, it is used to determine the underlying CDF of a dataset.

For a given dataset, $\{x_1, ..., x_n\}$, the ECDF is given mathematically by Eq. (A.1).

$$\hat{F}(x) = \frac{1}{n} \sum_{i=1}^{n} I\{x_i \leq x\} \tag{A.1}$$

where $I\{\cdot\}$ is the indicator function. It has two possible values:

$$I(x_i \leq x) = \begin{cases} 1 & \text{when } x_i \leq x \\ 0 & \text{when } x_i > x \end{cases} \tag{A.2}$$

A.2. OPTIMIZATION PROBLEM

This section describes the constraints for optimization problem described in Section 5.2.3. These constraints form the baseline DRP formulated in C1. The equality constraints are:

A

$$P_{\text{th,GH}} + P_{\text{th,B}} = P_{\text{th,TS}} + P_{\text{th,EB}} + P_{\text{th,PB}} \tag{A.3}$$

$$P_{\text{F}i} + P_{\text{EB}} + P_{\text{HP}} + \pi_i = P_{\text{FC}} + P_{\text{EG}} + P_{\text{ID}} \tag{A.4}$$

$$S_{\text{TS}}(t+1) = S_{\text{TS}}(t) - P_{\text{th,TS}}(t) - P_{\text{th,l}}(t) \tag{A.5}$$

$$\theta(t+1) = \theta(t) + \frac{P_{\text{th}}(t) - P_{\text{th,l}}(t)}{\dot{m} \cdot c} \tag{A.6}$$

$$P_{\text{th,EB}} = P_{\text{EB}} \cdot \eta_{\text{EB}} \tag{A.7}$$

$$P_{\text{th,B}} = P_{\text{th,HP}} = P_{\text{HP}} \cdot COP_{\text{HP}} \tag{A.8}$$

$$\sum_{t=0}^{N_t} P_{\text{F}i}^{DA} - \sum_{t=0}^{N_t} P_{\text{F}i} = 0 \tag{A.9}$$

$$\sum_{t=0}^{N_t} \tilde{P}_{\text{th,GB}}^{DA} - \sum_{t=0}^{N_t} P_{\text{th,GB}} = 0 \tag{A.10}$$

Equations (A.3) and (A.4) represent the thermal and electrical power balance constraints respectively. Constraints in Eqs. (A.5) and (A.6) represent the resource dynamics for thermal energy storage and general temperature evolution dynamics for building and greenhouses. η_{EB} represents the electrical boiler efficiency, while COP_{HP} represents the coefficient of performance of the HP. Constraints in Eqs. (A.7) and (A.8) relate the electrical and thermal powers for electric boiler and heat pump. Here, $P_{\text{th,B}}$ represents the thermal power consumption of the building. Equation (A.9) forms the load shifting constraint for flexible electrical loads in feeders F_i (F1 and F2). It ensures that no load shedding occurs by operating the loads flexibly. Equation (A.10) defines flexibility in operating GB. Since the amount of gas to operate the GB was brought on D-1 in the gas market, its operation is fuel constrained. Assuming a linear relationship between fuel used, power output, and hours of operation of the GB, Eq. (A.10) ensures that the rescheduling of the gas-based GB uses the same amount of gas as contracted in the day-ahead market on D-1.

In addition to the equality constraints, the following inequality constraints also apply.

$$\underline{\theta}_{\text{GH}} \leq \theta_{\text{GH}} \leq \overline{\theta}_{\text{GH}} \tag{A.11}$$

$$\underline{\theta}_{\text{B}} \leq \theta_{\text{B}} \leq \overline{\theta}_{\text{B}} \tag{A.12}$$

$$\underline{P}_{\text{F}i} \leq P_{\text{F}i} \leq \overline{P}_{\text{F}i} \tag{A.13}$$

$$r_{\text{F}i}^{\downarrow} \leq P_{\text{F}i}(t+1) - P_{\text{F}i}(t) \leq r_{\text{F}i}^{\uparrow} \tag{A.14}$$

$$0 \leq P_{\text{FC}} \leq \overline{P}_{\text{FC}} \tag{A.15}$$

Equations (A.11) and (A.12) represent the upper and lower bounds on thermal load (GH-A, GH-B, B) temperatures, Eqs. (A.13) and (A.14) represents the bounds on power and ramp rates on feeders F1 and F2, and finally, Eq. (A.15) describes the bounds on the power output of FC. The $abs()$ in calculation of UF signal introduces non-linearity in the optimization problem. This can however, easily be linearized by introducing a slack variable in the problem formulation. The reformulated problem then becomes a Mixed Integer Linear Programming (MILP) problem which is easily solvable.

List of Publications

First Author Publications

1. **Gusain D.**, Cvetković M., and Palensky P. *Simplifying multi energy system cosimulations using energysim*, SoftwareX **18**, 639 (2022).

2. **Gusain D.**, Cvetković M., and Palensky P. *Quantifying Operational Flexibility from a Portfolio of Flexible Energy Resources*, International Journal of Electric Power and Energy Systems **18**, 639 (2021).

3. **Gusain D.**, Cvetković M., Yagci C., and Palensky P. *Importance of Model Fidelity of Power to X Devices in Energy System Analysis*, IEEE Innovative Smart Grid Technologies (ISGT) North America 2022.

4. **Gusain D.**, Cvetković M., Bentvelsen R., and Palensky P. *Assessing Large Scale Electrolyzers as Flexibility Service Providers*, IEEE International Symposium on Industrial Electronics (ISIE) 2020.

5. **Gusain D.**, Cvetković M., and Palensky P. *Energy Flexibility Analysis using FMUWorld*, IEEE Innovative Smart Grid Technologies (ISGT) 2019.

Other Publications

1. Palensky, P., Cvetković, M., **Gusain, D.**, and Joseph, A., 2021. *Digital twins and their use in future power systems.* In Digital Twin, 1(4), p.4.

2. Shetgaonkar, A., Perilla, A., Tyuryukanov, I., **Gusain, D.**, López, C., and Rueda Torres, J.L., 2021. *Applications of PowerFactory for the Study of Basic Notions of Power System Dynamics in Graduate Courses.* In Modelling and Simulation of Power Electronic Converter Dominated Power Systems in PowerFactory (pp. 337-377). Springer, Cham.

3. Perilla, A., **Gusain, D.**, Torres, J.R., Palensky, P., van der Meijden, M., and Gonzalez-Longatt, F., 2020, October. *Optimal Tuning of Active Power Gradient Control for Frequency Support in Multi-Energy Systems.* In 2020 IEEE PES Innovative Smart Grid Technologies Europe (ISGT-Europe) (pp. 889-893). IEEE.

4. Cvetković, M., **Gusain, D.**, and Palensky, P., 2019, October. *Cossembler-Rapid Prototyping Tool for Energy System Co-simulations.* In IECON 2019-45th Annual Conference of the IEEE Industrial Electronics Society (Vol. 1, pp. 2138-2143). IEEE.

5. Cvetković, M., **Gusain, D.**, and Palensky, P., 2019, August. *Using Cossembler for Rapid Prototyping of Co-simulations for Power System Operations.* In 2019 IEEE Power & Energy Society General Meeting (PESGM) (pp. 1-5). IEEE.

6. Pan, K., **Gusain, D.**, and Palensky, P., 2019, January. *Modelica-supported attack impact evaluation in cyber physical energy system.* In 2019 IEEE 19th International Symposium on High Assurance Systems Engineering (HASE) (pp. 228-233). IEEE.

7. Rakhshani, E., **Gusain, D.**, Sewdien, V., Torres, J.L.R., and Van Der Meijden, M.A., 2019. *A key performance indicator to assess the frequency stability of wind generation dominated power system.* IEEE Access, 7, pp.130957-130969.